THE IMPACT OF PHYSICAL AND BIOLOGICAL FACTORS ON INTRACELLULAR UPTAKE, TRAFFICKING AND GENE TRANSFECTION AFTER ULTRASOUND EXPOSURE

A Thesis

Presented to

The Academic Faculty

by

Ying Liu

In Partial Fulfillment

of the Requirements for the Degree

Doctor of Philosophy in the

School of Chemical and Biomolecular Engineering

Georgia Institute of Technology

May 2011

THE IMPACT OF PHYSICAL AND BIOLOGICAL FACTORS ON INTRACELLULAR UPTAKE, TRAFFICKING AND GENE TRANSFECTION AFTER ULTRASOUND EXPOSURE

Approved by:

Dr. Mark R. Prausnitz, Advisor
School of Chemical & Biomolecular Engineering
Georgia Institute of Technology

Dr. John McDonald
School of Biology
Georgia Institute of Technology

Dr. Athanassios Sambanis
School of Chemical & Biomolecular Engineering
Georgia Institute of Technology

Dr. Philip J. Santangelo
Department of Biomedical Engineering
Georgia Institute of Technology

Dr. Hang Lu
School of Chemical & Biomolecular Engineering
Georgia Institute of Technology

Date Approved: March 07, 2011

ACKNOWLEDGEMENTS

I would like to thank many people who have been helping me and supporting me for these many years. I would like to thank my advisor, Dr. Mark R. Prausnitz, for giving me the opportunity to work in his lab, and for his patience, care and instruction in my research and thesis. As a person who is an inspiration to others, his diligence and respect to the research work will always be a model for me to follow. I would also like to thank Dr. Hang Lu, Dr. John McDonald, Dr. Athanassios Sambanis and Dr. Philip J. Santangelo for serving as members of my thesis committee, for their scientific advice and for the help from their lab members.

I wish to thank many people who have contributed to this work: Dr. Lilya Matyunina for handling the gene chip experiments; Dr. Nathan Bowen for his work on the microarray data analysis; Dr. Lijuan Wang for her help in RT-PCR; Dr. Roman Mezencev for the insightful discussion in cell cycle analysis; Aaron Lifland for his expertise in 3D image analysis; Dr. Kacy Cullen and Dr. Michelle LaPlaca for providing the cortical neurons; Dr. Heather Bara for her help in the experiments with adeno-associated virus; Dr. David A. Dean, Dr. Gill Heart and Dr. Al Merrill for the helpful discussion.

I would also like to acknowledge the staff in the IBB at Georgia Tech and Emory University who have helped in this work: Robert Karaffa and Nadia Boguslavsky for their assistance with cell sorting; Johnafel Crowe, Steven Woodard and Andrew Shaw for their confocal and flow cytometry expertise; Trudy Walker for her motherly greetings every day; Allen Echols for taking care of the packages and maintenance work. I want to

give my special thanks to Donna Bondy, the loveliest lady I have ever met, for her efficient and hard work on all the paper work and meeting schedules.

I would like to thank many past and present members of Dr. Prausnitz's research group: Dr. Robyn Schlicher and Josh Hutcheson for teaching me mammalian cell culture on my first day in the lab and other techniques in the following years; Dr. Vladimir Zarnitsyn for his insightful discussions and comments on my presentations all the time; Dr. Daniel Hallow for his ultrasound expertise; Christina A. Rostad for her help in siRNA experiments; Samirkumar Patel for solving the problems with computers and softwares every time; James Norman for helping me with statistics and driving to the AICHE annual conference in 2009; Aritra Sengupta for sharing all the "crazy" things he has done; Jing Yan, the undergraduate researcher who helped me with this work; Dr. Junghwan Park, Dr. Seong-O Choi, Dr. Jeong Woo Lee, Dr. Yeu-Chun Kim, Dr. Harvinder Gill and Yoo-Chun Kim for their kindness and friendship. I would especially like to thank Dr. Prerona Chakravarty and Dr. Samantha Andrews, for not only their help in my research but also their warm-heartedness in my everyday life in the lab.

I would also like to thank my friends in Atlanta, Dr. Jizhong Lou, Dr. Wei Chen, Weiwei Yin, Dr. Fang Kong, Dr. Tao Wu, Dr. Cho-Yin Lee, Dr. Liang Guo, Xue Xiang and Hui Yao for their friendship which made me feel at home.

It is never enough for me to say thanks to my parents for their unconditional and continuous love and support in my whole life. Finally, I thank Jun Chen, my husband, for making my life much more enjoyable and meaningful with his love.

TABLE OF CONTENTS

LIST OF TABLES

LIST OF FIGURES

LIST OF ABBREVIATIONS

DMEM	Dulbecco's Modified Eagle's medium
DNA	deoxyribonucleic acid
DTS	DNA nuclear targeting sequence
EDTA	ethylenediaminetetraacetic acid
EMS	ethyl methanesulfonate
FBS	fetal bovine serum
FCM	flow cytometry
FDA	Food and Drug Administration
FITC	fluorescein isothiocyanate
GADD	growth arrest and DNA-damage inducible gene
GAPDH	glyceraldehyde 3-phosphate dehydrogenase
GFP	green fluorescent protein
HEPE	4-(2-hydroxyethyl)-1-piperazineethanesulfonic acid
KEGG	Kyoto encyclopedia of genes and genomes
MW	molecular weight

NLS	nuclear localization signal
NMDA	N-methyl-D-Aspartate
PBS	phosphate buffered saline
pDNA	plasmid DNA
PNA	peptide nucleic acid
PVDF	poly vinylidene flouride
qRT-PCR	quantitative real-time polymerase chain reaction
RNA	ribonucleic acid
RPMI	Roswell Park Memorial Institute medium
RT	room temperature
siRNA	small interfering ribonucleic acid
SD	standard deviation
TOP2	Topoisomerase Ⅱ
US	ultrasound

LIST OF SYMBOLS

D	duty cycle [%]
G1	Gap 1 phase of cell cycle
G2	Gap 2 phase of cell cycle
J	acoustic energy [J/cm^2]
M	mitosis phase of cell cycle
N	the number of cells
ρ	density of water [g/mL]
S	synthesis phase of cell cycle
T, t	time [sec]
u	speed of sound in water [m/s]

SUMMARY

Ultrasound (US) is of interest among the current gene delivery systems due to its unique expected advantages, including: low toxicity, low immunogenicity, the potential for repeated application, organ specificity and broad applicability to acoustically accessible organs. Various US conditions have been tested for gene transfection among different types of cell *in vitro* (Liang et al. 2004; Michel et al. 2004; Zarnitsyn and Prausnitz 2004; Larina et al. 2005; Duvshani-Eshet et al. 2006; Fischer et al. 2006; Rahim et al. 2006), and with various organs and tissues *in vivo*, including skeletal muscle (Christiansen et al. 2003; Li et al. 2003; Pislaru et al. 2003; Wang et al. 2005), brain (Sheikov et al. 2004; Shimamura et al. 2004; Manome et al. 2005), heart (Bekeredjian et al. 2003; Guo et al. 2004; Tsunoda et al. 2005), liver (Miao et al. 2005) and kidney (Azuma et al. 2003; Lan et al. 2003; Koike et al. 2005; Ng et al. 2005). However, one problem in US-mediated gene transfection is the heterogenic bioeffects and thereby the low transfection efficiency.

In this work, we used megahertz pulsed ultrasound and studied gene transfection with a human prostate cancer cell line. We first studied the compromise of cell viability and uptake efficiency and found out that increasing sonication temperature or changing US contrast agents could improve drug/gene delivery mediated by US exposure. We also found that accounting for cell debris after sonication was important to correctly determine cell viability.

Next, we verified the capability of US to deliver DNA into the cell nuclei, which is necessary for successful gene transfection. Under the optimal sonication conditions, ~ 30% of cells showed DNA uptake right after US exposure and most had a portion of DNA already localized in the cell nuclei. The maximum transfection efficiency was ~ 12% at 8 h post US exposure. From the DNA perspective, ~ 30% of DNA was localized in the cell nuclei immediately after US exposure and ~ 30% was in the autophagosomes/ autophagolysosomes with the rest "free" in the cytoplasm. At later time up to 24 h, DNA continued to be distributed ~ 30% in the nuclei and most or all of the rest in autophagosomes/autophagolysosomes. Our results showed that US was able to deliver DNA into the cell nuclei shortly after the treatment and that the rest of DNA was mostly cleared by autophagosomes/autophagolysosomes.

To further increase transfection efficiency, we then studied the differences between live cells with DNA uptake and those with successful gene transfection post US exposure using cell sorting, cell cycle and microarray analysis. Cells with gene transfection were found to accumulate at the G1 phase of cell cycle and associate with the up-regulation of 32 genes (e.g., GADD45α) and the down-regulation of 46 genes (e.g., TOP2α). Drugs that regulate the expression levels of GADD45α and TOP2α were found to further enhance the transfection mediated by US. A maximun increase of ~ 2 fold in transfection efficiency was observed when cells were sonicated with 0.6 mg/mL ethyl methanesulfonate to up-regulate GADD45α. These results suggestted that using drugs that regulate certain introcellular processes could further enhance US-mediated gene transfection.

Over a broad range of US conditions, the integrity of three common gene delivery vectors, plasmid DNA, siRNA and adeno-associated virus, were not affected by US exposure. This thesis verified that US was able to delivery DNA into the cell nuclei to facilitate rapid gene transfection, and provided a proof of princible that by modulating certain intracellular processes, the efficiency of US-mediated gene transfection could be further increased. US could potentially be a safe and efficient method for gene therapy.

CHAPTER 1: INTRODUCTION

Gene therapy is promising as an effective way to treat many genetic disease, but limited by the lack of a safe and efficient gene delivery system. Ultrasound (US) has been explored as a physical gene delivery method ever since 1987, when Fechheimer reported US-mediated gene transfection in mammalian cells for the first time (Fechheimer et al. 1987). Various US conditions have been tested for gene transfection among different types of cell *in vitro* and organs and tissues *in vivo* (Azuma et al. 2003; Bekeredjian et al. 2003; Christiansen et al. 2003; Lan et al. 2003; Pislaru et al. 2003; Guo et al. 2004; Liang et al. 2004; Michel et al. 2004; Sheikov et al. 2004; Koike et al. 2005; Larina et al. 2005; Manome et al. 2005; Tsunoda et al. 2005; Fischer et al. 2006; Rahim et al. 2006). Compared to other methods (e.g., electroporation and chemical gene delivery vectors), US is a promising tool for gene therapy because of its unique advantages in safety, targeting and specificity. However, there are still many things that are not well understood and thereby prevent US from its clinical applications in gene therapy. For instance, the cavitation mechanism is not fully clear; the trafficking of exogenous gene in the cell cytoplasm is not well understood; how to effectively protect DNA from degradation and improve the nuclear import is under investigation. And most importantly, heterogeneous bioeffects were found in nearly all the studies using US for gene delivery, which is possibly the major reason of the low transfection efficiency.

Gene transfection requires overcoming several barriers: cell membrane, trafficking in the cytoplasm, nuclear entry, transcription and translation. To overcome

these barriers and enhance US-mediated gene transfection, many previous studies have focused on the optimization of physical parameters for US conditions, including acoustic pressure and energy, treatment time, US contrast agents and so on. Fewer studies looked into the biological regulation of intracellular processes such as facilitating the DNA trafficking and nuclear entry, and the regulation of gene expression, which could possibly be important to achieve high transfection rate. In this work, we hope to have a better understanding of the heterogeneous bioeffects caused by US exposure, including DNA uptake, gene expression, DNA localization in cell nuclei and cytoplasm. We expected to find the certain intracellular processes by regulating which US-mediated gene transfection can be further enhanced. We used megahertz pulsed ultrasound and studied gene transfection with a human prostate cancer cell line. We were particularly interested in:

- the compromise of cell viability and uptake/transfection efficiency post US exposure under optimal US conditions;
- the qualitative and quantitative analysis of the localization of plasmid DNA in the cell nuclei and cytoplasm;
- the differences between cells that have different bioeffects of DNA uptake or gene transfection post US exposure;
- the possibility to further enhance US-mediated gene transfection by regulating some intracellular processes with drug treatment.

This thesis seeks to characterize these processes associated with US-mediated gene transfection and offer strategies to increased transfection efficiency.

CHAPTER 2: BACKGROUND

Gene therapy is defined as the transfer of new genetic materials (DNA or RNA) into cells or targeted tissues for therapeutic benefits. It is proposed to be an effective way to treat genetic disease, such as monogenic disorders, cardiovascular disease and cancer (Miller 1992; Mulligan 1993; Crystal 1995). The major impediment to the successful application of gene therapy is not a paucity of therapeutic genes, but the lack of a safe, non-toxic and efficient gene delivery system (Young et al. 2006).

The therapeutic applications of ultrasound (US) have been studied and used ever since 1930s. The ability of US to transiently permeabilize cell membranes was investigated intensively to facilitate drug/gene delivery. Various US apparatus systems were designed and a variety of US exposure conditions (e.g., energy intensity, pulse length, acoustic pressure) were tested on different types of cells and tissues both *in vitro* and *in vivo*. The development in US contrast agents further enhanced drug/gene delivery using therapeutic US. Compared to other gene delivery systems, this approach is promising in clinics, because it is non-invasive, site-specific and easy to perform. US can be applied to both surface and deep tissues, both small and large tissues.

The low transfection efficiency is currently the major impediment to the clinical application of US-mediated gene transfection. US generates strong heterogeneous bioeffects and the transfection efficiency is strongly related to cytotoxicity, meaning that the compromise between cell viability and transfection efficiency is quite sensitive. Furthermore, the bioeffects caused by US exposure differs between the various types of cells and tissues. More research work is needed to fully understand the mechanisms of

US-mediated gene transfection. And based on those findings, better US delivery systems can be designed to achieve higher transfection efficiency.

Current Gene Delivery Strategies

An ideal gene delivery system should have these following characteristics:

- safety,
- resistance to metabolic degradation and/or attack by the immune system,
- specificity for the target cells or tissues,
- ability to express the therapeutic gene in a time period long enough.

Current gene delivery systems are generally classified as two categories: viral and non-viral methods.

Viral Gene Delivery System

Viral vectors are the most commonly used gene therapy method because of their nature to transfer DNA into cells. Currently a variety of virus vectors have been developed for gene delivery. Some of them like adenovirus and vaccinia virus can provide transient gene transduction, and others like retrovirus and adeno-associated virus can provide permanent transgene expression. Virus vectors can be easily manipulated according to the therapeutic genes and cell types, and provide high efficiency and possibility of long-term gene expression. They have been used in 70% of gene therapy clinical trials (Young et al. 2006). However, the introduction of foreign proteins may cause some unknown reactions that may be dangerous to patients. The acute immune response, immunogenicity, and insertion mutagenesis uncovered in gene therapy clinical trials have raised serious safety concerns about some commonly used viral vectors.

Several accidents associated with virus gene therapy have already been reported, including fatal accidents (Marshall 1999; Check 2002; Check 2003). Thus safety is a key problem when viral vectors are used in gene therapy. The maximum size of the transgene that recombinant viruses can carry is another potential limitation of viral gene delivery systems.

Non-viral Gene Delivery Systems

Non-viral gene delivery systems have been explored using chemical and physical approaches. These delivery systems are generally less efficient than viral vectors, especially *in vivo*. However, in contrast to viral delivery systems, DNA can be delivered without carrier proteins and therefore is typically non-immunogenic.

Chemical approaches (Nicolazzi et al. 2003; Dass 2004; Neu et al. 2005) use synthetic or naturally occurring compounds as carriers to deliver the DNA into cells. The therapeutic genes are usually immobilized, adsorbed, attached, or encapsulated into the chemical formulations, which are cationic lipid-based (lipoplexes) or cationic polymer-based (polyplexes) or lipid-polymer hybrid system. The DNA-containing particles are subsequently taken up by cells via endocytosis, macropinocytosis, or phagocytosis in the form of intracellular vesicles, and a small fraction of the DNA is released into the cytoplasm and migrates into the nucleus, where transgene expression takes place. Studies have been conducted to improve DNA uptake by cells and intracellular trafficking to the nucleus. Although these chemical approaches seem effective for *in vitro* gene delivery, they are not impressive in clinical trials due to the low transfection efficiency or toxicity because of the non-biodegradable nature of some gene carriers. And how to control the spatial delivery to the desired tissue is also a big challenge.

Gene delivery using chemical approaches involve such procedures as cell attachment, endocytosis and entrapment into endocytic vesicles, maturation of endosomes into lysosomes, escape from vesicular compartments, migration toward the nucleus periphery, dissociation between carriers and foreign DNA, and finally entry of DNA into the nucleus. In contrast, physical methods can bypass some of the above barriers. Physical approaches provide carrier-free gene delivery by employing a physical force that permeates the cell membrane and facilitates intracellular gene transfer. These systems include microinjection (King 2004), magnetofection (Scherer et al. 2002; Plank et al. 2003), laser irradiation, gene gun (Yang et al. 1990), hydrodynamic delivery (Zhang et al. 1999), electroporation (Andre and Mir 2004; Heller et al. 2005) and ultrasound (Newman and Bettinger 2007).

Microinjection

Microinjection is the direct-pressure injection of a solution into a cell through a glass capillary. It is an effective and reproducible method for introducing DNA into cells, and DNA can be delivered directly to the nucleus. However, microinjection is applied to cells one by one and therefore transfection is limited by the number of cells that can be treated. Currently this approach is the most common method for the production of transgenic animals (Uchida et al. 2001; Auerbach 2004; Hofmann et al. 2004).

Magnetofection

Magnetofection exploits paramagnetic particles made of iron oxide as drug carriers, guides their accumulation in target tissues with local strong magnetic fields. This method causes rapid sedimentation of nearly all gene delivery vectors on the target cells

and DNA uptake via endocytosis. It is also combined with chemical methods to develop gene carriers. More investigations need to be conducted. For example, changes in cellular physiology upon exposure to the magnetic field are not known yet (Plank et al. 2003).

Laser Irradiation

Laser irradiation requires a laser source to generate the laser beam, which focuses on the target cell and permeabilizes the cell membrane by a local thermal effect. There are reports showing that laser irradiation can also create transient pores on the cell membrane, which allow gene uptake (Kurata et al. 1986; Shirahata et al. 2001). The approach is not widely used mainly due to the high cost and physical size of the laser sources. The transfection efficiency depends on parameters like the pulse length and number, and total energy level.

Gene Gun

Gene gun was first used in plant cells in 1987 (Klein et al. 1987), and was applied to mammalian cells in the early 1990s (Yang et al. 1990). Gene gun deposits DNA on the surface of gold particles and accelerates the particles by pressurized gas. The particles penetrate into cells or tissues and release DNA for transfection. This method is also called particle bombardment and it may be good for DNA immunization to skin or exposed tissue (Eisenbraun et al. 1993; Wang et al. 2004). The depth of penetration is a big limitation and the device and gold particles are expensive. There are currently two major devices commercially available: Accell gene gun (Agracetus, Inc., Middleton, WI) and the Helios gene gun (BioRad Laboratories, Hercules, CA).

Hydrodynamic Delivery

Hydrodynamic gene delivery has been studied in the mouse model *in vivo*. The rapid tail vein injection of a large volume of DNA solution causes a transient overflow of injected solution at the inferior vena cava and induces a flow of DNA solution in retrograde into the liver. And thus a rapid rise of intrahepatic pressure, liver expansion, and reversible disruption of the liver fenestrae allow DNA to enter the hepatocytes (Liu et al. 2004; Zhang et al. 2004). The transfection efficiency depends on the structure of the organ and the volume and speed of injection. A big limitation of this method is that it is only applied to certain highly perfused organs like liver. And it is currently not applicable to inject large volume of solution in humans.

Electroporation

Electroporation is a common physical tool in gene delivery to cells. This approach applies electrical pulses to cells and creates a transient permeability of cell membranes which allows the entry of foreign DNA. Different electrode configurations and a wide range of pulse patterns have been developed depending on the cells or tissues to be treated. Electroporation has proved to be effective both *in vitro* and *in vivo*, including in various tissues like skin, liver, lung, kidney, bladder, retina, cornea, brain, skeletal muscle and so on (Wells 2010). Transfection efficiency mediated by electroporation is influenced by several physical (especially, pulse duration and electric field strength) and biological (including DNA concentration and conformation, cell size) factors.

Several major drawbacks exist for *in vivo* application of electroporation. Firstly, an invasive procedure is required to place the electrodes deep into the internal organs.

Secondly, it has a limited effective range (approximately 1 cm) between electrodes, which makes it difficult to transfect cells in a large area of tissue. Thirdly, electroporation for a cell suspension requires a voltage up to 1 kV (Gehl 2003). The high voltage applied to cells could affect the stability of genomic DNA, which is an additional safety concern. More investigations need to be conducted to address these concerns, maybe by optimizing the design of electrodes, their spatial arrangement, the field strength, and the duration and frequency of electric pulses.

Ultrasound

US-generated cavitation creates a transient permeability of cell membrane which allows the entry of DNA, like electroporation. US with US contrast agents has been studies as a promising method for gene therapy. US can penetrate tissues with the minimum damage and focus its energy to non-superficial objects within a small volume. These properties lead to non-invasive and site-specific gene delivery. The efficiency of US-mediated gene transfection is also influenced by physical (acoustic pressure, pulse length and exposure duration) and biological (including DNA concentration, cell concentration and size) factors. So far, the major problem for US-facilitated gene delivery is low gene transfection efficiency.

Ultrasound, Cavitation and Ultrasound Contrast Agents

Ultrasound

US is sound pressure with a frequency greater than the upper limit of human hearing, which is approximately 20 kHz. Therefore, US is classified as sound pressure at

frequencies above 20 kHz (Figure 2.1). US is widely used in clinics (e.g., imaging, cleaning, etc) and industries (e.g., welding).

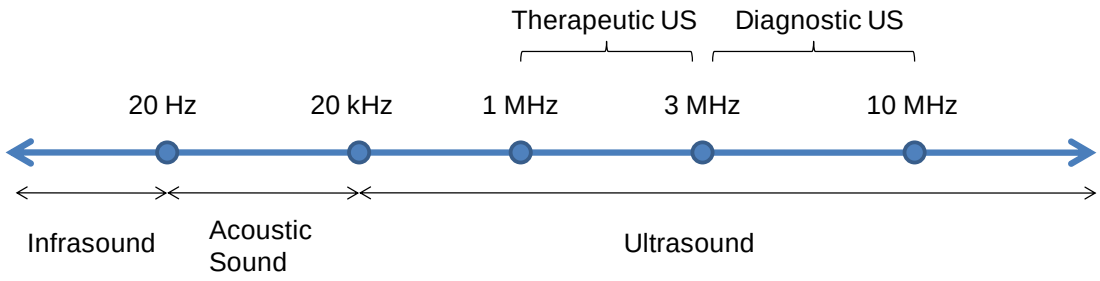

Figure 2.1: The frequencies of infrasound, acoustic sound and ultrasound.

Ultrasound is generated by a transducer which is usually made from piezoelectric materials like quartz or lead zirconate titanate (Asher 1997). A suitable alternating voltage is applied to the transducer. When the frequency of the input voltage reaches the resonance frequency for the vibration of the transducer, the piezoelectric material responds by undergoing vibrations. These vibrations are transmitted to the environment through a certain medium (e.g., water) as a periodic pressure wave (Pierce 1981).

Cavitation

Acoustic cavitation refers to the dynamical response of bubbles driven by acoustic pressure. When periodic positive and negative pressures generated by US produce a density gradient in the solution, the negative pressure could overcome a tension maintaining the liquid state, thereby generating a “cavity” in the solution. This is called cavitation. In the position of the cavity, microbubbles are produced. Two common sources for such bubbles are: pre-existing bubbles that are present in a liquid that is near

saturation with gas, or bubbles that form when the local pressure of the liquid decreases to below the vapor pressure of the liquid or decreases to such a low pressure that dissolved gas comes out of the solution.

Acoustic cavitation activity is classified as two categories: stable cavitation and transient cavitation (inertial cavitation). Stable cavitation refers to the repetitive pulsation of an acoustically driven bubble at an equilibrium radius. The bubbles vibrate in reaction to the pressure but undergo no change in size. Stable cavitation enhances the convective transport occurring within the liquid because the vibrating surface creates local swirling fluid convection, known as micro-streaming (Miller 1987). If the vibrating microbubbles expand during several cycles of growth under pressure and finally collapse, it is called transient cavitation. The collapse of bubbles is quite violent and is dominated by the inertia of the inrushing fluid. The physical effects of inertial cavitation include micro-streaming, fluid jetting, extreme thermodynamic conditions in the microbubble leading to light production (sonoluminescence) and chemical reactions (sonochemistry) (Leighton 1994). It is also noticed that the acoustic effects are associated with the frequencies and intensities of US (Carstensen et al. 1980; Muir and Carstensen 1980). For a given size of a microbubble, the intensity threshold to trigger inertial cavitation decreases as the US frequency decreases (Urick 1983). Low frequency US (< 1 MHz) causes strong cavitation, while higher frequency US causes more thermal energy deposition.

US Contrast Agent

US contrast agents are “soft-shelled” agents made of gas microbubbles. They have a gas core surrounded by a shell made from various materials, for example, polymer, lipid and protein. US contrast agents can serve as cavitation nuclei and enhance

the physical effects of US. Currently there are many commercially available US contrast agents, for instance, Optison®, Definity®, SonoVue® and so on. Table 2.1 briefly summarizes of the characteristics of some US contrast agents. Albunex®, Levovist®, Optison®, and Definity® have been approved by FDA.

Table 2.1: Physicochemical characteristics of US contrast agents.

US Contrast Agent	**Shell**	**Encapsulated Gas**	**Bubble Size Mean (Range)**
Sonazoid	Surfactant	Fluorocarbon	3.2 μm (1 – 10 μm)
Levovist	Galactose/palmitic acid	Air	2 – 3 μm (2 – 8 μm)
Optison	Albumin	Octafluoropropane	4.7 μm (1 – 10 μm)
SonoVue	Phospholipid	Sulphur hexafluoride	2.5 μm (1 – 10 μm)
Definity	Phospholipid	Perfluoropropane	1.5 μm (1 – 10 μm)
Albunex	Albumin	Air	4.5 μm (1 – 10 μm)

Besides the above soft-shelled US contrast agents, hard-shelled contrast agents (containing a rigid lipid or polymeric shell) have also be developed. These agents, although not currently commercially available, have been studied for diagnostic imaging (Schneider et al. 1991), drug delivery (Frinking et al. 1998), acoustic properties (Frinking and de Jong 1998; Hoff et al. 2000), and other biophysical applications (Bouakaz et al. 1999). Future studies in drug delivery are to develop US contrast agents with multiple functions, not only cavitation nuclei, but also drug carriers and tissue targeting for specific drug delivery purpose (Bekeredjian et al. 2006; Lum et al. 2006). For instance,

microbubbles can be prepared to encapsulate generic materials and to contain ligands like antibodies or specific peptides, which would bind to the specific target cells or tissues and therefore cause a close contact between microbubbles and the target of treatment (Feril 2009).

Ultrasound in Biomedical Applications

US is now broadly used in biomedical applications as a therapeutic, diagnostic or surgical instrument. The energy intensities for its therapeutic application generally range from 0.5 to 3 W/cm^2. Diagnostic US uses lower intensities (< 0.5 W/cm^2) and surgical US uses higher intensities (> 10 W/cm^2) (Ng and Liu 2002).

Therapeutic Applications

US was first introduced as a therapeutic method in 1930s, when the heating effects of US were applied to inner tissue for physical therapy. Ever since then, a variety of therapeutic US applications has been reported, for instance, rapid and localized tissue heating (Kennedy 2005; Haar and Coussios 2007), mechanical tissue damage and homogenization (Roberts et al. 2006), dissolution of blood clots (thrombolysis) (Everbach and Francis 2000; Datta et al. 2006), vascular occlusion (acoustic hemostasis) (Vaezy and Zderic 2007), locally enhanced and time-released activity of drugs (sonodymanic therapy) (Kinoshita and Hynynen 2006), reversible permeability to large molecules for drug delivery (sonoporation) (Mitragotri 2005), reversible opening of the blood-brain barrier (Mesiwala et al. 2002; Hynynen et al. 2005) and so on.

Diagnostic Applications

US has been used by radiologists and sonographers to image the human body for at least 50 years and has become one of the most widely used diagnostic tools in modern medicine without any known adverse "side effects". US-based diagnostic medical imaging techniques are used to visualize muscles, tendons, and many internal organs, to capture their size and structure. Diagnostic US is also used to visualize fetuses during routine and emergency prenatal care (so-called obstetric sonography), to confirm fetal viability, check for fetal movement and heartbeat, and determine the sex of the baby (Whitworth et al. 2010).

Surgical Applications

US surgery was first proposed as a tool of neurosurgical research in 1940s (Lynn et al. 1942). High intensity of US (> 10 W/cm^2) can be focused at a distance within the body and produce selective damage within the focal volume with no harm to the surrounding tissues. This technique has clear advantages over traditional forms of surgeries in clinics. Some examples are using US to kill tumor cells or break up kidney and gall bladder stones (lithotripsy) (Terhorst et al. 1972; Toth et al. 1988; Callans and Gadacz 1990; Mink et al. 1991; el Khader et al. 1995; Guo 1995; Yoshizawa et al. 2009; Gu et al. 2010).

Ultrasound-mediated Gene Transfection

US-mediated gene transfection is of interest due to its unique expected advantages, including: low toxicity, low immunogenicity, the potential for repeated application, organ specificity and broad applicability to acoustically accessible organs (Gao et al. 2007). However, it is in the early stage of clinical implementation with the major challenge of low transfection efficiency.

Current Research on US-mediated Gene Transfection

Ever since Fechheimer and his colleagues reported US-mediated gene transfection on mammalian cells in 1987 (Fechheimer et al. 1987), many groups have contributed to the study of gene transfection mediated by US with different types of cells *in vitro* (Liang et al. 2004; Michel et al. 2004; Zarnitsyn and Prausnitz 2004; Larina et al. 2005; Duvshani-Eshet et al. 2006; Fischer et al. 2006; Rahim et al. 2006), and with various organs and tissues *in vivo*, including skeletal muscle (Christiansen et al. 2003; Li et al. 2003; Pislaru et al. 2003; Wang et al. 2005), brain (Sheikov et al. 2004; Shimamura et al. 2004; Manome et al. 2005), heart (Bekeredjian et al. 2003; Guo et al. 2004; Tsunoda et al. 2005), liver (Miao et al. 2005) and kidney (Azuma et al. 2003; Lan et al. 2003; Koike et al. 2005; Ng et al. 2005). Besides reporter genes (e.g., plasmids encoding green fluorescent protein, β-galactosidase and luciferase), transfection with "therapeutic" genes using US exposure was also investigated (Kondo et al. 2004; Akowuah et al. 2005; Miao et al. 2005; Sakakima et al. 2005).

The development of stabilized microbubbles for increasing sensitivity and applicability further strengthened US as a powerful and safe tool for future gene delivery

(Bekeredjian et al. 2006). However, the US-mediated transfection efficiency is still comparatively low. The efficiency of gene transfection using liposomes can reach above 50% (Yamamoto et al. 1999), while US-mediated gene transfection only gives around 10% efficiency and fewer studies have shown transfection efficiency above 30% (Nozaki et al. 2006). Although a lot of work has been done to optimize the US parameters (e.g. pressure, exposure duration, energy intensity) and sonication conditions (e.g. cell concentration, US contrast agent concentration and plasmid concentration), low transfection efficiency is still the major challenge in US-mediated gene transfection. And transfection efficiency varies with different US contrast agents and different types of cells and tissues.

US exposure was found to generate heterogeneous bioeffects, which may be one of the major reasons of the low transfection efficiency. US opens the cell membrane so as to allow drug/gene entry, which is desired, but at the same time it puts cells in risk, which is unwanted. Cells close to the location of cavitation are likely destroyed by US exposure, cells at mid-distances from the microbubbles exhibit drug/DNA uptake with the cell membrane temporarily opened and rapidly resealed, and cells far from the cavitation microbubbles remain unaffected. Therefore, higher molecule uptake may be achieved under strong US conditions, but associated with higher cell death rate. To maintain a low death rate under gentle exposure conditions may lead to the uptake efficiency not high enough for applicable drug delivery. The compromise between high viability and high uptake efficiency is quite challenging. It is also worth noting that individual cells exposed *in vitro* may be more sensitive to US exposure than the tightly packed cells in tissues. Under similar US conditions which cause a lot of cell death *in vitro* may lead to

successful drug/gene delivery without much tissue damage *in vivo* (Danialou et al. 2002; Li et al. 2003).

Although cavitation is believed to play a major role in the cell membrane permeabilization (Miller et al. 1996; Kimmel 2006), the mechanisms by which US mediates gene transfection is not fully clear, particularly whether US affects later steps in gene transfection pathways, which are possibly the rate-limiting steps (e.g., DNA trafficking in the cytoplasm and entry into the nucleus). Along with the bioeffects of drug delivery and gene transfection, US was found to induce intracellular bioeffects as well. Changes in cell behavior after US exposure were reported, including morphology (Schlicher et al. 2010), proliferation (Bao et al. 1997; Lawrie et al. 1999), apoptosis (Ashush et al. 2000), migration and adhesion (Alter et al. 1998). Currently, limited expression profiling data provided by microarray analysis revealed that US regulated ribosomal proteins expression, influenced cell proliferation and differentiation, induced cell cycle arrest and apoptosis (Abdollahi et al. 2004; Tabuchi et al. 2007). These intracellular bioeffects may be cell-type specific and US-condition dependent. Whether these changes in intracellular processes are related to US-mediated gene transfection remains a question.

Research in US-mediated gene transfection still has a long way to go, with the major challenge of low transfection efficiency. More studies on the heterogeneous bioeffects, unclear mechanisms and unknown cellular pathways influenced by US exposure will possibly explain the reasons of low efficiency and further enhance gene transfection (Paliwal and Mitragotri 2006; Campbell and Prausnitz 2007).

Mechanisms of US-mediated Gene Transfection

Successful gene transfection requires both extracellular and intracellular barriers to be overcome. These barriers include plasma membrane, which is the barrier of DNA uptake, the cytoskeletal meshwork in the cytoplasm, which hinders DNA trafficking in the cytoplasm, and the nuclear envelope, which prevents DNA entry into the nucleus. The gene delivery system has to send the exogenous DNA to the nucleus before any transcription can take place. Although the mechanisms of US-mediated gene transfection are still under investigation and discussion, some theories and hypotheses have been proposed to explain how naked plasmid DNA comes into cells across the cell membrane, traverses in the cytoplasm, arrives inside the nucleus and gets ready for transcription and translation.

Plasmid DNA Uptake

Unlike chemical delivery systems, US-mediated DNA uptake is non-endocytotic, which allows a rapid and direct transfer of exogenous DNA into the cytoplasm. Cavitation is considered as one of the mechanisms of molecule uptake mediated by US. In transient cavitation, microbubbles collapse causes a sudden release of energy and in turn leads to a series of thermal, chemical and mechanical effects locally. The mechanical stress is thought to generate transient pores on the cell membrane close to the microbubbles, which allow an influx of external molecules into the cell (Schlicher et al. 2006). Strong correlation of cavitation caused by US with cellular uptake mediated by US has been demonstrated (Hallow et al. 2006). Some research found that the poration of the cell membrane could last from milliseconds (van Wamel et al. 2004) to nearly 24 h

(Taniyama et al. 2002), but efficient drug/gene delivery can be achieved within seconds (Schlicher et al. 2006).

The cavitation mechanism leads to the heterogeneous bioeffects of US exposure. Cells proximal to the cavitating microbubbles are mechanically destroyed, cells at mid-distances from the microbubbles exhibit reversible poration and drug/DNA uptake, and cells far from the microbubbles remain unaffected (Guzman et al. 2001; Schlicher et al. 2006). How to predict and control these heterogeneous bioeffects based on the understanding and measurement of the cavitation is under investigation.

Plasmid DNA Trafficking in Cytoplasm

DNA uptake is only the first step for gene transfection. After the plasmid DNA enters the cell successfully, it has to traverse the cytoplasm and enter the nucleus prior to transcription and translation. This process needs to be quick since nucleases in the cytoplasm start to degrade exogenous DNA in minutes (Lechardeur et al. 1999; Pollard et al. 2001).

The fluid-phase viscosity of the cytoplasm is in the range from 1.1 to 1.4 cP (Fushimi and Verkman 1991; Luby-Phelps et al. 1993), which is only slightly greater than water. However, the multiple cytoskeletal elements (e.g., microfilaments, microtubules and intermediated filaments) in cytoplasm form a complex and crowded latticework that significantly impedes the diffusion of large molecules. The passive diffusion of plasmid DNA in the cytoplasm is generally very slow, especially for DNA molecules lager than 1000 base pair (660 kDa). In fact, very few DNA molecules were found to be able to move away from the original site 1 h after microinjection into the cytoplasm (Lukacs et al. 2000). It has been shown in non-viral gene transfection that a

certain amount of plasmid DNA stays in the cytoplasm after entering the cell, which is considered as one of the reasons for low transfection efficiency by non-viral gene delivery methods.

Cytoskeleton regulates intracellular transport by impeding the passive diffusion of large molecules and providing active transport. One of the bioeffects mediated by US exposure is the alteration of cytoskeleton (Skorpikova et al. 2001; Raz et al. 2005), which may help in the passive diffusion of exogenous DNA by reducing crosslinks and actin fibers. And also, unlike chemical gene delivery systems, where gene vectors were found entrapped in large endocytic vesicles formed at the cell membrane, plasmid DNA was distributed throughout the cytoplasm right after US exposure (Zarnitsyn and Prausnitz 2004; Mehier-Humbert et al. 2005b; Duvshani-Eshet et al. 2006). Because of the above two possible reasons, naked exogenous DNA may be propelled into perinuclear region for nuclear import right after US exposure. Therefore the kinetics of plasmid internalization and gene expression was found faster in US-mediated gene transfection compared to chemical methods (Mehier-Humbert et al. 2005b).

Microtubule network is responsible for intracellular transport of cargos from the cell membrane to the nucleus. Dynein is one of the adaptor proteins associated with this process. Many viruses and endocytosed materials including some chemical gene delivery vectors are verified to utilize microtubules to reach the nucleus (Bukrinskaya et al. 1998; Suomalainen et al. 1999; Vihinen-Ranta et al. 2000; Ogawa-Goto et al. 2003; Bausinger et al. 2006). It is suggested that plasmid DNA may also utilize microtubules to transport from the cell membrane to the nucleus in other physical gene delivery systems, such as electroporation and microinjection (Vaughan and Dean 2006). However, it is believed

that intermediate adapter proteins may be required, since DNA cannot bind to the motor proteins directly. Besides microtubule, baculovirus and HIV virus were also found to use actin cytoskeletal network to traffic its genome toward the nucleus (van Loo et al. 2001; McDonald et al. 2002).

DNA Nuclear Import

Another barrier to gene transfection is the nuclear envelope, which separates the nucleus from the cytoplasm. The level of gene expression after delivery is limited by low quantities of exogenous DNA available for nuclear import (Brisson et al. 1999; Subramanian et al. 1999). Transport of molecules into the nucleus occurs through nuclear pores. Molecules with a diameter less than 10 nm or a molecular weight less than 70 kDa are able to diffuse passively through the nuclear pore (Melchior and Gerace 1995). Larger molecules including protein, DNA and RNA need to be transported actively by nuclear transport receptors through an energy-dependent process (Conti and Izaurralde 2001). It has been shown that the nuclear envelop is not a major hindrance to gene transfection in actively-dividing cells compared to non-dividing cells, where the nuclear envelope remains intact (Fasbender et al. 1997). Using chemical gene delivery methods, cells undergoing mitosis were found to be more ready for transfection (Wilke et al. 1996; Tseng et al. 1999), which suggests that nuclear envelope temporarily breaks down during mitosis therefore facilitates transfection and gene transfection efficiency may be dependent on the stage of cell cycle (Brunner et al. 2000). Synthetic nuclear localization signal (NLS) peptides can be recognized by nuclear pores and have been developed to bind to DNA and facilitate DNA delivery into the nucleus (Cartier and Reszka 2002). Nuclear import of plasmid DNA in non-dividing cells was also found to be DNA

sequence-specific and several DNA nuclear targeting sequences (DTS) were designed as an enhancer to help nuclear import in several cell lines (Graessmann et al. 1989; Dean 1997; Langle-Rouault et al. 1998).

Regulation of Intracellular Processes by US Exposure

It has been shown that a variety of cells behave differently under stress, including both chemical and mechanical stress (Ingber 2002). Signaling cascades, intracellular processes and transcription factors may be either up-regulated or down-regulated, and cytoskeleton may be reorganized as well. Under extreme stress, cells may even enter apoptosis. Similarly, cells may also undergo certain unknown intracellular processes regulation under the stress due to US exposure. Microarray and gene technology have been applied to the study of US-mediated regulation of intracellular signaling pathways (Tabuchi et al. 2007). Some research work has shown US-mediated regulation of ribosomal proteins (Abdollahi et al. 2004). The change in the ratio of ribosomes to mRNA can in turn affect protein synthesis. There are also reported results that US exposure activates DNA synthesis and promotes cell proliferation by activation of a Rho/Rock/ERK signaling pathway (Zhou et al. 2004). In brief, US may enhance gene transfection efficiency by regulating intracellular processes, and vice versa, facilitating these intracellular processes may also help in US-mediated gene transfection.

CHAPTER 3: MATERIALS AND METHODS

General Experimental Methods

Ultrasound Apparatus

The US transducer was an immersible, focused, piezoceramic transducer (Sonic Concepts, Woodinville, WA, USA, model no. H-101), supplied with two different matching resistance networks allowing production of sound at 1.1 MHz and 1 MHz. The transducer had a diameter of 70 mm, a 52 mm focal length and a 1.5 mm focal width at half-amplitude (-6 dB). A sinewave was provided by two programmable waveform generators (Standford Research Instruments, Sunnyvale, CA, USA, model no. DS345 and Agilent, Austin, TX, USA, model no. 33120A) and amplified by an RF broadband power amplifier (Electronic Navigation Industries, Rochester, NY, USA, model no. 3100LA).

The transducer was submerged in deionized and partially degassed water at 37 ℃ placed in a polycarbonate tank (30.5 x 29 x 37 cm) to sonicate a 375 μL sample held within a disposable micropipette (Samco, San Fernando, CA). A 5-cm thick acoustic absorber (SC-501 Acoustic Rubber, Sonic Concepts) was placed opposite the transducer in the tank to minimize standing-wave formation. A three-axis positioning system (10 μm resolution, Velmex, Bloomfield, NY, USA) was mounted on top of the tank to position samples and a hydrophone at desired locations in the tank.

The US transducer was calibrated versus the peak-to-peak voltage of the signal by a PVDF membrane hydrophone (NTR Systems, Seattle, WA, model no. HMA-0200) at a distance of 1 cm from the transducer (Appendix A). Sonication was carried out at

pressures (*p*) ranging from 0 MPa (i.e., "sham" exposure) to 2 MPa and the total treatment time (*t*) up to 60 min with a desired burst length at a desired duty cycle (*D*). Therefore the corresponding energy density (*J*) was calculated as

$$J = t \times D \times \frac{(\frac{p}{\sqrt{2}})^2}{\rho \times u},$$

where ρ is the density of water (1 g/mL) and u is the speed of sound in water (1,500 m/s). A typical US condition used for gene transfection study is:

- Peak-to-peak pressure: 0.78 MPa,
- Duty cycle: 25%,
- Pulse length: 0.25 ms,
- Total treatment time: 1 min.

Cell Culture

DU145 human prostate cancer cells (American Type Culture Collection, Manassas, VA, item no. HTB-81) in RPMI-1640 medium (Cellgro, Mediatech, Herndon, VA) and human HT-1080 fibrosarcoma cells (American Type Culture Collection, item no. CCL-121) in DMEM medium were cultured as monolayers in a humidified atmosphere of 95% air and 5% CO_2 at 37 ℃. The medium was supplemented with 10% heat-inactivated fetal bovine serum (FBS, Atlanta Biologicals, Atlanta, GA) and 1% penicillin/streptomycin (Cellgro).

Cell Samples for US-mediated Gene Transfection

DU145 cells were harvested according to the standard procedure (Hallow et al. 2006) and resuspended in RPMI-1640 medium at the final concentration of 1×10^7 cells/mL for US exposure. Cell concentration was determined by Multisizer™ 3 Coulter

Counter (Beckman Coulter, Inc. Fullerton, CA). The plasmid DNA (pDNA) encoding green fluorescent protein (GFP), gWiz™-GFP (Aldevron, Fargo, ND) was used in transfection. The pDNA was added to the cell suspension at a concentration of 20 μg/mL for US exposure.

Definity® US contrast agent (Bristol-Myers Squibb Medical Imaging, North Billerica, MA) was added to cell samples at a concentration up to 2 vol% to serve as cavitation nucleation sites.

General Fluorescent Probes

Plasmid DNA Labeling

To measure pDNA uptake efficiency and track the localization of pDNA in the cytoplasm, Mirus LabelIT® Tracker™ Cy™3 kit and Cy™5 kit (Mirus, Madison, WI) were used to label pDNA gWiz™-GFP and gWiz™ High-Expression control vector (gWiz™ Blank, Aldevron) before US exposure. The labeling reaction was conducted according to the procedure recommended by the manufacturer.

Nuclear Labeling

Hoechst 33342 (trihydrochloride, Invitrogen, Carlsbad, CA) and propidium iodide (PI, Invitrogen) were used to stain nuclei separately. Hoechst 33342 was added to cell samples at the final concentration of 10 μg/mL for 10 min at room temperature (RT). PI was added to sonicated cell samples at a concentration of 1 vol% for 5 min at RT to measure cell viability after US exposure (Liu et al. 2010).

Endosomes/lysosomes Labeling

LysoTracker® Green DND-26 (Molecular Probes, Invitrogen) was used to label acidic organelles in live cells. The reagent was added to cells in growth medium at a final concentration of 50 nM and incubated for 5 min at growth conditions. Cells were then washed three times before flow cytometry or microscopy analysis.

EEA-1 (final dilution rate 1:250, BD Bioscience, San Jose, CA), CD63 (final dilution rate 1:10, Developmental Studies Hybridoma Bank, Iowa City, IA) and LAMP-1 (final dilution rate 1:5, Developmental Studies Hybridoma Bank) were used as the primary antibody to label early endosomes, late endosomes and lysosomes, respectively. Alexafluor 488 Donkey anti Mouse A-21202 (Invitrogen) was used as the secondary antibody at a final concentration of 2 μg/mL. Cells plated on the coverslip (VWR International, West Chester, PA) were fixed in 2% formaldehyde for 10 min at RT and washed twice with PBS. Cells were treated with 10% serum and 0.02% (w/v) sodium azide in PBS for 5 min at RT and washed twice with PBS. Cells were then incubated with the primary antibody diluted in PBS with 10% serum and 0.2% saponin for 1 h in darkness at RT, and washed twice in PBS with 10% serum. After that, cells was incubated with the secondary antibody diluted in PBS with 10% serum and 0.2% saponin for 1 h in darkness at RT, and washed twice in PBS with 10% serum.

Flow Cytometry (FCM)

The pDNA uptake, transfection efficiency, cell viability and cell cycle were measured by a BD LSR benchtop flow cytometer (BD LSR, Becton Dickinson, San Jose, CA), and data were analyzed by FCS Express V3 (De Novo Software, Los Angeles, CA)

or FlowJo software (Tree Star, Ashland, OR). Typical analysis sampled approximately 10,000 cells. Samples were excited with a 488 nm laser to measure GFP expression (GFP fluorescence) with a 530/30 nm bandpass filter for emission. A 633 nm laser was used to measure pGFP uptake (Cy5 fluorescence) using a 660/20 nm bandpass filter for emission. Cell populations were first elucidated by gating (Figure 3.1a), and histogram data were then analyzed to determine % population (Figure 3.1b).

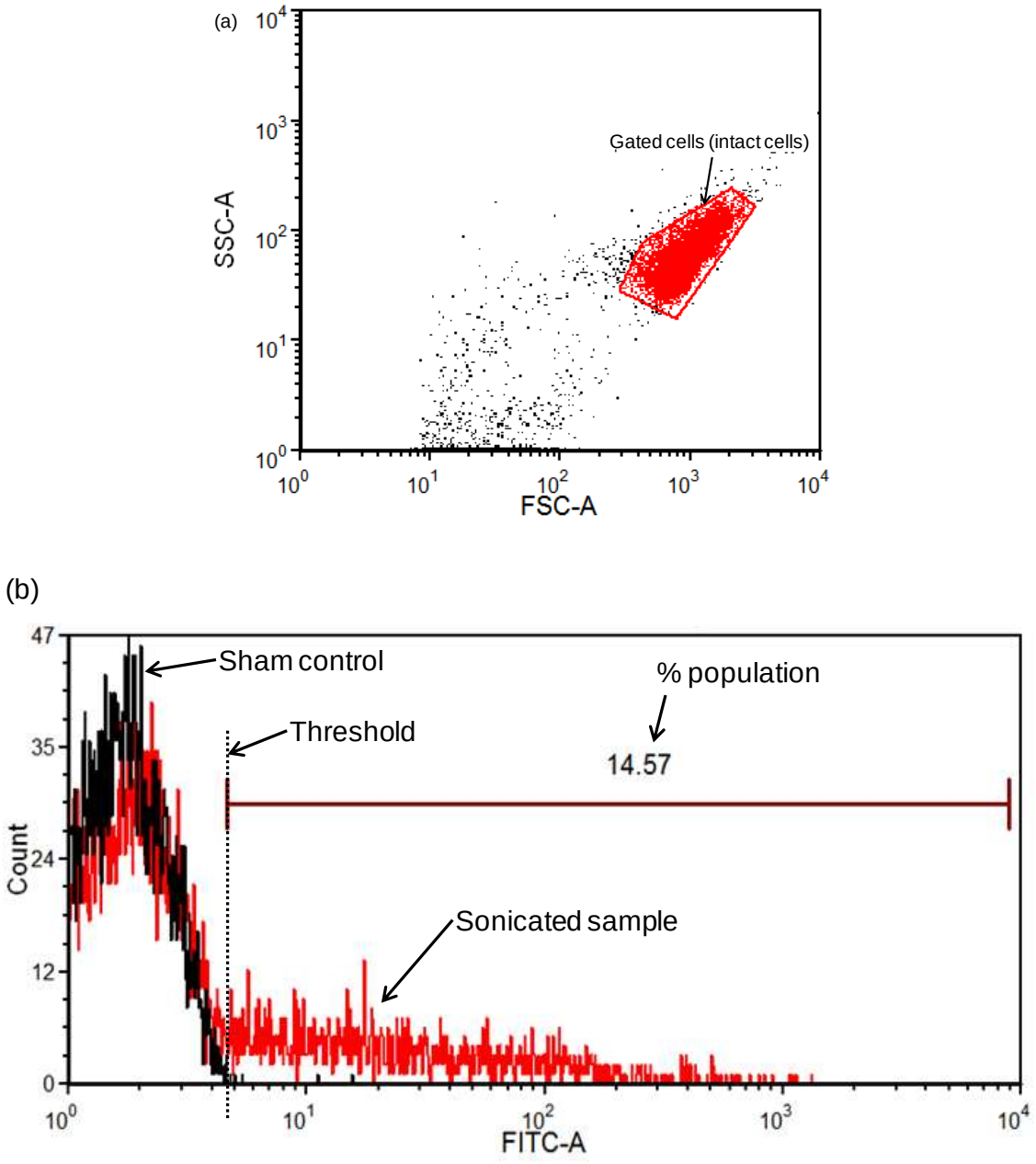

Figure 3.1: FCM analysis of cell samples after US exposure. (a) The scatter diagram of all the events with intact cells gated. FSC-A: forward scatter A is a parameter related to cell size by measuring light scattered less than 10 degrees as a cell passes through the laser beam. SSC-A: side scatter A is a parameter related to the internal granularity or complexity of a particle by measuring light scattered at a 90 degree angle as a cell passes through the laser beam. (b) The histogram of gated cells. FITC-A: a parameter indicating the light intensity of FITC.

The viability of DU145 cells post US-mediated gene transfection was determined by comparing the cell concentrations in samples to that in the "sham" exposure controls. Briefly, viable cells were counted in each sample, normalized based on the fluid volume analyzed by the flow cytometer and then normalized to the viability of a non-sonicated control sample. The analysis time of a sample in the flow cytometer was used as a measure of the sample volume analyzed, since the flow cytometer operated at a constant flow rate. Transfection efficiency and pDNA uptake were measured by determining the percentage of cells with the corresponding fluorescence greater than a threshold value based on untreated control cells (Figure 3.1b).

Confocal Microscopy

A Zeiss LSM 510 confocal laser-scanning microscope or Zeiss LSM META/NLO 510 multiphoton microscope (Zeiss, Thornwood, NY) was used to visualize the pDNA uptake and GFP expression. The lasers for blue, green and red fluorescence were UV (wavelength 364 nm), Argon (wavelength 488 nm) and Helium-neon (wavelength 543 nm). Images were captured by directing a 60× magnification oil objective or a 40× magnification objective. Hoechst 33342 was added to cell samples at the final concentration of 10 μg/mL for 10 min at RT. Cell samples were viewed on a 25 mm round glass cover slip in an Attofluor Cell Chamber (Molecular Probes, Invitrogen).

Image Analysis

Zen software (Zeiss) and Volocity 3DM software (Improvision, Lexington, MA) were used for 3D image analysis to identify and quantify colocalization.

Methods for Chapter 4

Experimental Protocols

US Procedures

DU145 cells at a final concentration of 1×10^6 cells/mL were mixed with 10 μM FITC–labeled dextran (70 kDa, Sigma, St. Louis, MO) and 2 vol% Optison® (GE Healthcare, Princeton, NJ) or 0.1 vol% Definity® for US exposure. The temperature for US treatment was either RT or 37 ℃. The peak-to-peak pressure was 0.39 MPa, duty cycle was 25% and total treatment time was 1 s. Samples were washed with PBS for three times after sonication to remove extracellular FITC-dextran and cells were resuspended in PBS.

Bioeffects Analysis

PI was added to cell samples at the final concentration of 1 vol% to measure cell viability after US exposure. A 488 nm laser was used in FCM for excitation and a 575/20 nm bandpass filter for emission to determine the number of intact cells lacking red fluorescence due to PI staining compared to untreated control cells. These cells were counted as intact viable cells. The viability of DU145 cells after US exposure was determined by normalizing the number of intact viable cells based on the fluid volume analyzed by the flow cytometer and then normalized to the number of intact viable cells

of a control sample in the fluid volume. The analysis time of a sample in the flow cytometer was used as a measure of the sample volume analyzed, because the flow cytometer operated at a constant flow rate. In this way, lysed cells, intact viable and dead cells were all taken in consideration. The following is an example.

In a "sham" control sample, the number of intact viable cells is N_0, and the time for FCM analysis is T_0. In a sonicated sample, the number of intact viable cells is N_1, the number of all the intact cells is N_s and the time for FCM analysis is T_s. Therefore, the number of intact dead cells is (N_s - N_1). The viability of intact cells is N_1/N_s (not accounting for cell debris generated by US exposure). When cell debris is accounted for, the overall viability after US exposure is:

$$\frac{N_1/T_s}{N_0/T_0}$$

The uptake efficiency of intact cells (not accounting for cell debris) after US exposure was measured by FCM with a 488 nm laser and a 530/30 nm bandpass filter for emission and determined by the percentage of cells showing green fluorescence compared to untreated control cells. The overall uptake efficiency is the uptake efficiency of intact cells multiplied by the overall viability.

The Analysis of Data from Literature

Cell viability and uptake efficiency data from various studies using a variety of cell types and tissues, different size of molecules and US apparatus and conditions were read and replotted as uptake efficiency versus viability. The papers and corresponding figures used are listed in Table 3.1.

Table 3.1: Data resource for Chapter 4.

Paper	Figure
Tata et al. 1997	Fig. 1, 2
Miller et al. 1999	Fig. 4
Cochran and Prausnitz 2001	Fig. 4
Guzman et al. 2001	Fig. 6, 7
Keyhani et al. 2001	Fig. 2
Guzman et al. 2002	Fig. 3, 4
Guzman et al. 2003	Fig. 1, 2
Larina et al. 2005	Fig. a, b
Mehier-Humbert et al. 2005a	Fig. 1
Hallow et al. 2006	Fig. 5
Hallow et al. 2007	Fig. 4
Hutcheson et al. 2010	Fig. 1
Karshafian et al. 2010	Fig. 4, 5

Experimental Methods for Chapter 7

Cell Sorting

Cells were suspended at a concentration of 5-10 $\times 10^6$ cells/mL in the sorting buffer containing 1 x PBS (Ca/Mg^{2+} free), 1 mM EDTA, 25 mM HEPES (pH 7.0, Invitrogen) and 1% heat-inactivated FBS, and then sorted by FACSVantage or FACSAria Cell-Sorting System (Becton Dickinson) using lasers and filters described previously.

Cell Cycle Analysis

The plasmid pBB14 encoding Us9-GFP (#18657, Addgene, Cambridge, MA) which retains GFP fluorescence quantitatively in cells following ethanol permeabilization (Kalejta et al. 1999) was used in US-mediated transfection for cell cycle analysis. Cells at a concentration of $1\text{-}2\times10^6$ cells/mL were mixed by vortexing with cold absolute ethanol at a volume ratio of 1 to 3 and incubated for at least 1h at 4 ℃. Fixed cells were washed twice with PBS and resuspended in PBS with 1 vol% PI and 10 vol% RNase A (Invitrogen) and incubated for 30 min at RT. Samples were analyzed by FCM. A 488 nm laser was used for excitation and a 575/26 nm bandpass filter for emission.

RNA Isolation and Microarray Hybridization

Cells isolated by FACS were suspended in Trizol (Invitrogen). RNA was isolated and purified with PicoPure RNA Isolation Kit (Arcturus, Mountain View, CA) and RNA quality was verified on the Bioanalyzer RNA Pico Chip (Agilent Technologies, Palo Alto, CA). All the procedures followed the manufacturers' protocols. Total RNA from the above extractions was processed using the RiboAmp HS kit (Arcturus) in conjunction with the IVT Labeling Kit (Affymetrix, Santa Clara, CA) to produce an amplified, biotin-labeled mRNA suitable for hybridizing to GeneChip Probe Arrays (Affymetrix). Labeled mRNA was then hybridized to GeneChip® Human Genome U133 Plus 2.0 Arrays (Affymetrix) according to the manufacturer's instructions.

Analysis of 3' Expression Microarray Results

Affymetrix .CEL files were processed using the Affymetrix Expression Console (EC) Software Version 1.1. Files were processed using the default MAS5 3' expression workflow which includes scaling all probes to a target intensity (TGT) of 500. Spiked in report controls used were AFFX-BioB, AFFX-BioC, AFFX-BioDn, and AFFX-CreX. Probe set results were further evaluated using Spotfire DecisionSite software. Probes were normalized across samples by Z-score calculation. In order to determine the differentially expressed probe sets between control and experimental groups, the t-test p-values were calculated for each group of probe set Z-score values. Genes with p values < 0.01 and fold changes > 2X or < -2X were considered for further analysis. In order to computationally cross-validate differentially expressed probe sets, .CEL files were converted to expression level values using the affy and GCRMA packages of the Bioconductor project (www.bioconductor.org) for the R statistical programming environment (www.rproject.org). After GCRMA preprocessing, differentially expressed probe sets were identified as above. The two lists of differentially expressed probes were compared and found to contain 86 overlapping probe sets. Duplicate probe sets representing the same gene and unnamed genes were removed to leave 78 unique genes for further functional characterization.

Websites Used for Functional Processing of Differentially Expressed Probe Sets

Genomica-http://genie.weizmann.ac.il/genomica_web/enrichment/gene_sets.jsp

GSEA-http://www.broad.mit.edu/gsea/

Pathway Express-http://vortex.cs.wayne.edu/projects.htm

DAVID Bioinformatics Resources-http://david.abcc.ncifcrf.gov/

Quantitative Real-Time Polymerase Chain Reaction (qRT-PCR)

1 μg of total RNA was reverse transcribed using Superscript III cDNA synthesis kit (Invitrogen) primed with random hexamers under conditions described by the supplier. cDNA from this reaction was cleaned up by gel extraction kit (QIAGEN, Chatsworth, CA). PCR was performed in DNA engine opticon 2 Continuous Fluorescence Detection System (MJ Research, Waltham, MA) using 1 μL of synthesized cDNA and iQ SYBR Green Supermix (Bio-Rad Laboratories, Hercules, CA) according to the manufacturer's protocols. Gene specific primers for two genes (TOP2α: Forward 5'- AGTCATTCCACGAATAACCA -3', Reverse 5'- TTCACACCATCTTCTTGAG -3'; GADD45α: Forward 5'- GAGAGCAGAAGACCGAAAGGA -3', Reverse 5'- CACAACACCACGTTATCGGG -3') were synthesized (Integrated DNA Technologies, Coralville, IA). RNA and cDNA concentration were determined by NanoDrop ND-1000 (NanoDrop Technologies, Wilmington, DE).

The expression levels of TOP2α and GADD45α were normalized to the expression of the housekeeping gene GAPDH and calculated according to the $2^{-\Delta\Delta Ct}$ method (Livak and Schmittgen 2001). The standard deviation was calculated for triplicate RT-PCR reactions.

Electrophoresis

The gel for DNA electrophoresis was made of 1.5% agarose (Denville Scientific, Inc., Metuchen, NJ). KODAK Gel Logic 100 imaging system (Scientific Imaging Systems; Eastman Kodak Co., New Haven, CT) was used for imaging.

Drug Treatment

The drugs tested in this study were purchased from Sigma. Their names and concentrations are listed in Table 3.2.

The drugs were added to the sample right before sonication at the desired concentrations. After US exposure, 40 μL of cells from the sample were plated in each well of a 6-well plate with total 2 mL growth medium under growth conditions. And therefore, the drug concentrations were diluted by 50 times for 8 h of incubation until further analysis.

Experimental Methods for Chapter 8

Samples for US Exposure

To test whether US exposure damages the integrity of pDNA, DNA samples were prepared by diluting plasmid gWizTM-GFP to a final concentration of 16 μg/mL in Opti-MEM medium (Gibco).

To test whether US exposure damages the integrity of RNA, survivin-siRNA (Silencer pre-designed siRNA, Ambion, Austin, TX) was diluted to a final concentration of 100 nM in Opti-MEM medium.

Table 3.2: Drugs and their concentrations.

Drugs	Final Concentration during US Exposure
Chloroquine diphosphate salt	100 μM
Amsacrine hydrochloride	200 nM
Mitoxantrone dihydrochloride	200 nM
Aclarubicin	50 nM
Etoposide	200 nM
Ethyl methanesulfonate (EMS)	0.6, 3 mg/mL
N-methyl-D-Aspartate (NMDA)	2 mM
PRIMA-1	1 mM
Taxol	16 μM
Docetaxel	16 μM
Bafilomycin A1	250 nM
Tetracaine	20 μM

To test whether US exposure damages the integrity of viral vectors, adeno-associated virus (provided courtesy of Dr. Athanasios Sambanis, Georgia Institute of Technology, Atlanta, GA) prepared as described previously (Tang and Sambanis 2003), was diluted in DMEM medium supplemented with 2% FBS to a concentration of 1.4×10^6 infectious units per mL.

Rat cortical neurons were freshly harvested from fetal E18 Sasco Sprague-Dawley rats (Charles River Laboratories, Wilmington, MA) with IACUC approval as previously

described (Cullen and LaPlaca 2006) and suspended in Neurobasal medium containing 2% B-27 and 500 μM L-glutamine (Gibco, Invitrogen) at a concentration of 1×10^6 cells/mL.

Sample Analysis

Possible damaging effects of US were assessed by measuring possible reductions in DNA's ability to transfect cells, siRNA's ability to knockdown protein expression, and adeno-associated virus' ability to transduce cells after sonication.

To measure DNA transfection efficiency, DU145 cells were mixed with sonicated pDNA and Lipofectamine 2000 (Invitrogen) according to the procedure recommended by the manufacturer. After incubation in the growth conditions in full culture medium for 24 h, cells were trypsinized, suspended in 300 μL PBS and placed on ice until analysis by FCM. Transfection efficiency was measured by determining the percentage of cells with green fluorescence due to GFP expression greater than untreated control cells.

To measure survivin knockdown, DU145 cells were transfected with sonicated siRNA using Lipofectamine 2000, as described above. After incubation in growth conditions in full culture medium for 48 h, cells were trypsinized, and washed with 500 μL PBS. A FITC-labeled anti-survivin monoclonal antibody (R&D Systems, Minneapolis, MN) was used to label the target protein according to the procedure recommended by the manufacturer. Survivin knockdown efficiency was quantified by measuring the decrease in mean FITC fluorescence by FCM.

To measure adeno-associated virus transduction efficiency, sonicated adeno-associated virus samples were incubated with HT-1080 fibrosarcoma cells (Tang and

Sambanis 2003). Briefly, a 375 μL sample of sonicated adeno-associated virus and 625 μl DMEM medium supplemented with 2% FBS were added to HT-1080 cells previously incubated for 1 day in 6-well plates. After incubation at 37 ℃ for 1 - 2 h, 1 mL pre-warmed DMEM medium supplemented with 18% FBS was added per well. Cells were then incubated and analyzed by FCM, as described above. Transduction efficiency was measured by determining the percentage of cells with green fluorescence due to GFP expression greater than untreated control cells.

The viability of rat cortical neurons immediately after US exposure was measured by determining the percentage of cells lacking red fluorescence due to PI staining compared to untreated control cells, as previously described.

Statistical Analysis

A minimum of three replicates were performed for all the samples. Replicates were used for calculation of experimental means and standard deviations. Paired or unpaired Student's t-test and analysis of variance (ANOVA) was applied to the data. Values of $p < 0.05$ were interpreted as significant.

CHAPTER 4: THE COMPROMISE OF UPTAKE EFFICIENCY AND CELL VIABILITY

Introduction

The first step of successful gene transfection is to get exogenous DNA into the target cells. In other words, to increase transfection efficiency, the uptake efficiency needs to be increased. However, cytotoxicity is found to be related to the uptake efficiency in US-mediated drug/gene delivery. US opens the cell membranes so as to allow drug/gene entry, which is desired, but at the same time it puts cells at risk of death, which is unwanted. Cells close to the location of cavitation are likely destroyed by US exposure, cells at mid-distances from the microbubbles exhibit drug/DNA uptake with the cell membrane temporarily opened and rapidly resealed, and cells far from the cavitation microbubbles remain unaffected (Guzman et al. 2001; Schlicher et al. 2006; Hutcheson et al. 2010). Therefore, higher molecule uptake may be achieved under strong US conditions, but associated with higher cell death rate. To maintain a low death rate under gentle exposure conditions may lead to the uptake efficiency not high enough for applicable drug delivery.

In this study, published cell viability and uptake efficiency data points from various studies using a variety of cell types and tissues, different size of molecules and US apparatus and conditions were combined and replotted as uptake efficiency versus viability (Tata et al. 1997; Miller et al. 1999; Cochran and Prausnitz 2001; Guzman et al. 2001; Keyhani et al. 2001; Guzman et al. 2002; Guzman et al. 2003; Larina et al. 2005; Mehier-Humbert et al. 2005a; Hallow et al. 2006; Hallow et al. 2007; Hutcheson et al.

2010; Karshafian et al. 2010). By investigating these data, we hope to have a better understanding of the compromise between cell viability and uptake efficiency – the heterogeneous bioeffects caused by US exposure.

To carry out this analysis, we first define uptake efficiency as the number of viable cells exhibiting uptake of a marker compound divided by the total number of cells originally in the sample. Because some cells often die during US exposure, the non-viable cells need to be accounted for. Some non-viable cells are present as intact cells that are stained with a marker of non-viability, such as propidium iodide. These non-viable cells are relatively easy to account for. Sometimes, cells can be lysed during US exposures and present as cellular debris. These non-viable cells are more difficult to account for, because each cell can be lysed into a variable number of pieces of debris. As discussed in chapter 3, we have developed a method to account for these cells turned into debris. Other studies have not always accounted for cells reduced to debris and therefore underestimate the total number of cells originally in the sample, which leads to an overestimate of uptake efficiency.

We are interested to compare uptake efficiency to cell viability. The highest possible uptake efficiency is equal to the cell viability, because by definition, only viable cells can be uptake cells. Because high uptake at high viability is desirable, in this chapter we test the hypothesis that high uptake at high viability cannot easily be achieved during US exposure. We test this hypothesis using 590 experimental data points taken from 13 different published studies.

Results

Uptake Efficiency versus Cell Viability

Data from 13 published papers were combined and replotted in Figure 4.1. The diagonal line on the graph corresponds to the maximum uptake efficiency, which equals cell viability. At very low viability, the uptake efficiency is close to this line, which means that the few remaining live cells have molecule uptake. At higher viability, the uptake efficiency generally diverts from the line, which means that although the US exposure did not cause as much cell death, only a portion of live cells had molecule uptake.

Among the 590 data points, there are 38 data points showing relatively high uptake (e.g., > 38%) at high viability (e.g., > 70%). It is therefore our goal to determine why these data points deviate from the rest and under what conditions these desirable delivery levels can be achieved. Several factors may contribute to these outlier results: the molecule size and other properties, the US conditions used, the cell type, the US contrast agent, the sonication temperature and the method of calculating cell viability (i.e., whether it accounted for cell debris generated by lysed cells). The 13 papers where we got these data points from, have covered a variety of cell types and tissues (e.g., DU145 human cells, rat mammary carcinoma cells, porcine carotid artery endothelium), a broad range of molecule size (e.g., calcein with the molecular weight of 623 Da, dextrans with a molecular weight ranging from 10 kDa to 2 MDa) and US conditions (e.g., acoustic energy up to ~ 800 J/cm^2), different US contrast agents (Albunex®, Optison®, Definity® and others) and sonication temperatures (room temperature, 37 ℃) and calculation of cell viability (accounting for cell debris or not) (Table 4.1).

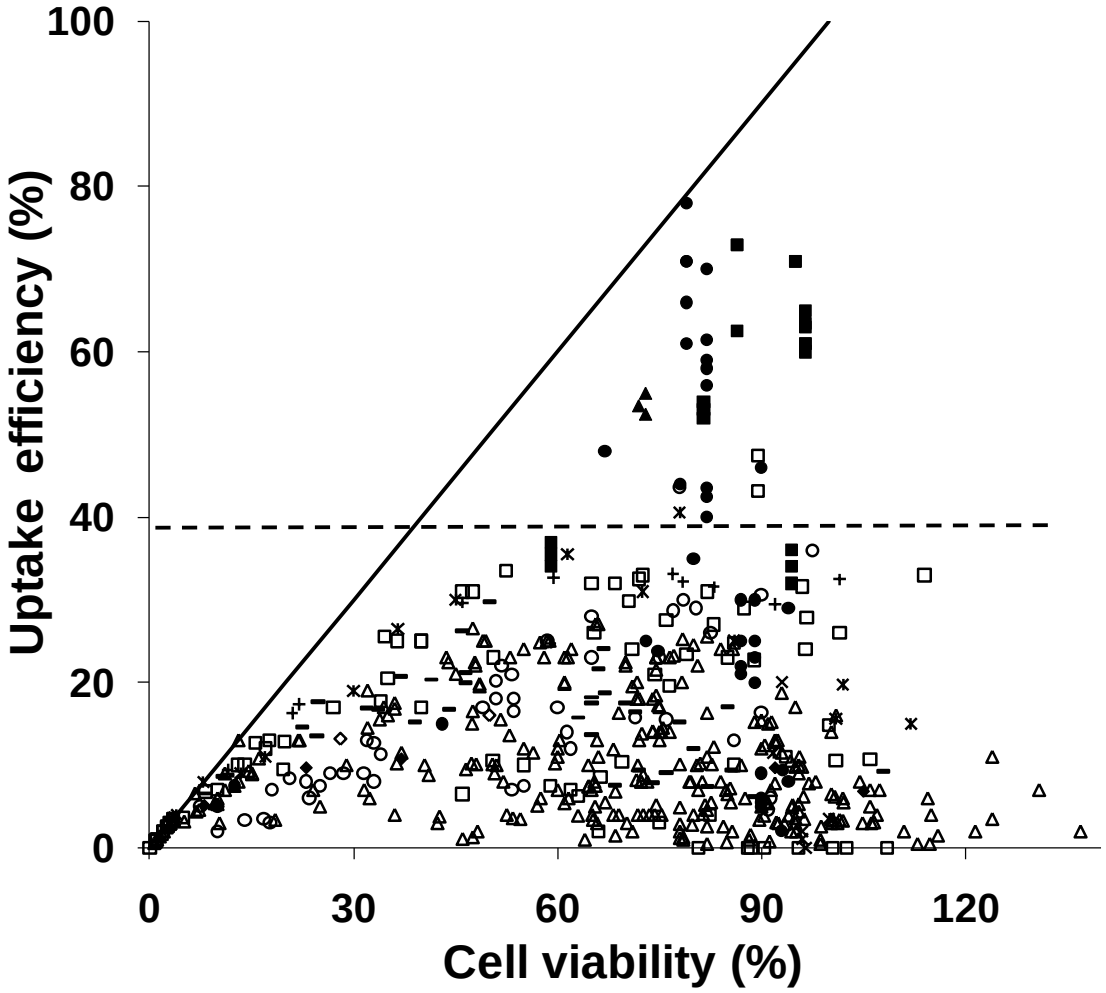

Figure 4.1: The uptake efficiency versus cell viability after US exposure. Data points were from literature: ◆, (Tata et al. 1997); ×, (Miller et al. 1999); □, (Cochran and Prausnitz 2001); +, (Guzman et al. 2001); ∗, (Keyhani et al. 2001); −, (Guzman et al. 2002); ○, (Guzman et al. 2003); ■, (Larina et al. 2005); ▲, (Mehier-Humbert et al. 2005a); △, (Hallow et al. 2006); ◇, (Hutcheson et al. 2010); ●, (Karshafian et al. 2010). Each data point represents the average of n ≥ 3 replicates. The solid line is where uptake efficiency equals cell viability. The dash line is where the uptake efficiency equals 38%.

Table 4.1: Summary of the methods used in the reference studies.

Reference	Cell/tissue type	Uptake molecules (MW)	US frequency	Contrast agent used (concentration)	Sonication temperature	US energies (J/cm^2)	Accounted for cell debris
Karshafian et al. 2010	KHT-C murine fibrosarcoma cells	Dextrans (10 kDa, 70 kDa, 500 kDa, 2 MDa)	500 kHz	Definity® (0.067 - 13.2 vol%), Optison® (0.067 - 13.2 vol%)	37 ℃	1.5 ~ 32	N*
Hutcheson et al. 2010	DU145 human prostate cancer cells	Calcein (623 Da)	24 kHz	None	RT+	8.6, 19.4	Y*
Hallow et al. 2007	Porcine artery (endothelial and smooth muscle cells)	TO-PRO®-1 (645 Da)	1.1 MHz	Optison® (1.7 vol%)	37 ℃	5.0 - 630	Y
Hallow et al. 2006	DU145 human prostate cancer cells, human aoric smooth muscle cells (AoSMC)	Calcein (623 Da)	1.1, 3.1 MHz	Optison® (0.25, 1.7, 14.3 vol%)	RT	0.03 - 405	Y
Mehier-Humbert et al. 2005a	Rat mammary carcinoma cells	Dextrans (77 kDa, 167 kDa, 464 kDa)	1.15 MHz	Fluorocarbon phospholipid-stabilized microbubbles (25 - 30 particles/cell)	37 ℃	27	N
Larina et al. 2005	MCF7 human breast adenocarcinoma, SK-BR-3 breast adenocarcinoma, HepG2 hepatocellular carcinoma, HeLa cervix epithelial adenocarcinoma, A549 lung carcinoma, T84 colorectal carcinoma, KM20 colon carcinoma	Dextrans (10 kDa, 70 kDa, 2 MDa)	3 MHz	Optison® (20 vol%)	37 ℃	180	N
Guzman et al. 2003	DU145 human prostate cancer cells	Calcein (623 Da)	500 kHz	Optison® (0.0056 - 14.4 vol%)	RT	2 - 817	Y
Guzman et al. 2002	DU145 human prostate cancer cells	Dextrans (42 kDa, 464 kDa), BSA (66 kDa), Calcein (623 Da)	500 kHz	Optison® (1.7 vol%)	RT	2 - 817	Y
Keyhani et al. 2001	DU145 human prostate cancer cells	Calcein (623 Da)	24 kHz	None	RT	1 - 114	Y
Guzman et al. 2001	DU145 human prostate cancer cells, aoric smooth muscle cells	Calcein (623 Da)	500 kHz	Optison® (1.7 vol%)	RT	2 - 817	Y
Cochran and Prausnitz 2001	DU145 human prostate cancer cells	Calcein (623 Da)	24 kHz	None	RT	0.003 - 32	Y
Miller et al. 1999	Chinese hamster ovary cells (CHO)	Dextran (850 kDa)	2.25 MHz	Albunex® (0 - 20 vol%)	37 ℃	80	Y
Tata et al. 1997	LnCap and PC-3 human prostate cancer cells	Plasmid DNA (~ 3 MDa)	932.7 kHz	None	37 ℃	7.9	N

+RT = room temperature. *Y = Yes and N = No.

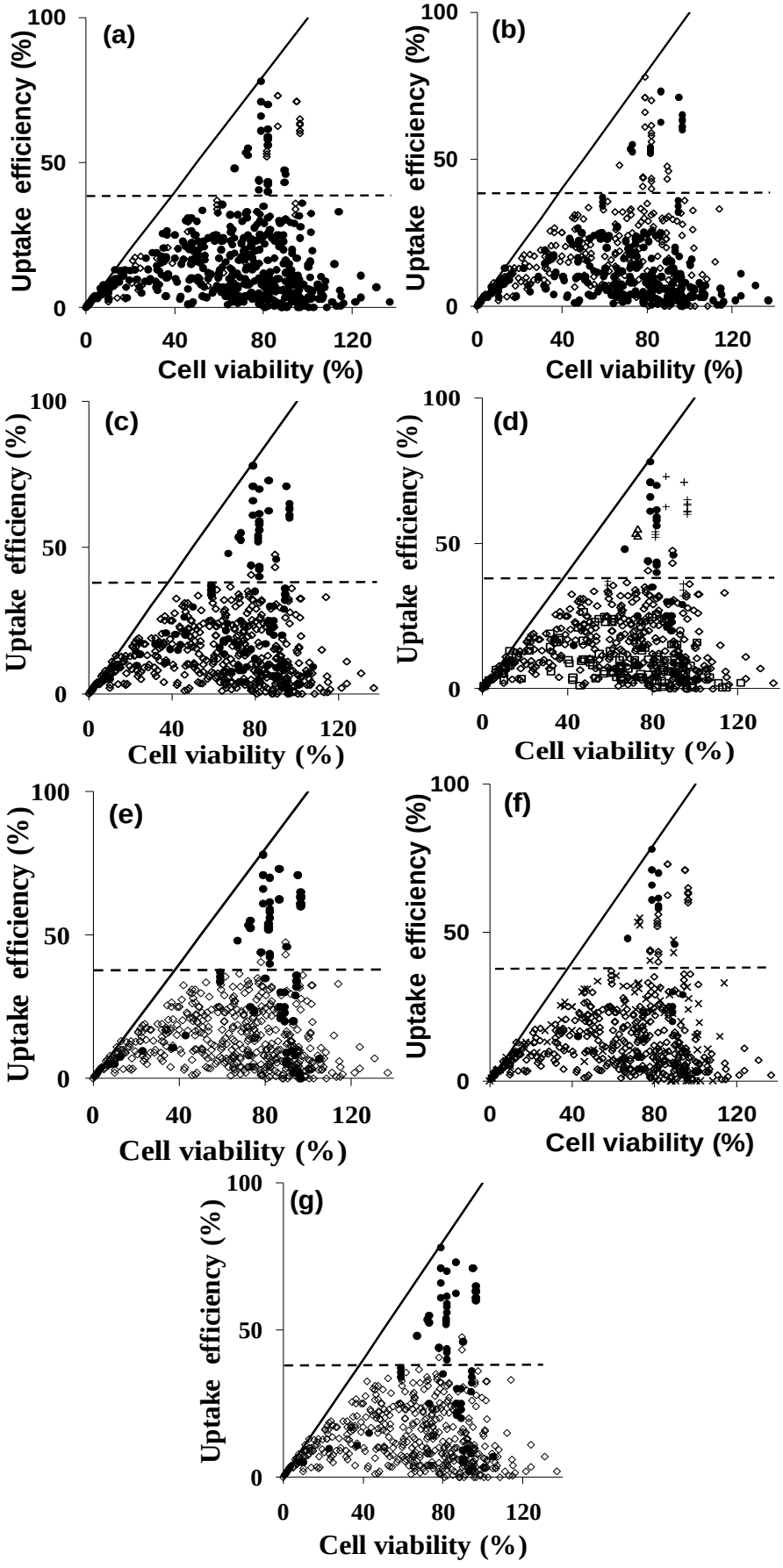
(a)
(b)
(c)
(d)
(e)
(f)
(g)
Uptake efficiency (%)
Cell viability (%)
0
50
100
0
40
80
120

Figure 4.2: The uptake efficiency versus cell viability after US exposure. Data points were from literature (see Figure 4.1). Each data point represents the average of n ≥ 3 replicates. The solid line is where uptake efficiency equals cell viability. The dash line is where the uptake efficiency equals 38%. (a) Data from studies using US energy lower (●) and higher (◇) than 100 J/cm^2. (b) Data from studies using megahertz US (●) and kilohertz US (◇). (c) Data from studies using large molecules (●, MW > 1 kDa, e.g., dextran, BSA and DNA) and small molecules (◇, MW < 1 kDa, e.g., calcein). (d) Data from studies using KHCT cells (●), prostate cancer cells (◇), CHO cells (○), AoSMC cells (□), rat mammary cells (△), *ex vivo* artery (×) and other cell lines (+). (e) Data from studies of US exposure at 37 °C (●) and room temperature (◇). (f) Data from studies using Definity® (●), Optison® (◇) and other contrast agents (×). (g) Data from studies accounting (●) and not accounting (◇) for cell debris in the calculation.

We put these 590 data points in groups according to the methods (e.g., whether or not accounting for cell debris, sonication temperature, US contrast agent, cell/tissue type, uptake molecule, US frequency and energy) used in the studies (Figure 4.2) and did a closer examination of the 38 outlier data (uptake threshold = 38%). To identify which parameters might influence whether a data point falls among the outliers, we looked for situations where one parameter value was much more highly represented among the outlier points. We considered these differences based on two types of analysis: (i) among the 38 outlier data points, we identified the fractions that were in each parameter group (Figure 4.3a) and (ii) among all the data points at each parameter value, we identified the fractions that were in the outlier group (Figure 4.3b).

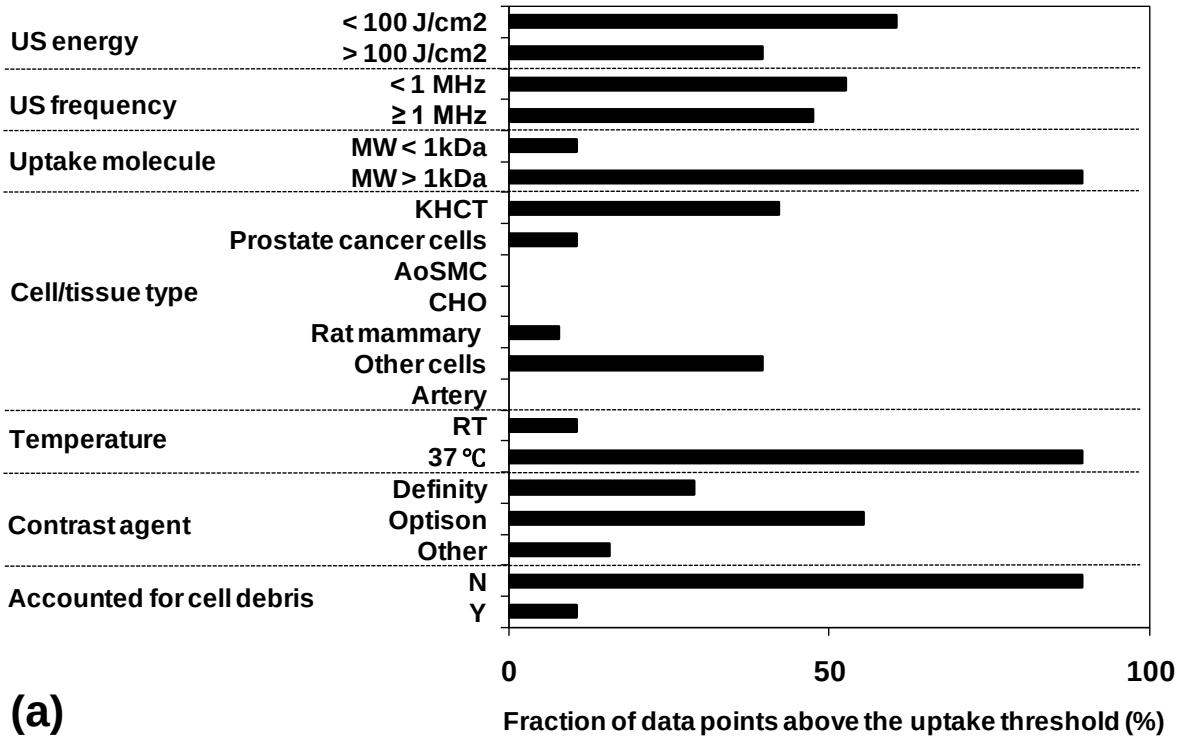

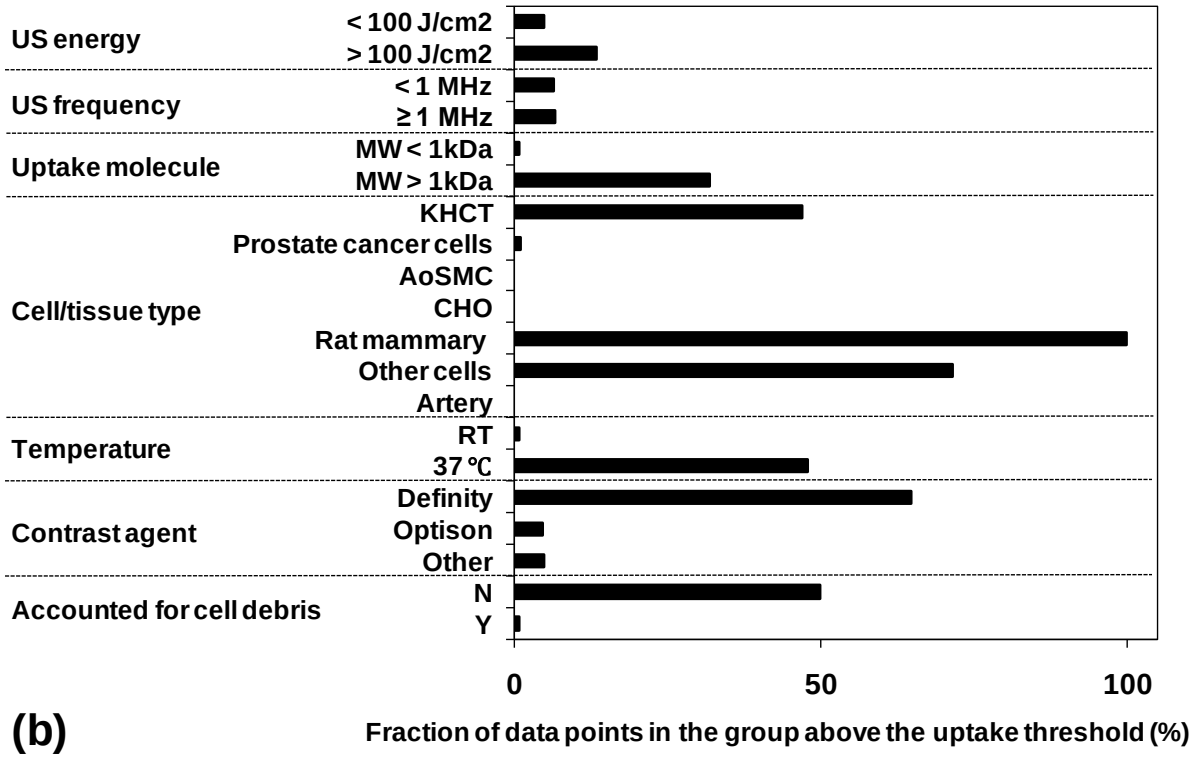

Figure 4.3: (a) The fraction of outlier data points (i.e., with uptake efficiency > 38%) that belong to each group. (b) The fraction of data points in each group that fall above the threshold.

As shown in Figure 4.3, there was no apparent preference for low (< 100 J/cm^2) vs. high (> 100 J/cm^2) acoustic energy or low (< 1 MHz) vs. high (≥ 1 MHz) US frequency. Among the uptake molecules, there was a higher incidence of high (> 1 kDa) vs. low (< 1 kDa) molecular weight compounds. We believe this difference is an artifact of the data set, such that these studies using conditions associated with the outlier data happened to use high molecular weight dextrans. The literature shows that uptake of high molecular weight molecules is not easier or more extensive than low molecular weight molecules (Guzman et al. 2002; Larina et al. 2005; Mehier-Humbert et al. 2005a; Karshafian et al. 2010). Moreover, the inert matter compounds used in these studies are not expected to affect viability. Similarly, the outlier data points were not associated with a particular cell type, although one of the studies generating the outlier data happened to use rat mammary carcinoma cells.

We did, however, notice that the outlier data were associated with sonication at higher temperature of 37 ℃, rather than room temperature. 89% of the 38 outlier data were from the studies of US exposure at 37 ℃ (Figure 4.3a) and 71% of the data from the studies of US exposure at 37 ℃ were above the uptake threshold (Figure 4.3b). Among the 38 outlier data, 30% were from studies using Definity® as a contrast agent and 55% were from studies using Optison® (Figure 4.3a). While 65% of the data from the studies using Definity® were outlier and only 4% of the data from the studies using Optison® were above the uptake threshold (Figure 4.3b). Thus, US contrast agents may also contribute to the higher uptake efficiency. Finally, we noticed that whether accounting for cell debris in the calculation of cell viability made a big difference.

Among the 38 outlier data, 90% did not account for cell debris (Figure 4.3a) and 50% of data that did not account for cell debris were outlier, while only 0.7% of the data that accounted for cell debris were above the uptake threshold (Figure 4.3b). In the following section we analyze the effects of these three features of the outlier cells.

The Influence of Temperature and US Contrast Agents

To test the effect of sonication temperature and the type of contrast agent on uptake efficiency, we conducted US exposure using DU145 cells as target cells and FITC-dextran (70 kDa) as the uptake marker compound with 1 MHz US. As shown in Figure 4.4, US exposure at the temperature of 37 ℃ resulted in higher uptake efficiency in the presence of Definity® (but not Optison®). Definity® led to higher uptake efficiency compared to Optison® at both temperatures. Under all these four sonication conditions, similar cell viability (~ 55%, $p > 0.05$) was achieved.

Figure 4.4 shows that increasing temperature to 37 ℃ in the presence of Definity® increased uptake efficiency by 51±34% relative to cells sonicated at room temperature. Changing temperature in the presence of Optison® did not have a significant effect on uptake efficiency. It is worth noting that 30% of the 38 outlier data points were from the studies of US exposure at 37 ℃ in the presence of Definity®. Thus, it is possible that if the data points generated at room temperature that show lower uptake had instead been taken at 37 ℃, they would have had higher uptake efficiency. This is in agreement with previous studies that showed enhanced delivery at elevated temperature (Kim et al. 1996; Poling et al. 2001; Nozaki et al. 2003; Zarnitsyn and Prausnitz 2004).

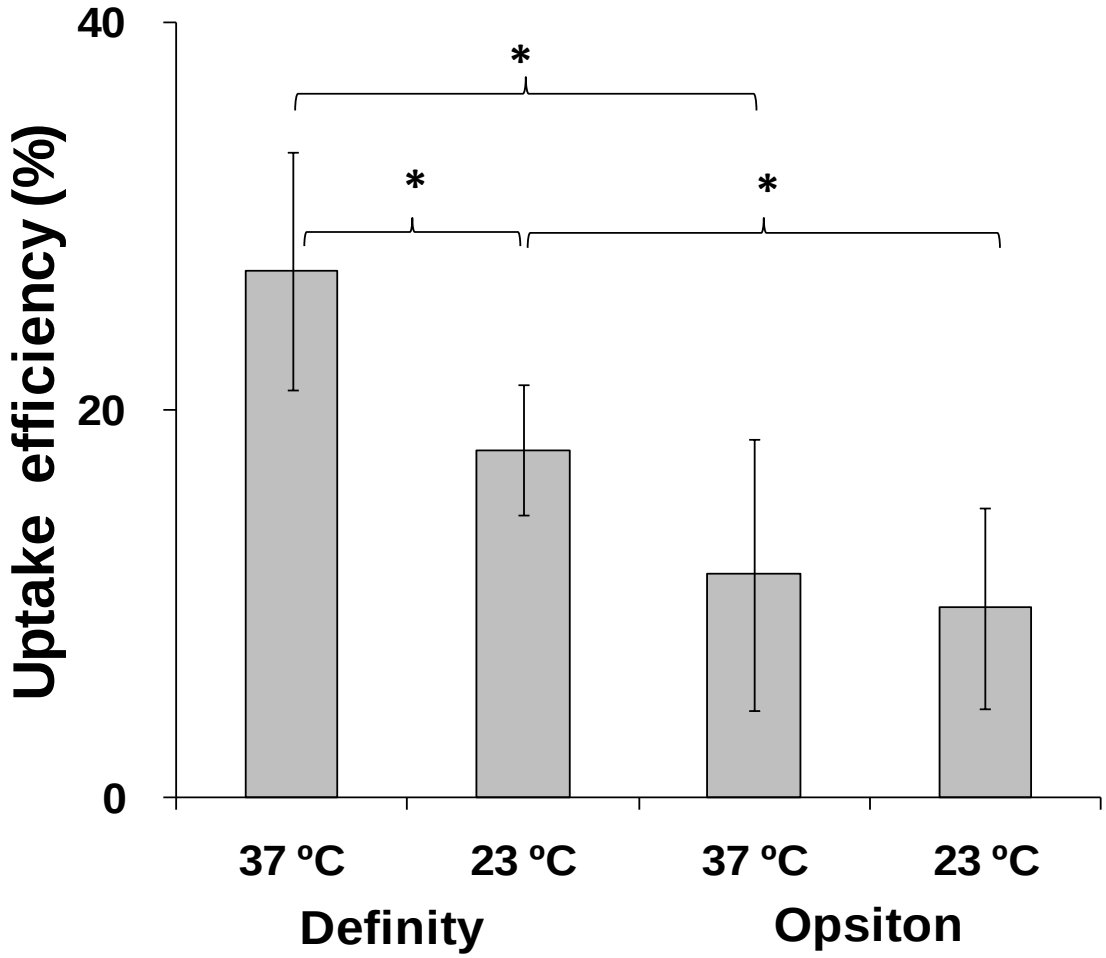

Figure 4.4: The overall uptake efficiency among DU145 cells after US exposure at 23 ℃ or 37 ℃ with 0.1 vol% Definity® or 2 vol% Optison® (*p < 0.05, n = 3 replicates, data points show average ± SD). US pressure: 0.39 MPa, duty cycle: 25%, total treatment time: 1 s.

Figure 4.4 also shows that 0.1% Definity® led to 83% – 136% greater uptake efficiency than 2% Optison® depending on the temperature. These concentrations were selected to get an equal bubble concentration (~ 1.2×10^7 bubbles/mL), because the native microbubble concentration in Definity® is 20-fold higher than that in Optison® (Karshafian et al. 2010). And these concentrations were in the range of what the reference studies used. Among the data from the studies using Optison® (the concentration range:

0.067 - 20 vol%), 75% were using the concentration of ~ 2% (0.67 – 3.3 vol%). Among the data from the studies using Definity® (the concentration range: 0.067 – 13.2 vol%), 12% were using the concentration of ~ 0.1% (0.067 – 0.67 vol%). It is possible that if the data points generated using 2% Optison® that show lower uptake had instead been taken using 0.1% Definity®, they would have had higher uptake efficiency. It is also expected that we may get higher uptake efficiency if higher Definity® concentration is used, as shown previously (Moran et al. 2002; Li et al. 2004; Miller and Dou 2004b; Koike et al. 2005; Rahim et al. 2006; Karshafian et al. 2010; King et al. 2010).

A different temperature or US contrast agent may improve the molecule uptake without affecting cell viability, but these may not be the only two factors. Therefore we finally looked into the issue of cell debris in the calculation of uptake efficiency and cell viability.

Accounting for Cell Debris in the Calculation of Uptake Efficiency and Viability

As shown in Figure 4.3, whether or not accounting for cell debris in the calculation of cell viability made a big difference. If cells reduced to debris are not accounted for, then uptake efficiency and cell viability can both be increased (i.e., the denominator would be smaller in the calculation of percent cells with uptake and viability), which would significantly affect our analysis. Although we do not have access to the original data and it would be very difficult to account for cell debris after the fact in those studies with high uptake at high viability, we do have access to the original data for some of the data points that were generated by accounting for cell debris, and can work backwards to find out what the uptake efficiency and cell viability would be if cell debris had not been accounted for.

Using this approach, we replotted 280 data points from a large study using DU145 cells and calcein with 1.1 and 3.1 MHz US in Figure 4.5a (Hallow et al. 2006). In this figure, the same 280 experimental data points were each plotted twice in two different formats: accounting and not accounting for cell debris in the calculation. Accounting for the debris, the cell viability is $\frac{N_1/T_s}{N_0/T_0}$ (see Chapter 3). Not accounting for cell debris, the viability is N_1/N_s. This analysis shows that not accounting for cell debris in the cell viability calculation has a significant effect. If these data are presented without accounting for cell debris, many of the data points are in the region of high uptake at high viability. If presented with accounting for cell debris, then the data points are all below 38%, the uptake efficiency threshold (Figure 4.5a).

We next calculated the difference in uptake efficiency and cell viability for each of the pairs of data points with and without accounting for cell debris and present them in Figure 4.5b and 4.5c. These graphs show that both uptake efficiency and cell viability can be increased by tens of percent if cell debris is not accounted for. In addition, the degree of deviation increases with increasing energy for both uptake efficiency and cell viability (ANOVA, $p < 0.01$). Although the data are not shown graphically, the absolute value for uptake efficiency (calculated without accounting for cell debris) also increases with increasing energy (ANOVA, $p < 0.05$), which means that the greatest deviations are seen at the conditions with the highest uptake efficiency.

(a)

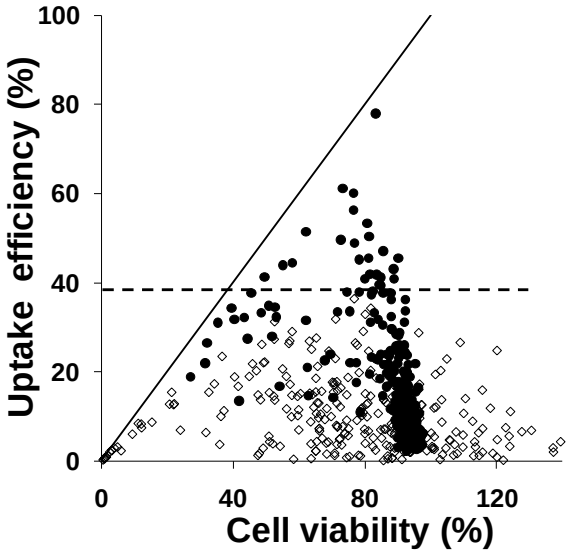
Uptake efficiency (%)
100
80
60
40
20
0
0
40
80
120
Cell viability (%)

(b)

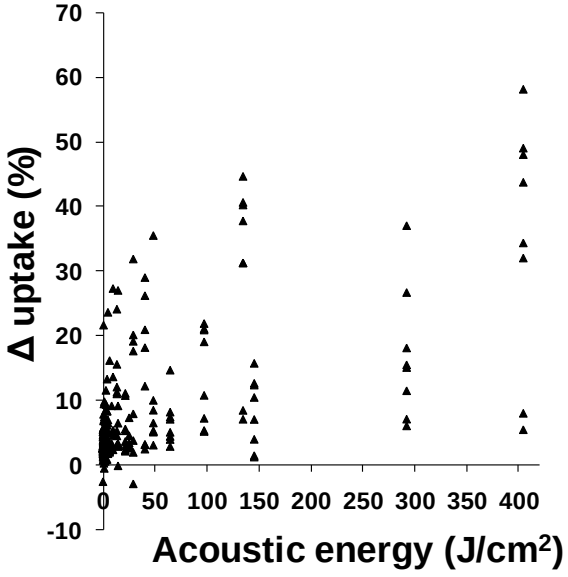
Δ uptake (%)
70
60
50
40
30
20
10
0
-10
0
50
100
150
200
250
300
350
400
Acoustic energy (J/cm²)

(c)

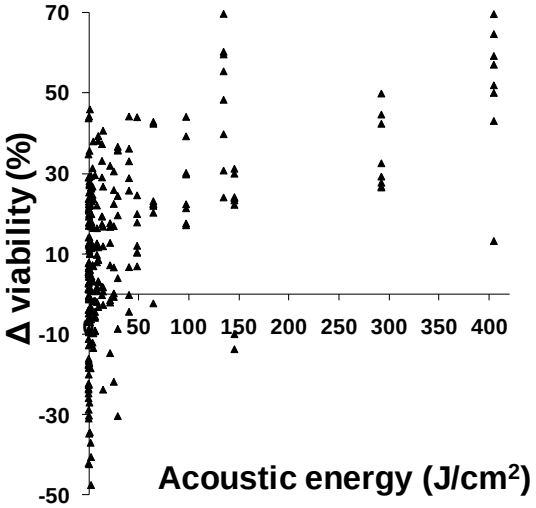
Δ viability (%)
70
50
30
10
-10
-30
-50
50
100
150
200
250
300
350
400
Acoustic energy (J/cm²)

Figure 4.5: (a) The uptake efficiency versus cell viability after US exposure. White diamonds represent data in the calculation accounting for cell debris caused by US exposure. Black circles represent the same experimental data but in the calculation not accounting for cell debris. Each data point represents the average of $n \geq 3$ replicates. The solid line is where uptake efficiency equals cell viability. The dash line is where uptake efficiency equals 38%. (b, c) The differences between the two ways in calculating uptake efficiency and cell viability over a range of acoustic energy intensities. (b) Δuptake and (c) Δviability were calculated by subtracting the data in the calculation accounting for cell debris from that in the calculation not accounting for cell debris.

Discussion

Various US apparatus systems have been designed and a variety of US exposure conditions (e.g., frequency, energy intensity, pulse length, acoustic pressure) were tested on different types of cells and tissues both *in vitro* and *in vivo* to facilitate drug/gene delivery (Mitragotri 2005). Although the bioeffects caused by US exposure was found to differ due to the US conditions and cell/tissue types, nearly all the studies reported the heterogeneous bioeffects. It is difficult to achieve both high viability and high uptake efficiency or transfection efficiency.

US temporarily opens cell membranes and allows molecules to diffuse into cells. The diffusion may be enhanced by increasing temperature (Kim et al. 1996; Poling et al. 2001; Nozaki et al. 2003; Zarnitsyn and Prausnitz 2004). In this study, US exposure at 37 ℃ increased uptake efficiency without decreasing the cell viability compared to sonication at RT. Similar results were found in some previous drug/gene delivery studies using US exposure (Kim et al. 1996; Nozaki et al. 2003; Zarnitsyn and Prausnitz 2004) and other delivery systems (Croaker et al. 1990; Fregeau and Bleackley 1991; Rols et al. 1994).

The bioeffects mediated by US may be dependent on the US contrast agent (Moran et al. 2000; Chen et al. 2002; Moran et al. 2002; Sonne et al. 2003; Li et al. 2004; Miller and Dou 2004b; Koike et al. 2005; Rahim et al. 2006; McDannold et al. 2007; Karshafian et al. 2010; King et al. 2010). Definity® and Optison® were tested in this study at a concentration of 0.1 and 2 vol%, separately. This comparison of contrast agents is complicated because the concentrations were not the same. In terms of bubble concentration, 2% Optison® corresponds to ~ 1.2×10^7 bubbles/mL and 0.1% Definity® corresponds to ~ 1.2×10^7 bubbles/mL. In terms of volume fraction of bubbles, 2% Optison® corresponds to 0.04 vol% gas and 0.1% Definity® corresponds to 0.005 vol% gas. Under the same US conditions, Definity® showed higher uptake efficiency, which is consistent with some previous studies (Moran et al. 2000; Li et al. 2004; Miller and Dou 2004b; King et al. 2010). It is also expected that higher uptake efficiency may be reached if higher Definity® concentration is used, as shown previously (Koike et al. 2005; Rahim et al. 2006; Karshafian et al. 2010).

US generates heterogeneous bioeffects among sonicated cells, including (i) viable cells that appear unaffected, (ii) viable cells reversibly permeabilized, as evidenced by intracellular uptake of molecules, (iii) cells that appear to be viable shortly after sonication, but later undergo apoptosis and die, and (iv) nonviable cells during sonication, as shown by an irreversible loss of the plasma membrane barrier or lysis of the cell into debris (Hutcheson et al. 2010). Quantification of cells lysed into debris was difficult, because a single lysed cell produced multiple debris events. By investigating the methods in related literature, we found whether or not accounting for cell debris in the calculation of uptake efficiency and viability made a significant difference. Without accounting for

the debris from lysed cells, the uptake efficiency and viability were calculated as those among the intact cells, while cells that were destroyed by US were omitted. Therefore, the uptake efficiency in live cells seems high, but the overall, actual uptake efficiency may be much lower (Figure 4.5). As shown in Figure 4.2g and 4.3, 90% of the 38 outlier data points did not account for cell debris and 50% of data points that did not account for cell debris were among the outliers, while only 0.7% of the data that accounted for cell debris were among the outliers. Among the data points in Figure 4.5, up to 90% of cells could be turned into debris by US, depending on the conditions used. Therefore, not accounting for cell debris in the calculation could not completely reflect the bioeffects caused by US exposure.

This is more significant under strong US conditions when more cell debris is possibly generated ($N_s < N_0$ and $T_s > T_0$) (Figure 4.5). Under gentle US conditions when most cells remain intact, $N_s \approx N_0$ and $T_s \approx T_0$. Therefore, the cell viability is $\frac{N_1/T_s}{N_0/T_0} \approx N_1/N_s$, and accounting for cell debris in the calculation of viability may cause some noise (Figure 4.5c) due to the measurement of three more numbers, N_0, T_0 and T_s. Since the overall uptake efficiency is the uptake efficiency of live cells multiplied by the overall viability, not accounting for debris also affects the calculation of uptake efficiency by making it higher.

To summarize, after investigating the quantitative bioeffects caused by US exposure in the previous studies, we found regardless the cell types, US conditions, sonication temperature or US contrast agents, the bioeffects of US exposure are heterogeneous, which means it is difficult to achieve high uptake efficiency and low

cytotoxity at the same time. To reflect the actual bioeffects, the results of uptake and viability should be reported with the cell debris taken into consideration.

CHAPTER 5: THE OPTIMIZATION OF US CONDITIONS FOR GENE TRANSFECTION

Introduction

Because US-mediated drug/gene delivery caused heterogeneous bioeffects, to increase the overall gene transfection efficiency, it is a challenge to find an optimal US condition that compromises the viability and transfection efficiency. In this study, DU145 cells were exposed with 1 MHz US for gene transfection. US exposure conditions were optimized by testing these parameters: acoustic pressure and energy intensity, US pulse length and duty cycle, US contrast agent and the osmotic condition. We expected to find an US condition that maintains low death rate (~ 80% cell viability) and at the same time achieves a transfection efficiency as high as possible.

Results

US Pressure and Energy Intensity

Three acoustic pressures were tested with different total treatment time, which gave three acoustic energy intensities at each pressure: 200, 306 and 400 J/cm^2 (Figure 5.1). The transfection efficiency in live cells increased and cell viability decreased with the increase of US pressure (two-way ANOVA, $p < 0.05$). US exposure at 0.78 MPa for 1 min (the energy intensity of 306 J/cm^2) showed the highest transfection efficiency (~ 21%) in all the cells with the average cell viability of 84%.

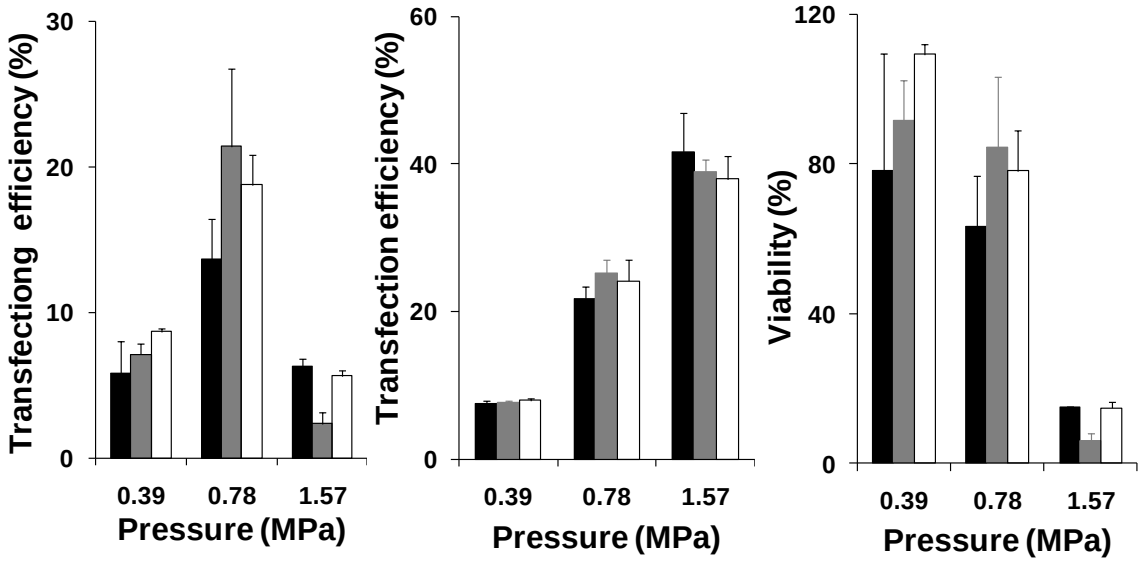

(a) **(b)** **(c)**

Figure 5.1: Transfection efficiency among all the cells (a) and live cells (b) and the cell viability (c) at 8 h after US exposure at different acoustic pressures and energy intensities (n ≥ 3 replicates, data points show average ± SD) with a pulse length of 0.25 ms, duty cycle of 25% and Definity® concentration of 2 vol%. Black bar: acoustic energy of 200 J/cm^2. Grey bar: acoustic energy of 306 J/cm^2. White bar: acoustic energy of 400 J/cm^2.

Pulse Length

The pulse length or pulse repetition frequency was previously found to affect cell viability and transfection efficiency (Tata et al. 1997; Huber et al. 1999). In our study, the transfection efficiency in live cells increased and cell viability decreased with the increase of pulse length (one-way ANOVA, $p < 0.01$). US exposure at the pulse length of 0.25 ms showed an average cell viability of 75% with the average transfection efficiency of 6% among all the cells at the energy intensity of 102 J/cm^2 (Figure 5.2).

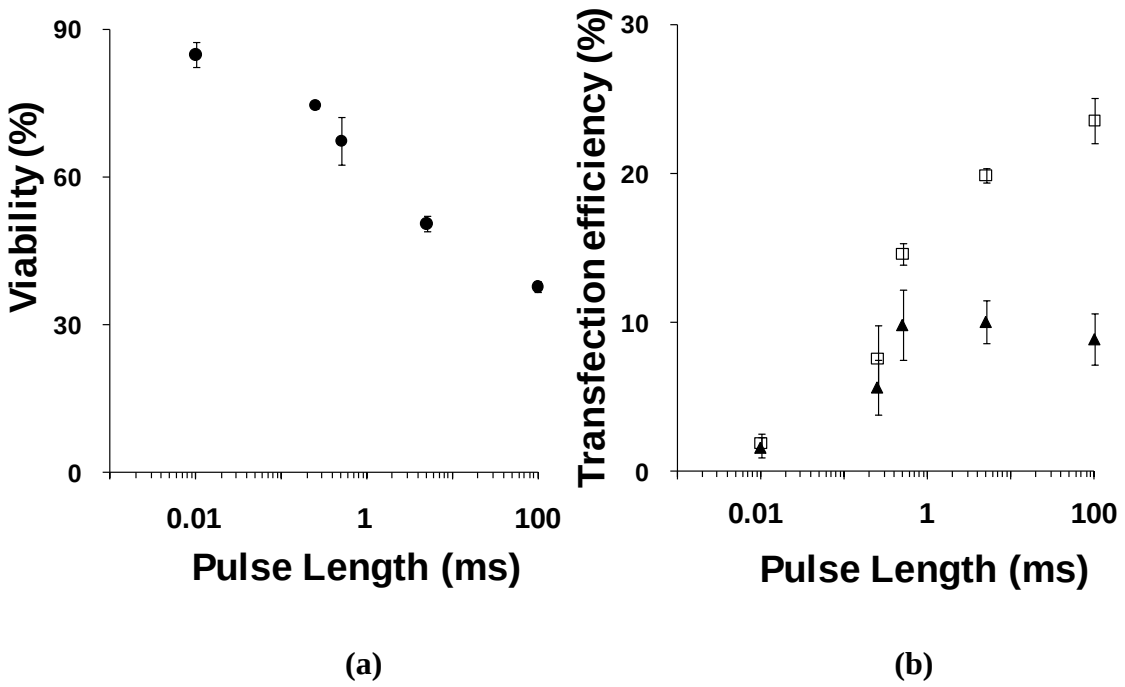

(a) **(b)**

Figure 5.2: Cell viability (a) and transfection efficiency (b) at 8 h after US exposure at different pulse length (n ≥ 3 replicates, data points show average ± SD) with the acoustic pressure of 0.78 MPa, energy intensity of 102 J/cm^2, duty cycle of 4%, total treatment time of 125 s and the Definity® concentration of 2 vol%. Rectangle: transfection efficiency in live cells. Triangle: transfection efficiency in all the cells.

Duty Cycle

We tested the influence of duty cycle at the pulse length of 0.25 ms and 0.5 ms (Figure 5.3). Overall, the bioeffects at different duty cycles were significant (one-way ANOVA, $p < 0.01$), which is consistent with some previous studies (Larina et al. 2005; Pan et al. 2005). US exposure at the duty cycle of 25% showed comparatively both high viability and high transfection efficiency.

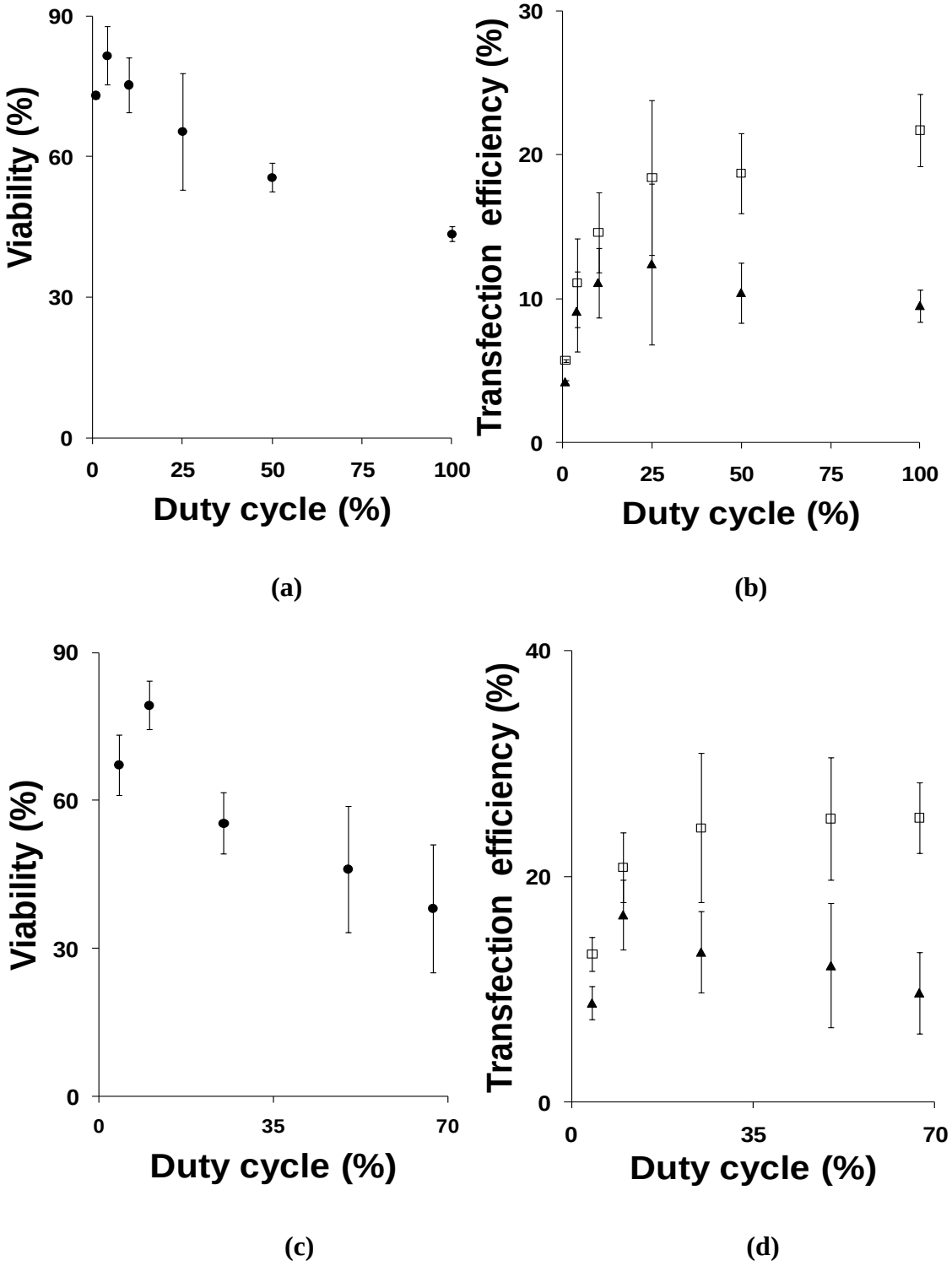

Figure 5.3: Cell viability (a, c) and transfection efficiency (b, d) at 8 h after US exposure at different duty cycle (n ≥ 3 replicates, data points show average ± SD) with the acoustic pressure of 0.783 MPa, energy intensity of 102 J/cm^2, pulse length of 0.25 (a, b) or 0.5 (c, d) ms, and the Definity® concentration of 2 vol%. Rectangle: transfection efficiency in live cells. Triangle: transfection efficiency in all the cells.

US Contrast Agent

The concentration of US contrast agent affects microbubble-cell spacing and therefore has been shown to affect the bioeffects caused by US exposure (Guzman et al. 2003; Ohl et al. 2006; Miller et al. 2008). With the increase of Definity® concentration, cell viability decreased and the transfection efficiency in live cells increased reaching a maximum, beyond which it decreased (one-way ANOVA, $p < 0.01$). Similar results were found in other studies of US-mediated drug delivery (Karshafian et al. 2010). At the concentrations we tested, adding 2 vol% of Definity® to the sonication samples showed an average cell viability of 77% with the average transfection efficiency of 18% among all the cells (Figure 5.4).

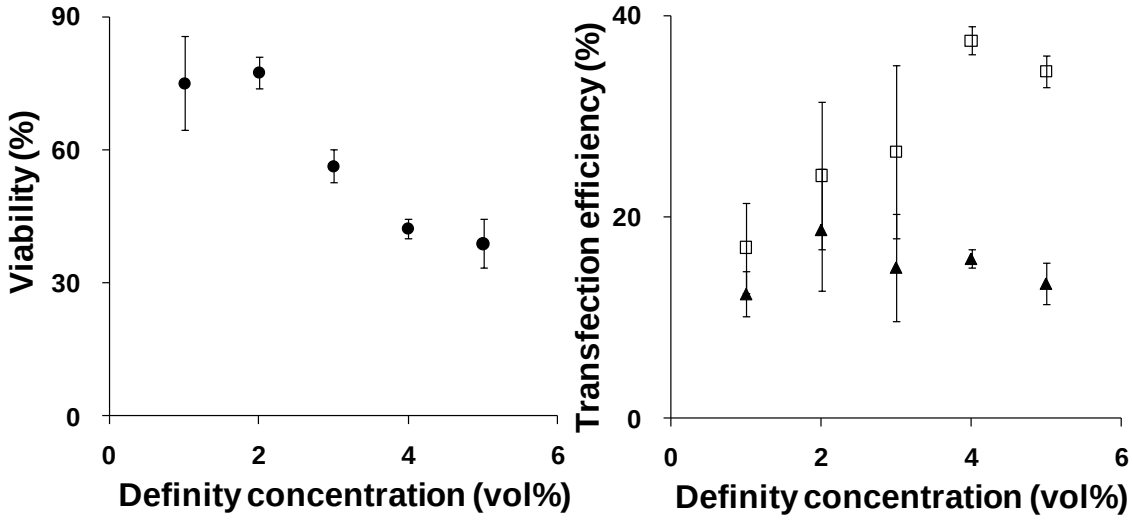

(a) **(b)**

Figure 5.4: Cell viability (a) and transfection efficiency (b) at 8 h after US exposure at different Definity® concentration (n ≥ 3 replicates, data points show average ± SD) with the acoustic pressure of 0.783 MPa, energy intensity of 306 J/cm^2, duty cycle of 25%, total treatment time of 1 min and the pulse length of 0.25 ms.

Rectangle: transfection efficiency in live cells. Triangle: transfection efficiency in all the cells.

Osmotic Conditions

The osmotic pressure of the external aqueous medium may cause cells to swell and make the cell membranes more permeable for drug/gene delivery. The microbubble-cell spacing may be changed to make cells easier to be targeted by US. The osmotically driven convective flow may also facilitate drug/gene delivery. As a result shown in Figure 5.5, transfection efficiency was increased when cells were suspended in a low osmotic strength buffer of RPMI mixed with water at a RPMI:water volume ratio of 3:1, compared to cells sonicated in pure RPMI medium.

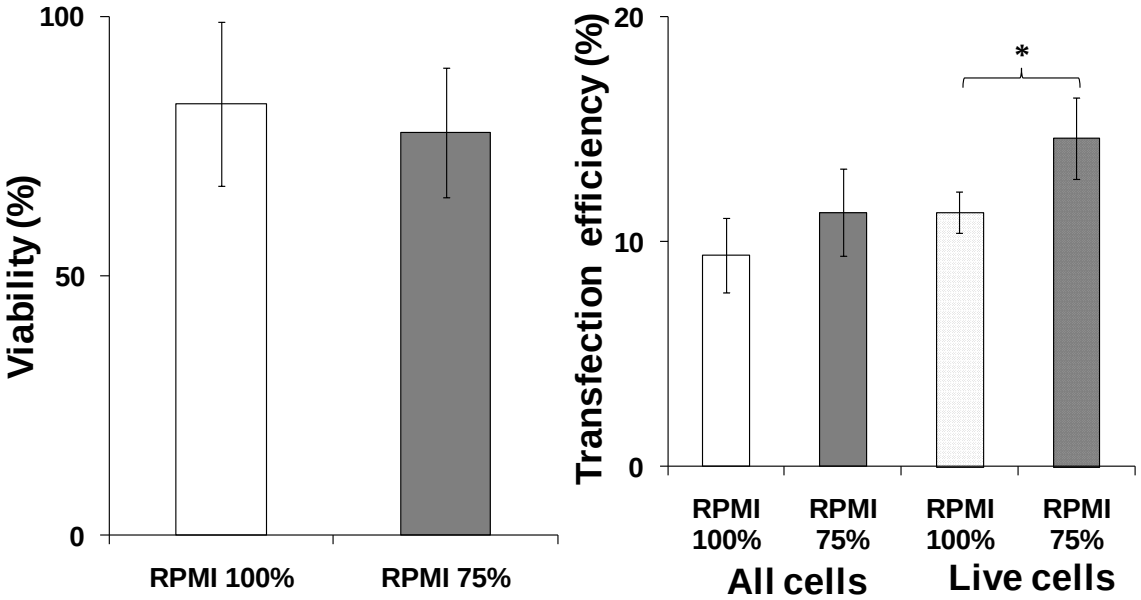

(a) **(b)**

Figure 5.5: Cell viability (a) and transfection efficiency (b) under different osmotic conditions. The volume ratio of water over RPMI medium is 0 to 1 or 1 to 3. ($n \geq 3$ replicates, data points show average ± SD). US conditions: acoustic pressure of 0.783

MPa, total treatment time of 1 min, energy intensity of 306 J/cm^2, duty cycle of 25%, the pulse length of 0.25 ms and the Definity® concentration of 1 vol%.

Discussion

To find an optimal US condition for gene transfection, we measured the cell viability and transfection efficiency at different acoustic pressures, energy intensities, pulse lengths, duty cycles, the concentrations of Definity® US contrast agent, and the osmotic conditions of the extracellular medium.

The bioeffects caused by US was previously found to be related to the acoustic energy intensity, but at higher energy intensities (i.e., > 100 J/cm^2) where the US exposure was well above the cavitation threshold, this dependence was not that significant (Guzman et al. 2001; Zarnitsyn and Prausnitz 2004). Our data showed the US pressure had a strong impact on gene transfection and cell viability. Pulse length affects the threshold for gas fragmentation and inertial cavitation nucleation caused by US (Atchley et al. 1988; Chen et al. 2003c; Miller and Dou 2004a). In a pulse length long enough, additional microbubbles may be activated due to the fragmentation of mother bubbles into daughter microbubbles and therefore a cascade of cavitation may be generated (Chen et al. 2003c).

Under the same acoustic energy intensity, the bioeffects mediated by US exposure were found to increase with the increasing pulse length (Kober et al. 1989; Brayman and Miller 1999; Huber et al. 1999; Chen et al. 2003b; Chen et al. 2003c; Tu et al. 2006). We got comparatively higher viability and transfection efficiency in all the cells at the pulse length of 0.25 ms and 0.5 ms. Changing duty cycle did not affect the bioeffects mediated by US. However, longer duty cycle may lead to the increase of temperature. We

measured the temperatures of sonication samples before and immediately after US exposure. The changes of temperature in the sonication samples were less than 1 ℃ at most duty cycles tested, except the duty cycle of 100% when continuous US was applied, rather than pulsed US, and a temperature rise of 1.2 ℃ was measured. The transfection efficiency was increased by changing the osmotic pressure of the extracellular medium. However, to better mimic the *in vivo* conditions, we choose to use pure RPMI as the medium for cell samples.

Based on these data, the following parameters were chosen for a typical US condition to facilitate gene transfection in DU145 cells *in vitro*.

- Frequency: 1 MHz
- Peak-to-peak pressure: 0.78 MPa,
- Duty cycle: 25%,
- Pulse length: 0.25 ms,
- Total treatment time: 1 min,
- Acoustic energy intensity: 306 J/cm^2,
- Definity® concentration: 1 ~ 2 vol%.

CHAPTER 6: DNA TRAFFICKING AND LOCALIZATION

Introduction

DNA entry to the cells is only the first step for gene transfection. The exogenous DNA has to traverse the cytoplasm and enter the nucleus prior to transcription and translation. This process needs to be quick since nucleases in the cytoplasm start to degrade exogenous DNA in minutes (Lechardeur et al. 1999; Pollard et al. 2001). However, the passive diffusion of plasmid DNA in the cytoplasm is generally very slow, especially for DNA molecules lager than 1000 base pair (660 kDa), because the multiple cytoskeletal elements (e.g., microfilaments, microtubules and intermediated filaments) in the cytoplasm form a complex and crowded latticework that significantly impedes the diffusion of large molecules (Lukacs et al. 2000). It has been shown in non-viral gene transfection that a certain amount of plasmid DNA stays in the cytoplasm after entering the cell, which is considered as one of the reasons for low transfection efficiency by non-viral gene delivery methods (Vaughan et al. 2006). Therefore, it is important to better understand DNA trafficking in cytoplasm to enhance gene transfection.

Current studies on DNA trafficking are mainly focused on chemical gene delivery systems (Colin et al. 2000; Fisher et al. 2000; Tachibana et al. 2002; Akita et al. 2004), where multiple trafficking steps are required, such as cell attachment, endocytosis and entrapment into endocytic vesicles, maturation of endosomes into lysosomes, escape from vesicular compartments, migration toward the nucleus periphery, dissociation between carriers and foreign DNA, and finally entry of DNA into the nucleus. There are fewer reports of DNA trafficking studies using physical delivery systems such as US

(Duvshani-Eshet et al. 2006) , electroporation (Golzio et al. 2002) and microinjection (Wilson et al. 1999; Vaughan et al. 2008). US-mediated gene transfection temporarily opens cell membranes and does not require endocytosis to allow pDNA entry. US was found to deliver pDNA to the periphery of cell nucleus and facilitate rapid transfection, possibly due to the alteration of cytoskeleton (Skorpikova et al. 2001; Raz et al. 2005), although this only happened to a small fraction of cells.

In this study, we use both flow cytometry and confocal microscopy to analyze the localization of pDNA in cell cytoplasm and nuclei post US exposure both qualitatively and quantitatively. We hypothesize that DNA introduced into the cytoplasm during sonication is either transported into the nucleus within hours or removed by autophagosomes/autophagolysosomes. DNA that reaches and remains in the nucleus is efficiently transcribed and translated to produce its expression product. We expect to have a better understanding of the kinetics of pDNA uptake, gene expression, pDNA colocalization in the cell nuclei and other organelles in the cytoplasm.

Results

Heterogeneous Bioeffects Caused by US Exposure

We first looked at the heterogeneous bioeffects among viable cells after 8-h incubation post US exposure. Three kinds of viable cells were observed under confocal microscope (Figure 6.1): cells with pDNA uptake (cells with red fluorescence), cells with GFP transfection (cells with green fluorescence) and cells with neither of these bioeffects. To achieve successful gene transfection, it is necessary to get DNA into the

cell nuclei. We further evaluated the capability of US to deliver DNA to the nuclei by confocal microscopy and colocalization analysis.

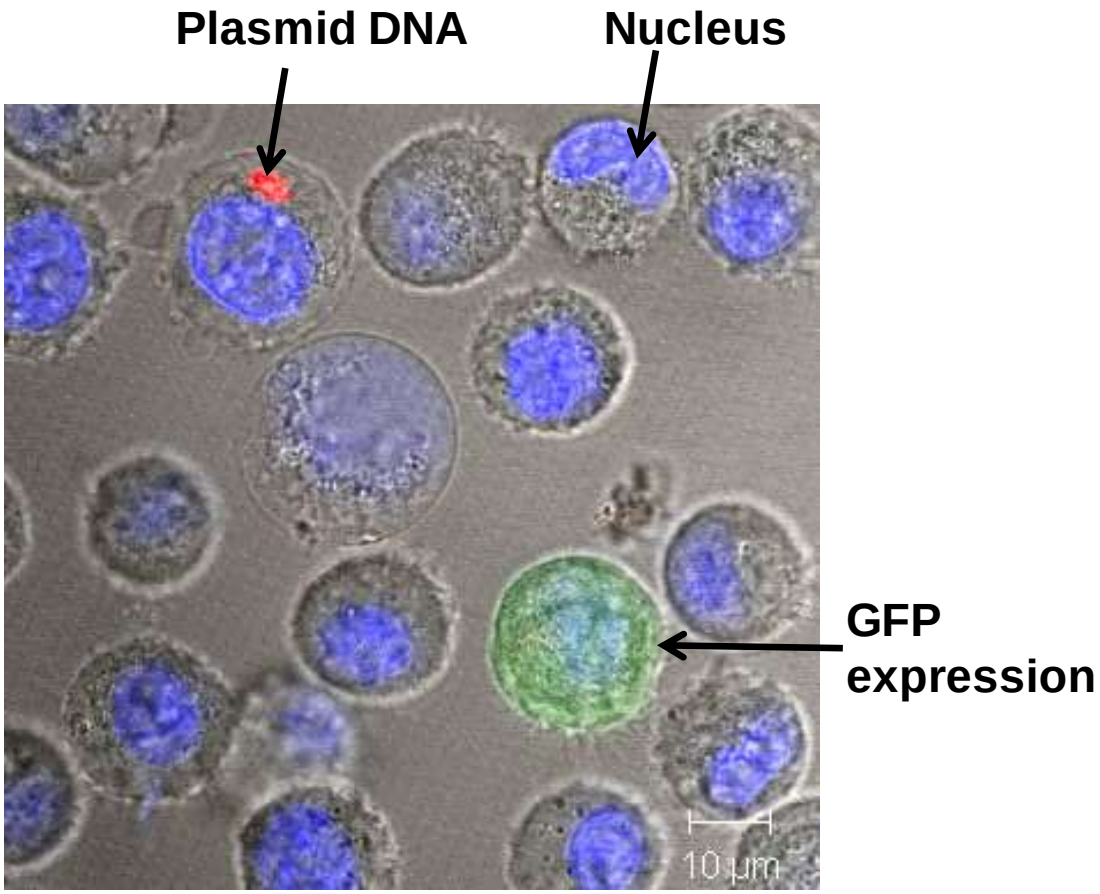

Figure 6.1: Confocal micrograph showing Cy3-labeled pDNA uptake (red) and GFP expression (green). Cells were harvested after incubation for 8 h post US exposure and stained with a nuclear counterstain, trihydrochloride (blue). US exposure conditions: pressure amplitude of 0.78 MPa, total treatment time of 1 min with a pulse length of 0.25 ms at a duty cycle of 25%, Definity® concentration of 1 vol%.

Colocalization of pDNA with Nuclei post US Exposure

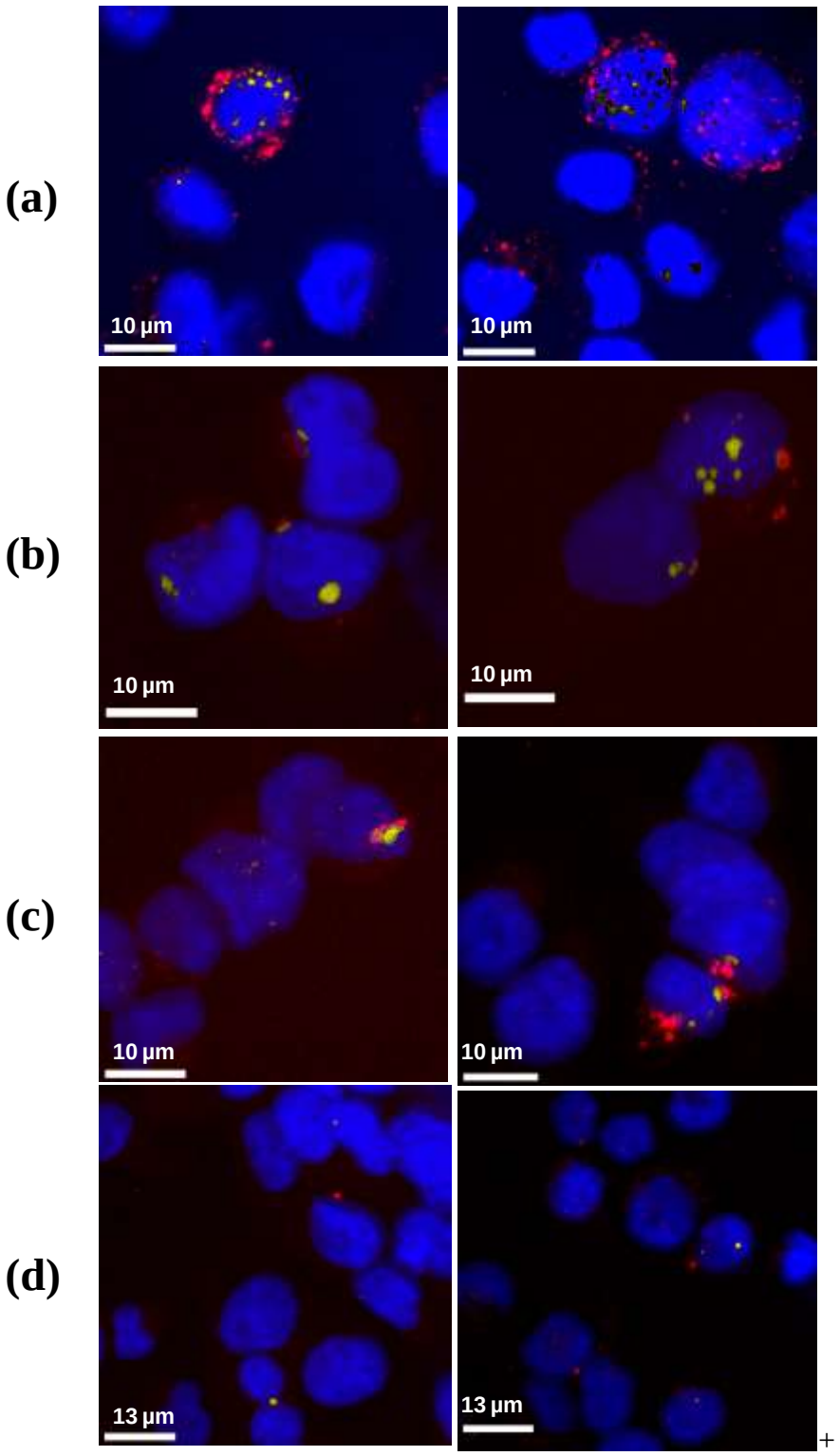

Figure 6.2: Representative microscopy images (two images at each time point) of Cy3-labled pDNA and cell nuclei at 30 min (a), 8 h (b), 16 h (c) and 24 h (d) post US

exposure. The red color indicates pDNA. The blue color indicates cell nuclei. The yellow pseudo-color indicates colocalization.

Representative microscopy images showed the colocalization of pDNA with the cell nuclei immediately after US exposure (Figure 6.2a), which indicated US could deliver pDNA to the nuclei to facilitate rapid gene transfection. The colocalization of pDNA and nuclei was observed from 30 min to 24 h post US exposure. At earlier time points post US exposure, pDNA spread out in cells as many small red dots under the confocal microscope (Figure 6.2a). Over time, the red dots became less in number and larger in size (Figure 6.2b, c), indicating pDNA aggregated in the perinuclear region of the cell and were possibly "packaged together" by some intracellular organelles. Therefore the light intensity of red fluorescent and the pseudo-yellow color indicating colocalization right after US exposure was not as strong as we observed at later time points. It was hard to find the location of pDNA at later time points (Figure 6.2d) presumably because of the less number of pDNA left due to degradation or cell division.

Quantitative Analysis from the Cellular Perspective

The microscopy images showed that US was able to deliver DNA to the cell nuclei within a short time after the treatment. We next investigated DNA delivery from the cellular perspective by measuring the fraction of cells containing DNA (Figure 6.3a), with DNA in their nuclei (Figure 6.3b) and the fraction of cells with GFP expression (Figure 6.3c). Immediately after US exposure, about 32% of all the cells showed labeled pDNA uptake (Figure 6.3a). The uptake efficiency decreased over time (one-way ANOVA, $p < 0.01$) possibly due to DNA degradation and cell division. The uptake efficiency determined by FCM (black triangles, Figure 6.3a) was higher than that

determined by confocal microscopy (white triangles, Figure 6.3a) (two-way ANOVA, $p < 0.05$), mainly because FCM is more sensitive. It was observed that at 30 min after US exposure, the red dots indicating pDNA were small in size and weak in light intensity, therefore hard to recognize with naked eyes (Figure 6.2a). Counting cells under microscope gave a lower fraction of cells with DNA uptake, compared to the measurement using FCM.

Figure 6.3b shows the fraction of cells with pDNA in the nuclei determined by confocal microscopy and 3D image analysis. Previous work has suggested that cells only need three plasmid copies per nucleus to express detectable transgene product (Ludtke et al. 2002). We found that 30 min after US exposure about 12% of cells had pDNA in the nuclei, at 4 h this number became 14% (Figure 6.3b). Gene transfection was observed as early as 4 h (~ 10%) post US exposure (Figure 6.3c). Transfection efficiency increased over time, peaked at 8 h (~ 12.3%) and then decreased (one-way ANOVA, $p < 0.01$). Similar results were found in some previous studies (Mehier-Humbert et al. 2005b; Ohl et al. 2006). The transfection efficiency of unlabeled pDNA was higher than labeled pDNA (two-way ANOVA, $p < 0.01$) probably because the side effects of Cy5 labeling, which was investigated and discussed previously (Gasiorowski and Dean 2005).

It was suggested that once pDNA entered the cell nucleus, protein expression took place within 3 h (Mehier-Humbert et al. 2005b). The rapid transfection observed after US exposure together with the colocalization of pDNA in the cell nuclei confirmed that US could not only open the cell membranes and allow pDNA to diffuse into the cytoplasm, but also possibly deliver pDNA to the perinuclear region to facilitate nuclear uptake or directly to the nuclei and thus achieve rapid gene transfection. Several reasons could

possibly contribute to the decrease of GFP-positive cells at 20 h post-transfection. Firstly, naked pDNA could be partially degraded by DNases in cytoplasm over time. Secondly, the half-life of GFP in mammalian cells is between 20 and 30 h (Corish and Tyler-Smith 1999). Thirdly, the decrease could also be explained by cell growth and division, thereby reducing the quantity of GFP copies per cell.

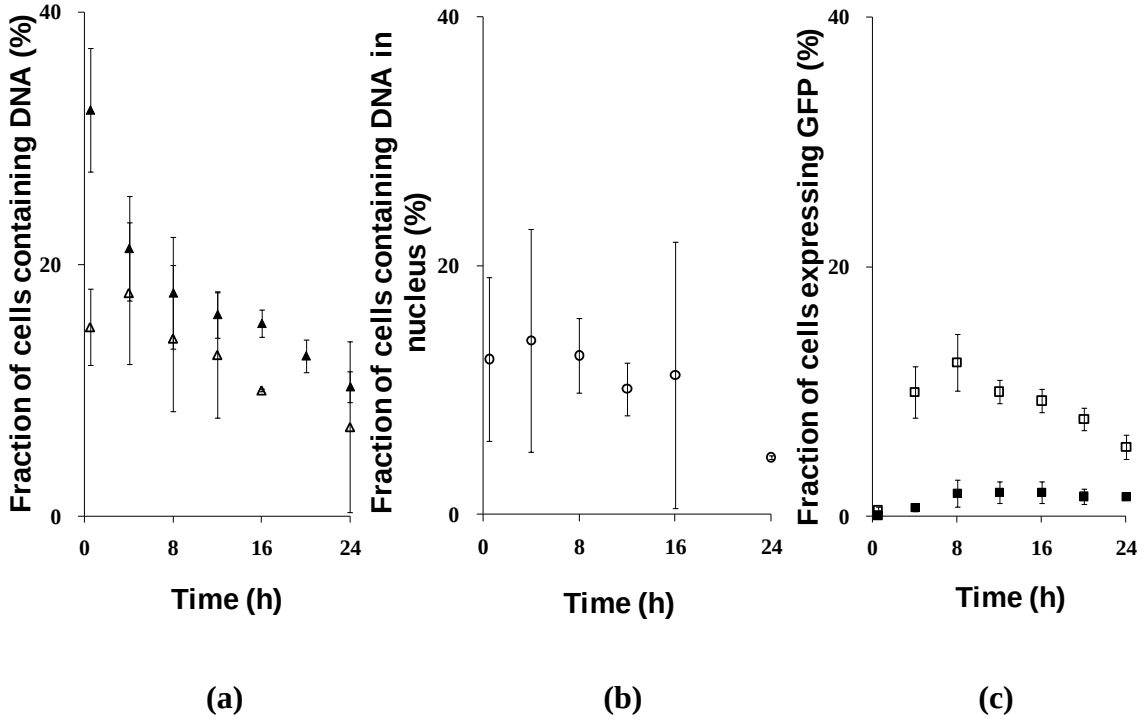

Figure 6.3: (a) Kinetics of labeled pDNA uptake determined by FCM (black triangle, n ≥ 4 replicates, data points show average ± SD, one-way ANOVA, p < 0.01) and microscopy (white triangle). (b) The fraction of cells with labeled pDNA colocalized with the nuclei determined by microscopy. (c) Transfection efficiency of labeled pDNA (black rectangle) and unlabeled pDNA (white rectangle) determined by FCM (n ≥ 4 replicates, data points show average ± SD, two-way ANOVA, p < 0.01). (a, b) Data points from quantitative microscopy images analysis represent the average ± SD of 3 biological samples with ≥ 5 images for each (one-way ANOVA, p > 0.05). Totally over 100 cells at each time point were examined under microscope. US exposure conditions: pressure amplitude of 0.78 MPa, total treatment time of 1 min with a pulse length of 0.25 ms at a duty cycle of 25%, Definity® concentration of 1 vol%.

Overall, we found ~ 30% of cells had DNA uptake right after US exposure and most of these uptake cells had pDNA in the nuclei. We found the maximum gene transfection efficiency was ~ 12% at 8 h post US exposure, which is close to the fraction of cells that had pDNA in the nuclei (two-way ANOVA, $p > 0.05$). These findings support our hypothesis that DNA that reaches and remains in the nucleus is efficiently transcribed and translated to produce its expression product.

Quantitative Analysis from the DNA Perspective

We next analyzed DNA delivery from the DNA perspective by determining the fraction of DNA delivered into the cell nuclei. Right after US exposure, nearly 30% of pDNA were colocalized with cell nuclei and this number remained nearly constant till 24 h of incubation (Figure 6.4, one-way ANOVA, $p > 0.05$). This result confirmed that US was able to deliver pDNA directly to the nuclei and facilitate rapid transgene expression.

We also randomly picked individual cells with pDNA uptake, measured the fraction of pDNA in the nucleus per cell and put it in the histograms (Figure 6.5). The geometric means were found similar in each histogram at different time point post US exposure, which were close to the results in Figure 6.4, that is, 25 - 30% of DNA were colocalized with the nuclei when the whole microscopy images were analyzed.

These histograms confirmed that most of the cells with DNA uptake had at least some DNA in the nuclei, as shown previously in Figure 6.3. At early time point (30 min post US exposure), cells had a variety amount of DNA in the nuclei (Figure 6.5a). At later time points (e.g., 24 h post US exposure), cells had most of DNA either in the nuclei of in the cytoplasm (Figure 6.5d). These results were consistent with the previous observations under microscope that DNA spread out in cells as many small red dots

initially and aggregated, became larger in size but less in number over time (Figure 6.2), therefore we did not see many cells with the fraction of DNA in the nuclei in the range of 20% ~ 80% at later time points.

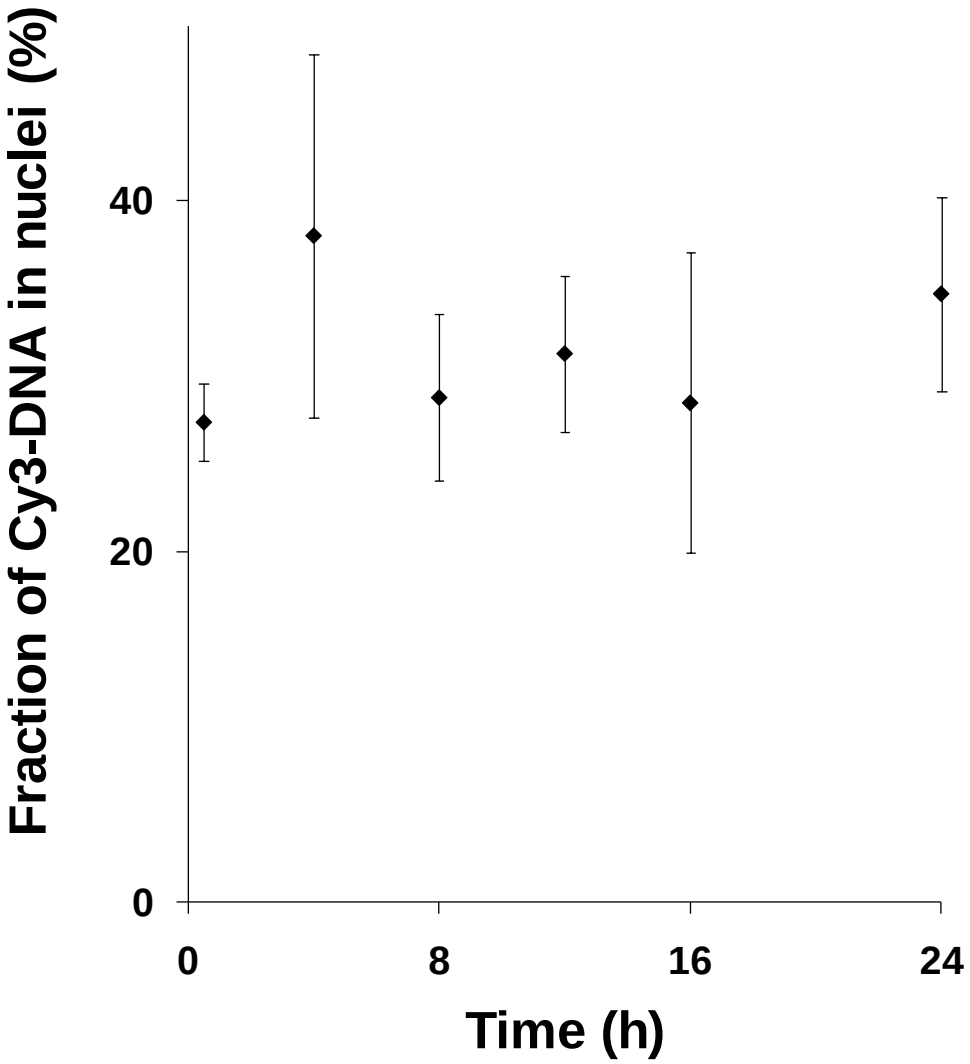

Figure 6.4: The fraction of Cy3-labeled pDNA that colocalized with the cell nuclei. Data points represent the average ± SD of 3 biological samples with ≥ 5 images for each (one-way ANOVA, $p > 0.05$). Totally over 100 cells at each time point were examined under microscope.

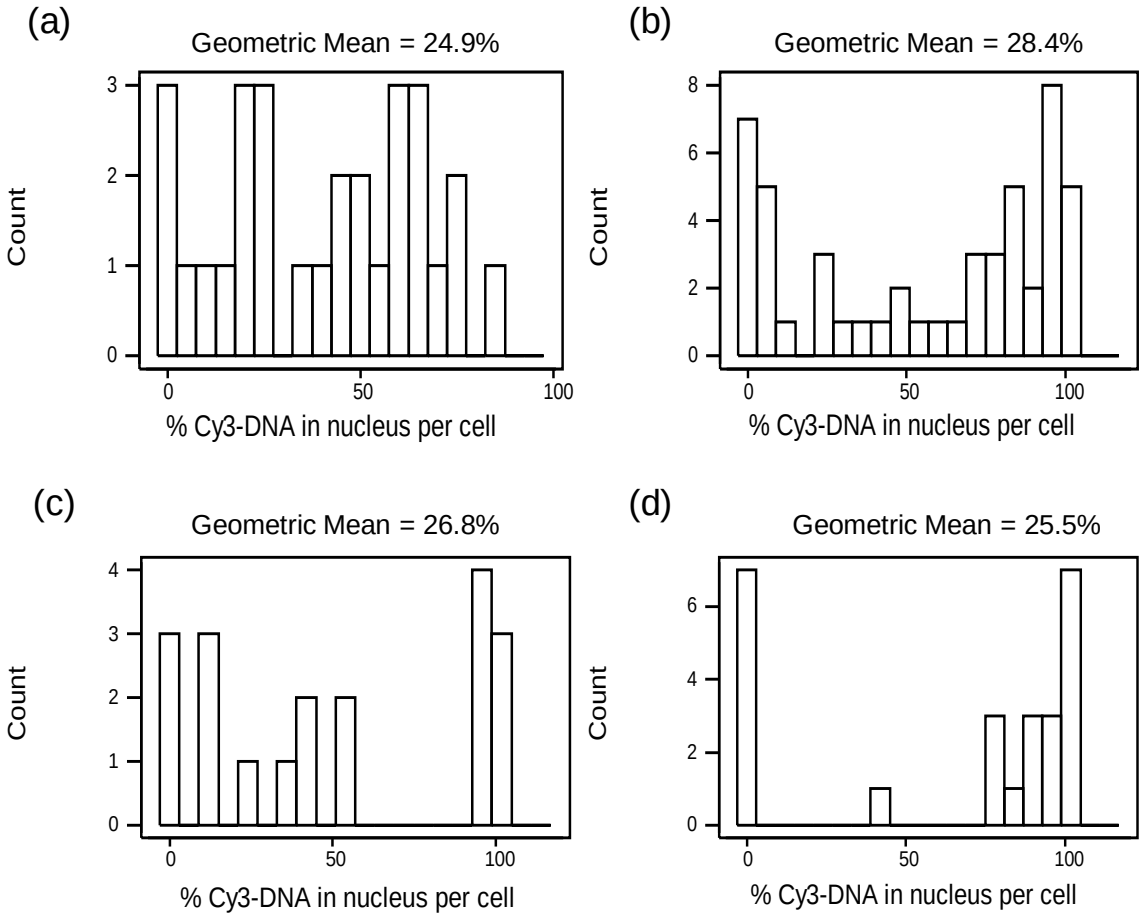

Figure 6.5: Histograms of the fraction of Cy3-labled pDNA in the cell nucleus per cell. Cells were examined under microscope at (a) 30 min (n = 29), (b) 8 h (n = 50), (c) 16 h (n = 19) and (d) 24 h (n = 25) post US exposure at the pressure amplitude of 0.78 MPa for 1 min with a pulse length of 0.25 ms at a duty cycle of 25% and Definity® concentration of 1 vol%.

DNA Trafficking in Cytoplasm post US Exposure

We previously found US was able to deliver DNA to the cell nuclei and we were also interested in the location of the rest of DNA in the cytoplasm. Figure 6.2 suggested that after pDNA were delivered into cells, pDNA aggregated in the perinuclear region of

the cell and were possibly "packaged together" by some intracellular organelles. To better understand it, we used specific antibodies to label early endosomes, late endosomes and lysosomes separately in cells incubated for 0 ~ 24 h after US-mediated gene transfection, and looked for the colocalization of pDNA with these organelles. Under confocal microscope, colocalization was not found between pDNA and early endosomes (Figure 6.6a) or late endosomes (Figure 6.6b) at all the time points post US exposure. In most cases, pDNA was not found colocalized with lysosomes (Figure 6.6c), except two colocalization cases was found in all the images (2 out of ~ 700 cells) investigated (Figure 6.6d). These results indicated that US-mediated gene delivery was not through endocytosis.

We also used LysoTracker® to generally label acidic organelles including endosomes/lysosomes and autophagosomes/autophagolysosomes. Colocalization was found within 30 min after US exposure (Figure 6.7), which indicated that pDNA in cytoplasm was entrapped by autophagosomes/autophagolysosomes and possibly transported or degraded by autophagosomes/autophagolysosomes, since pDNA were not found to colocalize with specifically antibody-labeled early endosomes, late endosomes or lysosomes (Figure 6.6).

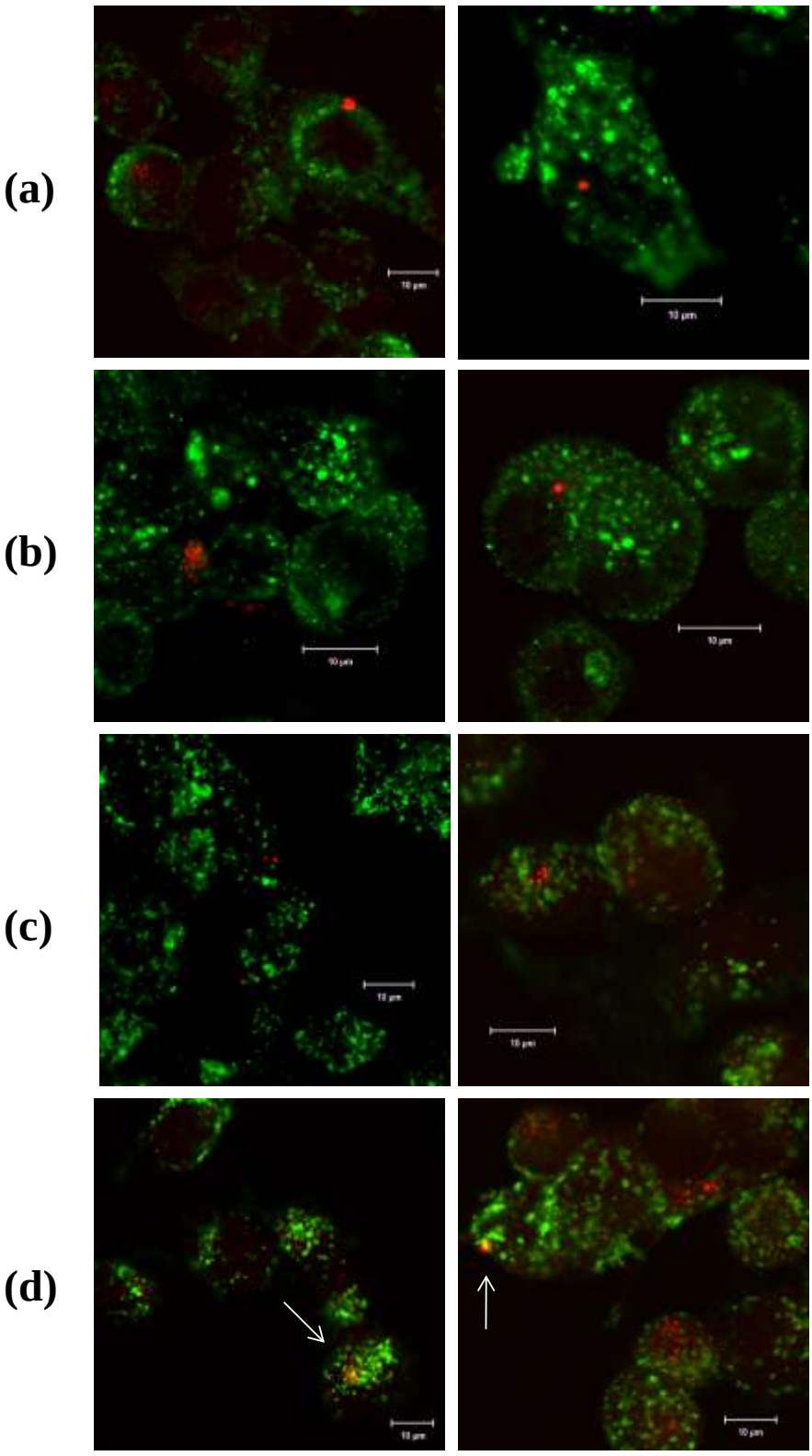

Figure 6.6: Representative microscopy images of Cy3-labled pDNA and antibody-labeled early endosomes (a), late endosomes (b) and lysosomes (c, d) in cells incubated for 8 h post US exposure. The red color indicates pDNA. The green color

indicates early endosomes (a), late endosomes (b) and lysosomes (c, d). The yellow color indicates colocalization.

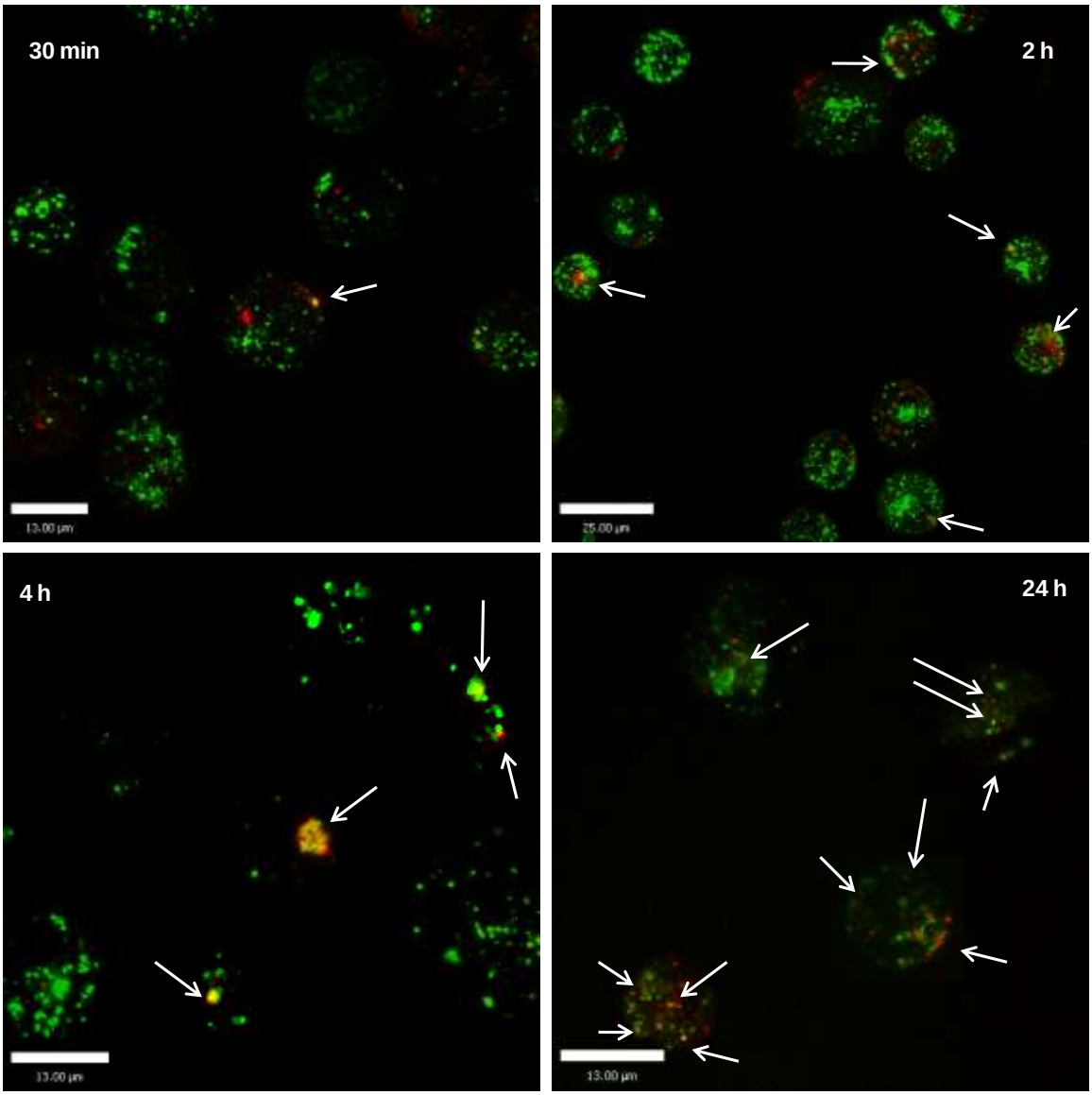

Figure 6.7: Representative microscopy images of Cy3-labled pDNA and LysoTracker®-labeled endosomes/lysosomes and autophagosomes/ autophagolysosomes in cells at 30min, 2 h, 4 h and 24 h post US exposure. The red color indicates pDNA. The green color indicates endosomes/lysosomes and autophagosomes/autophagolysosomes. The yellow color indicates colocalization (also indicated by arrows).

We determined the fraction of pDNA colocalized with autophagosomes/ autophagolysosomes and put the results together with the fraction of pDNA colocalized with the cell nuclei (data from Figure 6.4). As shown in Figure 6.8, 30 min after US exposure, about the same amount of pDNA were colocalized with the cell nuclei and autophagosomes/autophagolysosomes, and the rest of pDNA (~ 60%) were "free" in the cytoplasm. At 4 h post US exposure, most of the pDNA in the cytoplasm were colocalized with autophagosomes/autophagolysosomes, leaving only ~ 10% "free" in the cytoplasm ($p < 0.01$). And at 24 h, all the pDNA that were not in the cell nuclei were colocalized with autophagosomes/autophagolysosomes. It is likely that these pDNA were finally degraded.

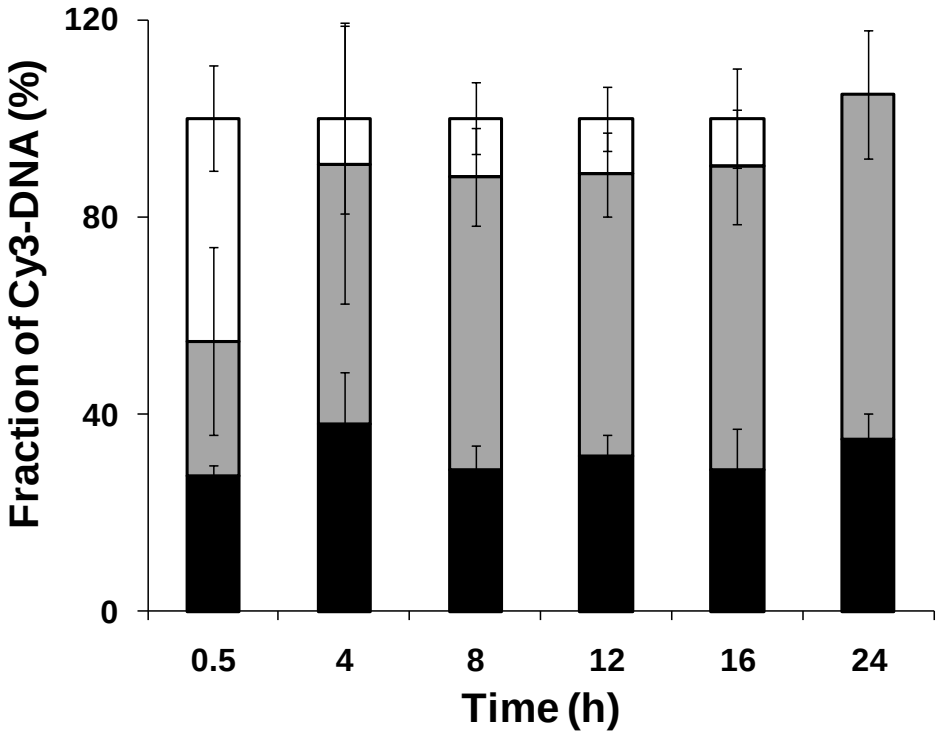

Figure 6.8: The fraction of Cy3-labeled pDNA that colocalized with the cell nuclei (black bar, one-way ANOVA, $p > 0.05$), autophagosomes/autophagolysosomes (grey bar, one-way ANOVA, $p < 0.01$) and "free" in the cytoplasm (white bar, one-way

ANOVA, $p < 0.01$). Data points represent the average ± SD of 3 biological samples with ≥ 5 images for each. Totally over 100 cells at each time point were examined under microscope.

Discussion

We studied the capability of US to deliver DNA in the cell nuclei from the cellular perspective and DNA perspective. The results support our hypothesis that DNA introduced into the cytoplasm during sonication is either transported into the nucleus within hours or removed by autophagosomes/autophagolysosomes, and DNA that reaches and remains in the nucleus is efficiently transcribed and translated to produce its expression product. We found that within 30 min after sonication, up to ~ 30% of cells had DNA uptake and most had a portion of the DNA already in the nuclei (Figure 6.3). Overall, ~ 30% of intracellular DNA was in the nuclei, ~ 30% was in the autophagosomes/autophagolysosomes and the rest was free in the cytoplasm (Figure 6.8). After 4 h, the percentage of cells with DNA uptake decreased to ~20% and half of those cells (i.e. ~ 10% of all cells) exhibited expression of the reporter protein GFP (Figure 6.3). The percentage of intracellular DNA remains at ~ 30% in the nuclei, but increased to ~ 60% in the autophagosomes/autophagolysosomes, leaving just ~ 10% free in cytoplasm (Figure 6.8). At later time up to 24 h, the percentage of cells with DNA uptake decreased continuously to ~ 10%, with most of these cells exhibiting GFP expression (Figure 6.3). DNA continued to be distributed ~ 30% in the nuclei and most or all of the rest in autophagosomes/autophagolysosomes (Figure 6.8).

US was found to be able to deliver pDNA into cell nuclei within 30 min in our study and other studies (Duvshani-Eshet and Machluf 2005). This could explain the rapid

gene transfection observed within 3 ~ 4 h after US exposure, compared to the kinetics of gene transfection mediated by chemical vectors like liposomes, in which it takes ~ 3 times longer to start seeing gene expression (Mehier-Humbert et al. 2005b). Since the protein expression took place after about 3 h once the DNA entered the cell nucleus (Mehier-Humbert et al. 2005b), the cells showing early GFP expression probably had pDNA in the nuclei shortly after US exposure. Over time, we observed the decrease in DNA uptake efficiency possibly due to DNA degradation and cell division. The maximum GFP expression was observed at 8 h post US exposure and transfection efficiency decreased significantly after 20 h, possibly due to DNA degradation, cell division and the limited lifetime of GFP in mammalian cells (Corish and Tyler-Smith 1999).

FCM is generally more sensitive to measure the fraction of cells with pDNA uptake, compared to microscopy where uptake cells were counted by naked human eyes. This could explain the difference between the uptake efficiency in Figure 6.3a. To get the fraction of cell nuclei with pDNA (Figure 6.3b), 3D image analysis was used to quantify the colocalization and therefore provided a better method than counting cell nuclei with naked human eyes. It also is worth noting that the Cy3/Cy5 labeling process could alter pDNA and affect DNA trafficking, localization, uptake and transfection (Gasiorowski and Dean 2005). For instance, the fluorophores were randomly attached on the plasmids with an alkylating aromatic nitrogen mustard (Belikova et al. 1967) and the bulky fluorophores that coat the plasmid may block transcription factors from binding to the DNA (Slattum et al. 2003). This could explain the fact that transfection efficiency of unlabeled pDNA was higher than labeled pDNA (Figure 6.3c).

It is interesting to see that 30 min post US exposure, pDNA spread out in cells as many small red dots under the confocal microscope (Figure 6.2a). After 4h, the red dots became less in number and larger in size (Figure 6.2b, c, d), indicating pDNA aggregated or were possibly "packaged together". The histograms showing the fraction of pDNA in the nucleus per cell were consistent with these observations (Figure 6.5). At 30 min after US exposure, the DNA uptake cells were found with various amount of pDNA in the nuclei (Figure 6.5a). At later time points, the DNA uptake cells had most of the pDNA either in the cytoplasm or in the nuclei (Figure 6.5d).

Although gene transfection mediated by US dose not involve endocytosis (Figure 6.6), pDNA was found to entrap in large vesicles like autophagosomes and autophagolysosomes (Figure 6.7), which were generally thought to originate randomly throughout the cytoplasm from the endoplasmic reticulum (Deretic 2005), the post-Golgi compartment or the phagophore (Juhasz and Neufeld 2006). Autophagosomes/ autophagolysosomes were found to move bidirectionally along microtubules towards and away from the cell nuclei with the help of the motor protein dynein (Jahreiss et al. 2008). The colocalization of pDNA and autophagosomes/autophagolysosomes was observed as early as 30 min after US exposure (Figure 6.7 and 6.8). About 27% of pDNA were colocalized with autophagosomes/autophagolysosomes and about 45% of pDNA were possibly free in the cytoplasm (Figure 6.8). At 4 h post US exposure, the majority of pDNA in the cytoplasm were colocalized with autophagosomes/autophagolysosomes. Because naked pDNA could not bind to the adaptor proteins directly, the colocalization of pDNA and autophagosomes/autophagolysosomes could possibly facilitate the active transport to the cell nuclei, as suggested by some gene therapy studies using other

delivery systems (Bukrinskaya et al. 1998; Suomalainen et al. 1999; Vihinen-Ranta et al. 2000; Ogawa-Goto et al. 2003; Bausinger et al. 2006; Vaughan et al. 2008). The final fate of autophagosomes/autophagolysosomes is the same as endosomes/lysosomes. The colocalized pDNA could be degraded as their cargo (Eskelinen 2005). As shown in Figure 6.8, one day after US exposure, all the pDNA that stayed in the cytoplasm were entrapped by autophagosomes/autophagolysosomes. The formation mechanism and intracellular itinerary of autophagosomes/autophagolysosomes are not fully clear. Further study is needed to better understand how their colocalization with pDNA in US-mediated gene transfection affects the exogenous gene trafficking and transfection efficiency.

Although further study is needed, these data suggest the following sequence of events. Sonication initially delivers DNA into about one third of cells exposed to US. In about half of those cells, significant amounts of DNA reach the nucleus within 30 min. Overall, approximately one third of DNA that is delivered into cells makes it into the nucleus within 4 h and the rest is removed by autophagosomes/autophagolysosomes. Over time, the fraction of cells containing DNA decreases to 10% after 24 h. Most of the cells that contain DNA in the nucleus express that DNA, which peaks at 8 h after sonication.

Thus, there are a number of rate-limiting steps to increase DNA transfection by US. (i) DNA is delivered into only one third of cells exposed to ultrasound. (ii) Only half the cells with intracellular DNA achieve significant DNA levels in the nucleus. (iii) Over time, DNA leaves the nucleus and transfection levels drop correspondingly.

These observations suggest opportunities to increase DNA transfection by US. (i) Increase the fraction of cells that receive intracellular DNA and survive. As shown in the

previous chapters, it is difficult to achieve high uptake and high cell viability at the same time. Given the known trade-off between increased uptake and cell viability, strategies to protect cell viability under conditions that deliver DNA effectively into cells may be useful. Some studies have shown the possibility to increased cell viability after US exposure by the chelation of intracellular Ca^{2+} and the supplement of ATP energy (Schlicher et al. 2006; Hutcheson et al. 2010). (ii) It appears that there is a race between DNA transporting to the nucleus before autophagosomes/autophagolysosomes take it away. Thus, methods that increase/target DNA trafficking to the nucleus by enhancing active transport and methods that decrease clearance by inhibiting autophagosomes/ autophagolysosomes may be useful. Microtubule stabilizers (Ogawa-Goto et al. 2003; Vaughan and Dean 2006), DNA interchelators (Chu et al. 1987), nuclear localization signals (Cartier and Reszka 2002) and DNA targeting sequences have been studies for this purpose (Dean et al. 1999). (iii) Loss of DNA from the nucleus may be associated with loss of nuclear structural integrity during cell division. Thus, slowly dividing cells in the body (as opposed to rapidly dividing cancer cell culture used in this study) may retain DNA in the nucleus longer and thereby sustain expression levels longer.

CHAPTER 7: MICROARRAY STUDY AND DRUG TREATMENT COMBINED WITH US EXPOSURE

Introduction

The previous chapters have shown that just by optimizing the US exposure conditions, we still could not overcome the compromise of cell viability and uptake/transfection efficiency, and we also found heterogeneous bioeffects among the viable cells, including cells with successful gene transfection, cells with only pDNA uptake but no transfection and cells with neither of these bioeffects. In this chapter, we were looking for methods other than optimizing the physical parameters of US to increase gene transfection.

Novel transcriptional profiling technologies such as microarray analysis allow the simultaneous measurement of changes in expression of hundreds and thousands of genes. It has been used for the characterization of gene expression patterns during diseases and normal biological processes, as well as for the identification of specifically expressed genes induced by physical and chemical stress (Schena et al. 1995; Cheung et al. 1999; Butte 2002). Several studies have utilized this technology for identifying changes in gene expression induced by a fairly intense continuous wave (4.9 W/cm^2 for 1 min) (Schena et al. 1995; Tabuchi et al. 2002), focused US (75 W/cm^2 for 1 min) (Abdollahi et al. 2004), continuous high-intensity focused US (6,731 W/cm^2 for 20 sec) (Hundt et al. 2007), short-pulse high-intensity focused US (134 W/cm^2 for 16.5 min) (Hundt et al. 2007), and

low-intensity pulsed US (0.3 W/cm^2 for 1 min) (Tabuchi et al. 2007). These limited expression profile data provided by microarray analysis revealed that US may regulate ribosomal proteins expression, influence cell proliferation and differentiation, induce cell cycle arrest and apoptosis. These intracellular bioeffects may be cell-type specific and US-condition dependent.

Unlike these previous studies, we were not investigating the changes in transcriptional profile caused by US exposure. We applied microarray technology to exploring the differences between sonicated cells with transfection and sonicated cells with uptake but no transfection, and looked for biological factors that could increase gene transfection efficiency after US exposure. In this present study, gene expression among DU145 human prostate cancer cells after US-mediated transfection was analyzed using Affymetrix GeneChip® Human Genome U133 Plus 2.0 Arrays. The goal of this study is to determine the differences between a cell that takes up DNA after sonication but is not transfected and a cell that similarly takes up DNA but is transfected. Our hypothesis is that differences in transcriptional profile determined by gene chip analysis will correlated with differences in transfection status among cells with DNA uptake. We then seek to use this information to identify drugs that mediate the cell's transcriptional profile to increase transfection rates. Stated differently, we seek to learn how to turn cells with DNA uptake but no transfection into cells that are transfected by controlling targeted transcriptional pathways. We hope these findings can help to better understand the heterogeneous bioeffects of US and further suggest additional regulation of intracellular processes to enhance gene transfection mediated by US.

Results

Cell Sorting

To study the difference between transfection cells expressing GFP and uptake cells without the expression of GFP, we first identified and sorted the three populations of cells at 8 h after US exposure (Figure 6.1): cells with GFP transfection (green fluorescence), cells with labeled pDNA uptake (red fluorescence) and cells with neither of these bioeffects. As shown in Figure 7.1, after sorting the purity of each population was above 98% (Figure 7.1c, d).

Gene Chip and Cell Cycle Analysis

Affymetrix GeneChip® Human Genome U133 Plus 2.0 Arrays can analyze the relative expression level of more than 47,000 transcripts including over 38,500 well-characterized genes. Transcriptional profiling using these microarrays was performed to generally characterize the differences between cells with pDNA uptake and GFP expression. 78 genes were found differentially expressed between the two groups of cells, 32 of which were up-regulated in transfected cells and 46 were down-regulated relative to cells with pDNA uptake but lacking expression (Figure 7.2a). The names of these 78 genes and their fold changes were listed in Appendix B. This result confirmed our hypothesis that differences in transcriptional profile correlate with differences in transfected status among cells with DNA uptake.

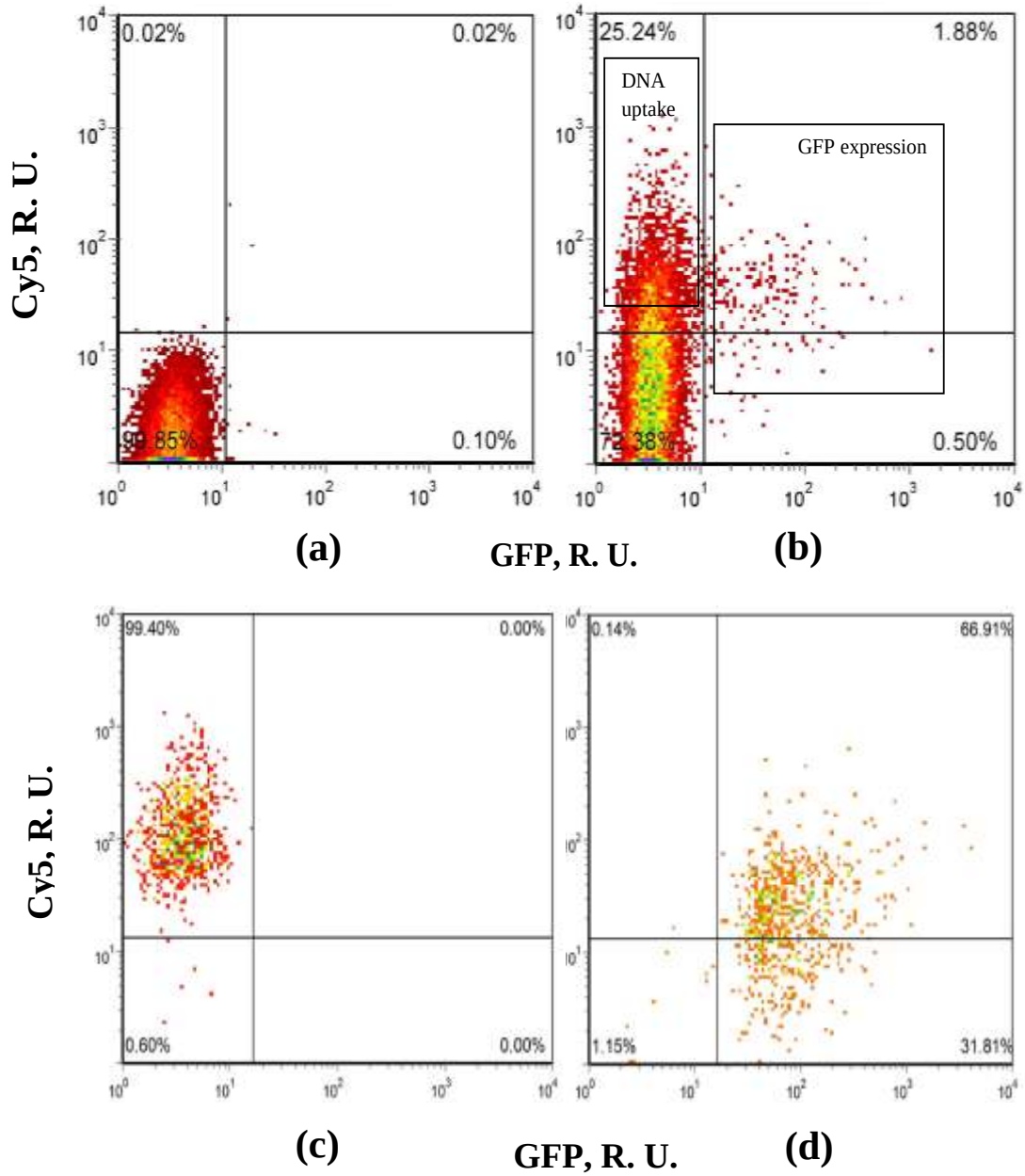

Figure 7.1: Representative FCM density plots showing the three populations of DU145 cells after incubation for 8 h post US exposure. (a) "sham" exposure before sorting; (b) sonicated sample before sorting; (c) cells with pDNA uptake after sorting and (d) cells with GFP expression after sorting. Both axes have relative units. US exposure conditions: pressure amplitude of 0.78 MPa, total treatment time of 1 min with a pulse length of 0.25 ms at a duty cycle of 25%, Definity® concentration of 1 vol%.

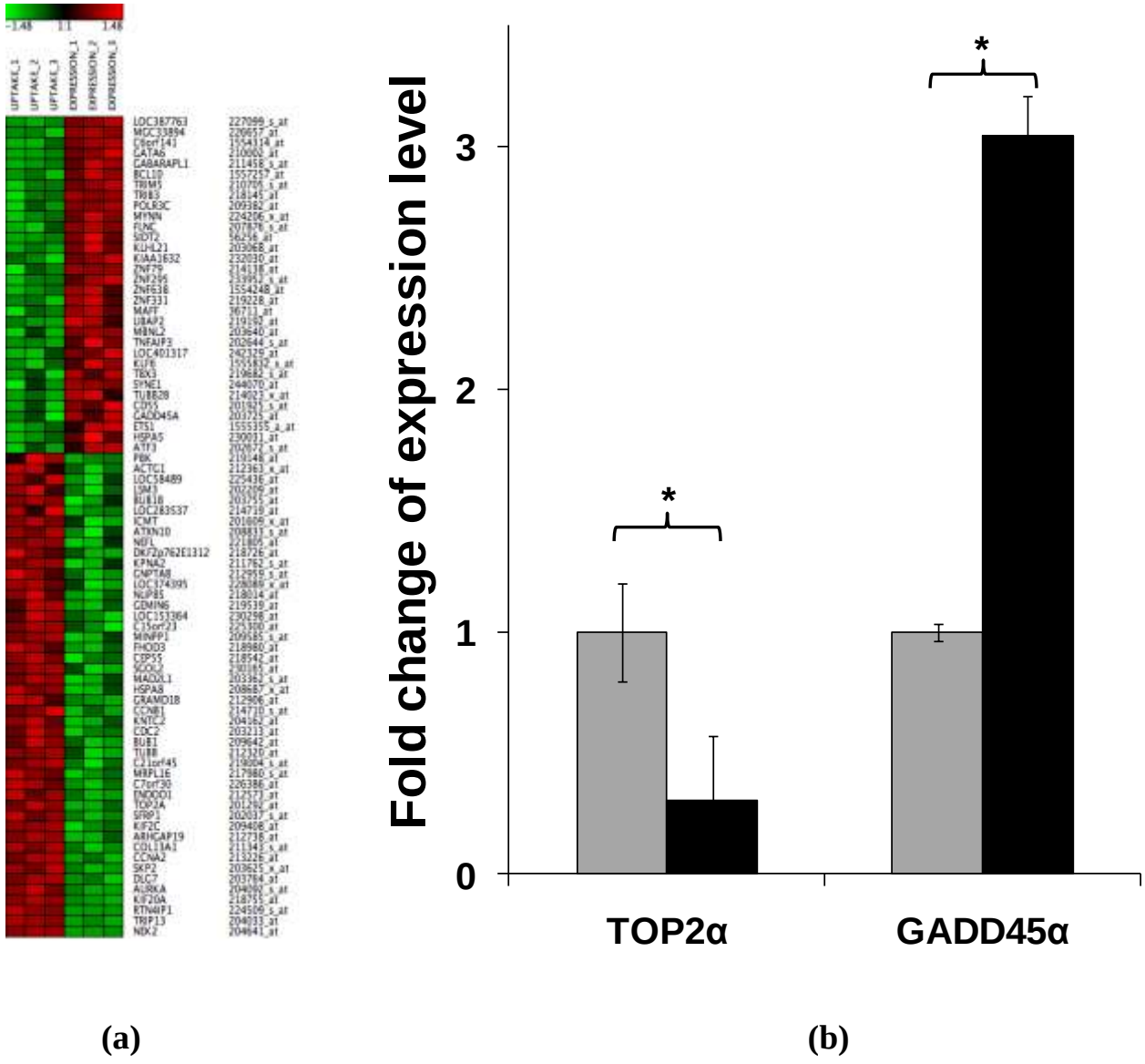

Figure 7.2: Gene expression analysis. (a) The heat map of Z-scores of 78 differentially expressed genes between the two groups of cells with pDNA uptake and GFP expression, sorted by descending Δ Z-score. The green color indicates lower expression and the red indicates higher expression level. (b) The expression levels of TOP2α and GADD45α in the two cell populations were determined using qRT-PCR. Data represent the means of n = 3 replicates with standard deviation (*p < 0.01). Grey bar: cells with pDNA uptake but no transfection. Black bar: cells with GFP expression.

The expression levels of two representative genes (TOP2α, Topoisomerase IIα and GADD45α, one of the arrest and DNA-damage inducible genes) were measured using qRT-PCR to independently test the validity of the differential gene expression determined by microarray, because they were two of the most down/up-regulated genes (Appendix B). The qRT-PCR results confirmed the differences detected in the microarray study (Figure 7.2b, Appendix C). The expression level of TOP2α in transfected cells decreased to 30%, while the expression of GADD45α increased by 3 fold, compared to cells with pDNA uptake (Figure 7.2b).

Kyoto Encyclopedia of Genes and Genomes (KEGG) pathway (Homo sapiens) analysis was applied to the list of genes as shown in Table 7.1. We found that the genes involved in cell cycle regulation involved the largest number of genes (8 genes, ~ 10% of the total number of the gene list). These 8 genes were mapped to KEGG cell cycle pathway (Figure 7.3) and their full names and fold changes were listed in Table 7.2. These genes indicated some type of cell cycle arrest present in the transfected cells.

We then performed cell cycle analysis and found that cells with pDNA uptake and cells without bioeffects did not show significant difference in each cell cycle stage. However, cells with GFP transfection were found to accumulate in the G1 phase of cell cycle compared to the other two populations (Figure 7.4). The promoter of the GFP encoding plasmid we used is a constitutively active cytomegalovirus (CMV) promoter, which is cell cycle independent (Zhao et al. 2000).

Table 7.1: KEGG pathway analysis.

Enriched terms associated with the gene list	Gene count	% involved genes/total genes	P-value*
Cell cycle	8	9.9	2.70E-06
Progesterone-mediated oocyte maturation	5	6.2	9.90E-04
Oocyte meiosis	5	6.2	2.50E-03
Pathogenic Escherichia coli infection	3	3.7	3.60E-02
p53 signaling pathway	3	3.7	5.00E-02
Gap junction	3	3.7	8.00E-02

*Modified Fisher Exact p-value, EASE Score. The smaller, the more enriched.

Table 7.2: KEGG cell cycle enriched genes by PATHWAY EXPRESS (Bonferroni corrected $p = 2.8 \times 10^{-7}$).

Gene Symbol	Gene Name	Fold Change
BUB1B	BUB1 budding uninhibited by benzimidazoles 1 homolog beta	-3.80
SKP2	S-phase kinase-associated protein 2 (p45)	-3.40
CDC2	cell division cycle 2, G1 to S and G2 to M	-3.20
BUB1	BUB1 budding uninhibited by benzimidazoles 1 homolog (yea	-2.90
MAD2L1	MAD2 mitotic arrest deficient-like 1 (yeast)	-2.60
CCNB1	cyclin B1	-2.50
CCNA2	cyclin A2	-2.40
GADD45A	growth arrest and DNA-damage-inducible, alpha	3.10

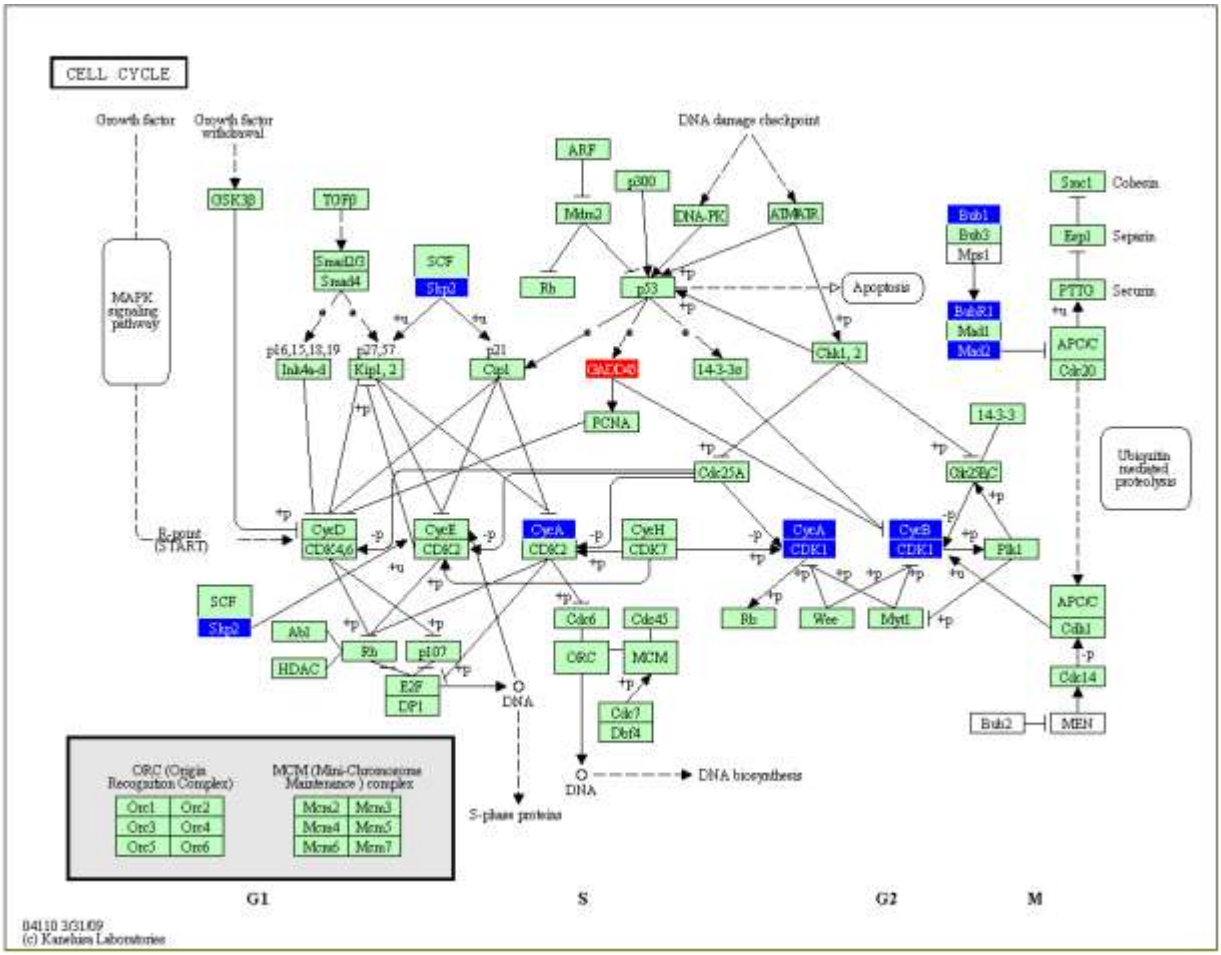

Figure 7.3: Pathway Express rendering of enriched genes on KEGG Cell Cycle Pathway Map. Each box represents a particular gene. The blue color represents down-regulated genes and the red represents up-regulated genes in cells with GFP expression relative to cells with pDNA uptake.

Both the cell cycle and microarray analysis indicated cell cycle arrest in the cells with gene transfection. Among all the genes of interest, TOP2α and GADD45α were chosen for further study because they were two of the most down/up-regulated genes and they were both involved in cell cycle regulation. GADD45α is one of the growth arrest and DNA-damage inducible genes. It is a p53-regulated gene as shown in the KEGG cell cycle pathway analysis (Figure 7.3) (Kastan et al. 1992). The expression level of

GADD45 has been found to be associated with cell cycle, being the maximal in G1 phase (Kearsey et al. 1995). Overexpression of GADD45α *in vitro* retarded cell growth and increased accumulation in G1 phase or G2/M boundary of cell cycle (Fan et al. 1999; Harkin et al. 1999; Wang et al. 1999; Liebermann and Hoffman 2008). It is hypothesized that the interaction of GADD45 with p21, another p53-regulated gene (Figure 7.3), leads to G1 phase arrest, although the mechanism is not well understood (Kearsey et al. 1995).

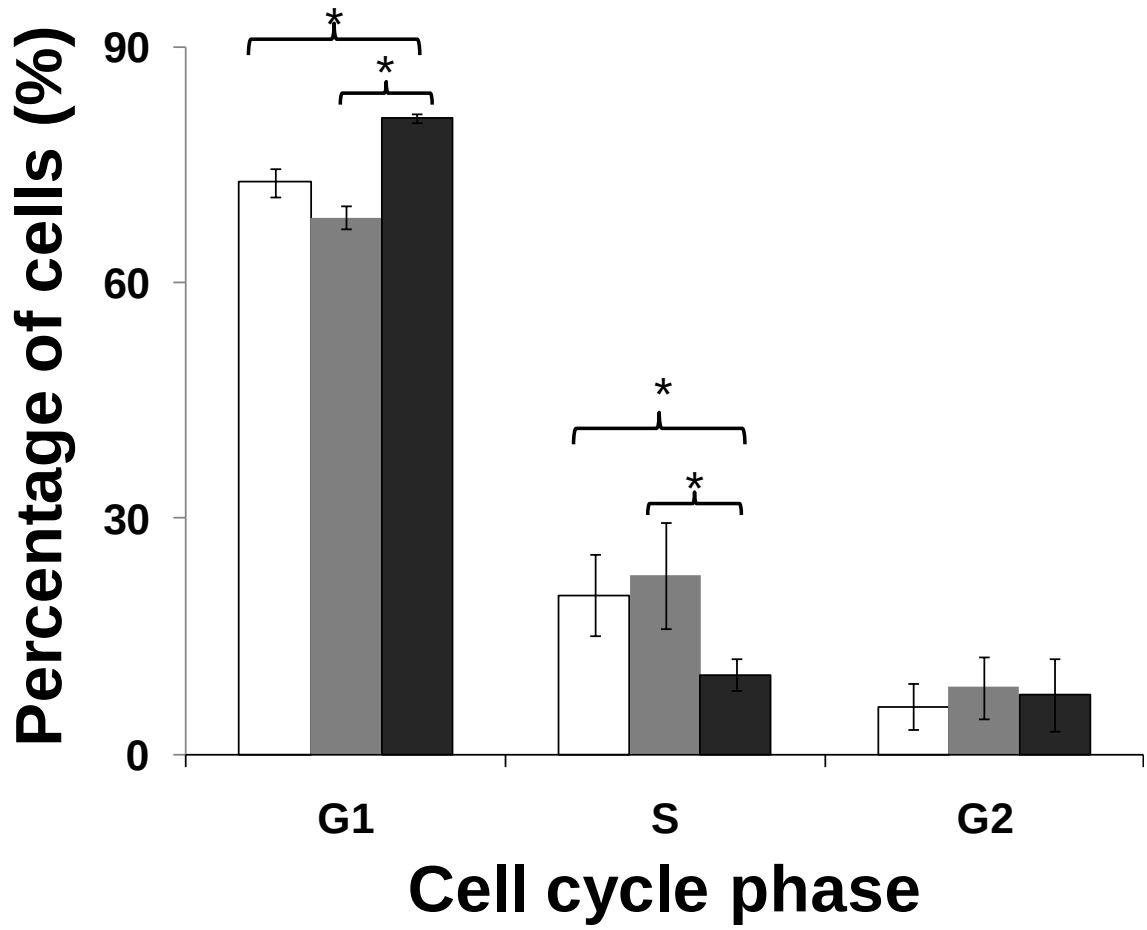

Figure 7.4: Cell cycle analysis of the three populations at 8 h post US exposure: cells without bioeffects (white bar), cells with pDNA uptake (grey bar) and cells with GFP transfection (black bar). Data represent the averages of n ≥ 3 replicates with standard deviation (*p < 0.05). US exposure conditions: pressure amplitude of 0.78 MPa, total treatment time of 1 min with a pulse length of 0.25 ms at a duty cycle of 25%, Definity® concentration of 1 vol%.

Topoisomerase II is a dimeric enzyme involved in altering DNA topology (Champoux 2001). TOP2α isoform is necessary for chromosome condensation and segregation in mitosis. The concentration of TOP2β isoform is relatively constant over cell cycle, while the expression of TOP2α is coupled with cell cycle. The level of TOP2α protein synthesis is significantly higher in the late S and G2/M phase than during G1 phase (Goswami et al. 1996). That is, TOP2α is down-regulated in the G1 phase of cell cycle. Our results found its expression level decreased in GFP-expressing cells together with increased expression level of GADD45α. The down-regulation of TOP2α and up-regulation of GADD45α in GFP-expressing cells were consistent with our cell cycle analysis, which indicated that cells with GFP transfection accumulated in the G1 phase of cell cycle.

Drug Treatment Combined with US Exposure

Three strategies were proposed to further enhance US-mediated gene transfection in DU145 cells: inhibiting the expression of TOP2α, enhancing the overexpression of GADD45α, and regulating the active transport and trafficking in the cytoplasm. We then selected drugs that regulate these intracellular processes, combined drug treatment with US exposure, and analyzed the bioeffects including gene transfection efficiency, DNA uptake efficiency and cell viability. Considering the possible additional damage to the cell integrity caused by the drug treatment, we determined the transfection efficiency in the cells remaining viable after 8-h incubation post US exposure and also the transfection efficiency in all the cells by comparing the number of cells in the sonication samples with that in the “sham” controls.

Drugs that Induce GADD45α Expression

Ethyl methanesulfomate (EMS), N-methyl-D-Aspartate (NMDA) and PRIMA-1 (p53 reactivation and induction of massive apoptosis) were chosen to enhance the expression of GADD45α because they were suggested to induce the overexpression of GADD45α via different mechanisms.

EMS

The expression level of GADD45α was previously found to be increased by 1 ~ 5 fold in cultured cells by the exposure to alkylating agents such as EMS (Papathanasiou et al. 1991). The ethyl group of EMS reacts with guanine in DNA, induces DNA damage and therefore causes the overexpression of GADD45α. In this study, EMS was added to the cell sample at a final concentration of 0.6 or 3 mg/mL for US exposure. With EMS treatment, the transfection efficiency was increased by 2 fold, while the cell viability was not affected compared to US exposure alone (Figure 7.5). The effect of different concentrations was not significantly different ($p > 0.05$).

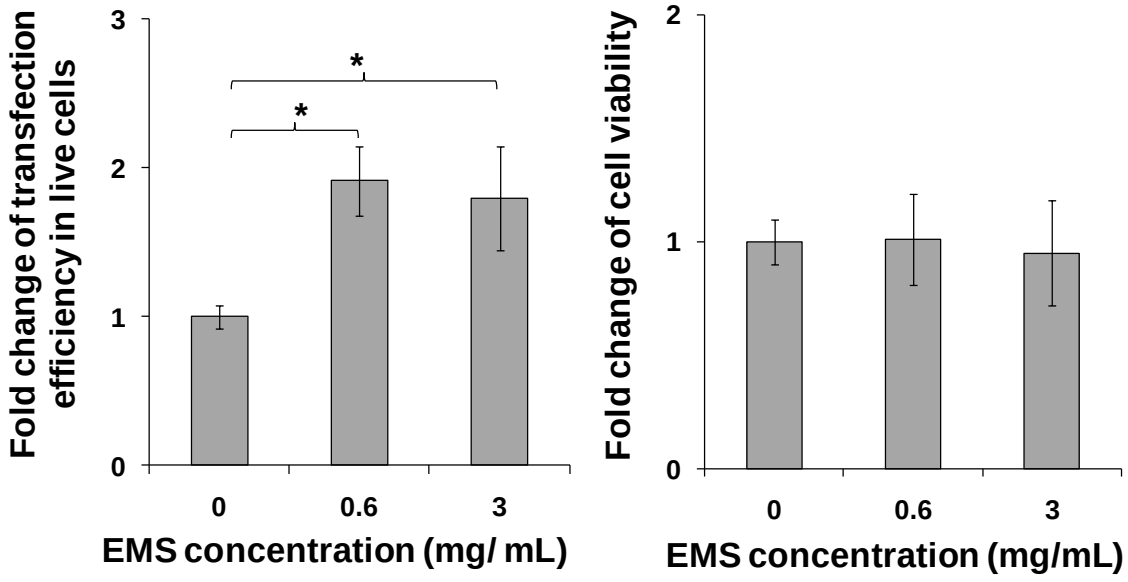

Figure 7.5: EMS treatment increased the transfection efficiency mediated by US without affecting the cell viability. Data represent the averages of n ≥ 3 replicates with standard deviation (*paired Student's t-test, p < 0.01). US conditions: pressure amplitude of 0.78 MPa, total treatment time of 1 min with a pulse length of 0.25 ms at a duty cycle of 25%, Definity® concentration of 1 vol%.

NMDA

NMDA is a known excitotoxin and has been shown to increase the expression level of GADD45α in neuronal cells (Laabich et al. 2001; Uberti et al. 2002). NMDA-induced GADD45α expression generally requires the activation of NMDA receptors (Uberti et al. 2002). Treating DU145 cells with NMDA for US exposure, we found the transfection efficiency in live cells was increased by 12%, while the cell viability was decreased compared to US exposure alone. The overall transfection efficiency among all the cells was not changed (Figure 7.6).

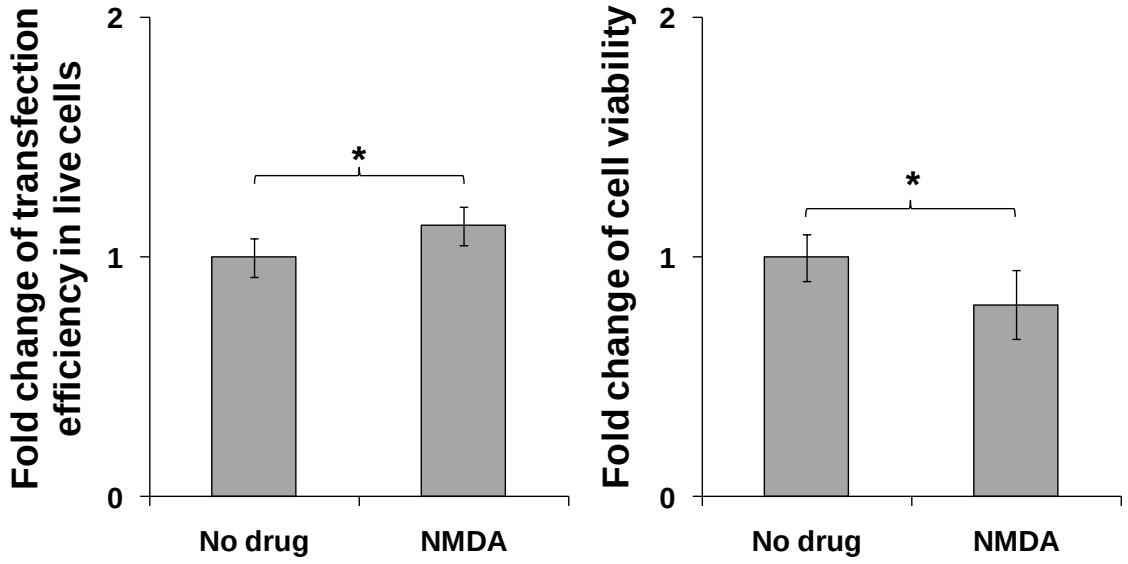

Figure 7.6: NMDA treatment (2 mM) increased the transfection efficiency mediated by US in live cells, but decreased the cell viability. Data represent the averages of n ≥ 3 replicates with standard deviation (*paired Student's t-test, p < 0.05). US

conditions: pressure amplitude of 0.78 MPa, total treatment time of 1 min with a pulse length of 0.25 ms at a duty cycle of 25%, Definity® concentration of 1 vol%.

PRIMA-1

PRIMA-1 was previously found to reactivate mutant p53 (Kastan et al. 1992; Lambert et al. 2009), which was supposed to up-regulate the expression level of GADD45α (Figure 7.3). We treated DU145 cells with up to 1 mM PRIMA-1 for US exposure and did not find any enhancement in gene transfection (Figure 7.7). A possible reason is that the regulation of GADD45α was not direct but through reactivating p53 in DU145 cells and therefore not as effective as when the overexpression of GADD45α was induced directly.

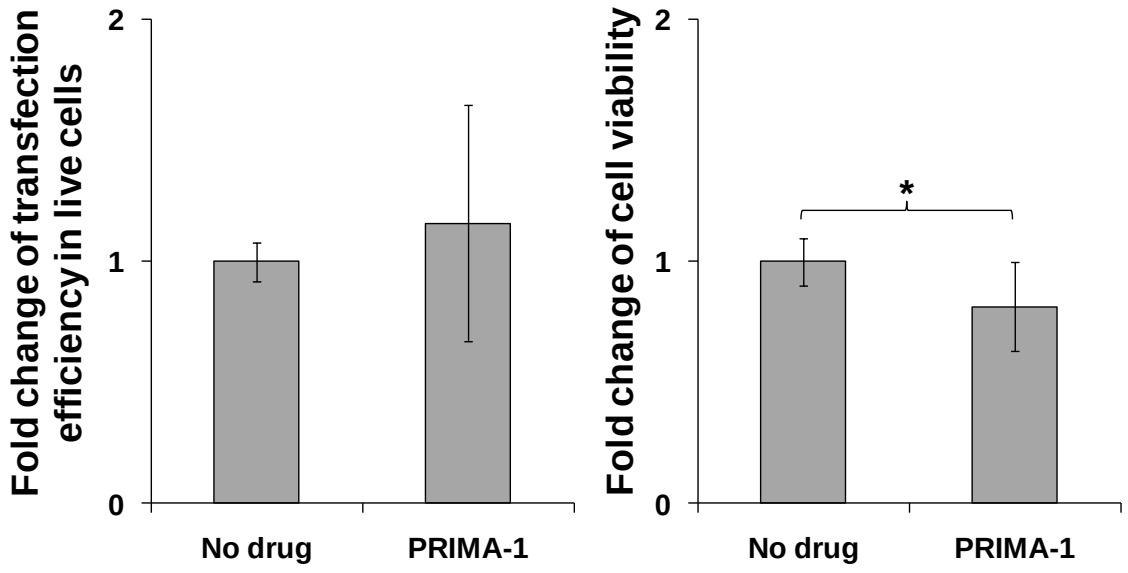

Figure 7.7: PRIMA-1 treatment (1 mM) did not affect the transfection efficiency mediated by US but decreased the cell viability. Data represent the averages of n ≥ 3 replicates with standard deviation (*paired Student's t-test, p < 0.05). US conditions: pressure amplitude of 0.78 MPa, total treatment time of 1 min with a pulse length of 0.25 ms at a duty cycle of 25%, Definity® concentration of 1 vol%.

Drugs that Inhibit TOP2α Expression

There are several kinds of TOP2α inhibitors based on the action mechanisms of eukaryotic TOP2 (Sehested and Jensen 1996; Burden and Osheroff 1998). In the present study, chloroquine, aclarubicin, amsacrine, mitoxantrone and etoposide were tested. Chloroquine and aclarubicin were two representative catalytic inhibitors of TOP2α by inhibiting the enzyme in binding to its substrate DNA (Andoh and Ishida 1998). Amsacrine, mitoxantrone and etoposide were representative TOP2α poisons that stabilize the structure of the DNA/TOP2 complex and so that the closure of TOP2-catalyzed DNA break is not possible (Nelson et al. 1984).

Amsacrine Hydrochloride

Amsacrine can poison TOP2α by stabilizing the structure of the DNA/TOP2 complex and so that the reaction cannot move forward (Nelson et al. 1984). When amsacrine was added to the cell samples for US exposure, the transfection efficiency was increased by ~ 50%. Although the cell viability was decreased, the overall transfection efficiency among all the cells was increased (Figure 7.8).

Chloroquine Diphosphate Salt

Chloroquine is a DNA interchalater that inhibits TOP2α by preventing this enzyme from binding to its substrate DNA (Andoh and Ishida 1998). When we treated cells with chloroquine for US exposure, the transfection efficiency was found increased by ~ 30%, and the cell viability was not affected compared to US exposure alone (Figure 7.9).

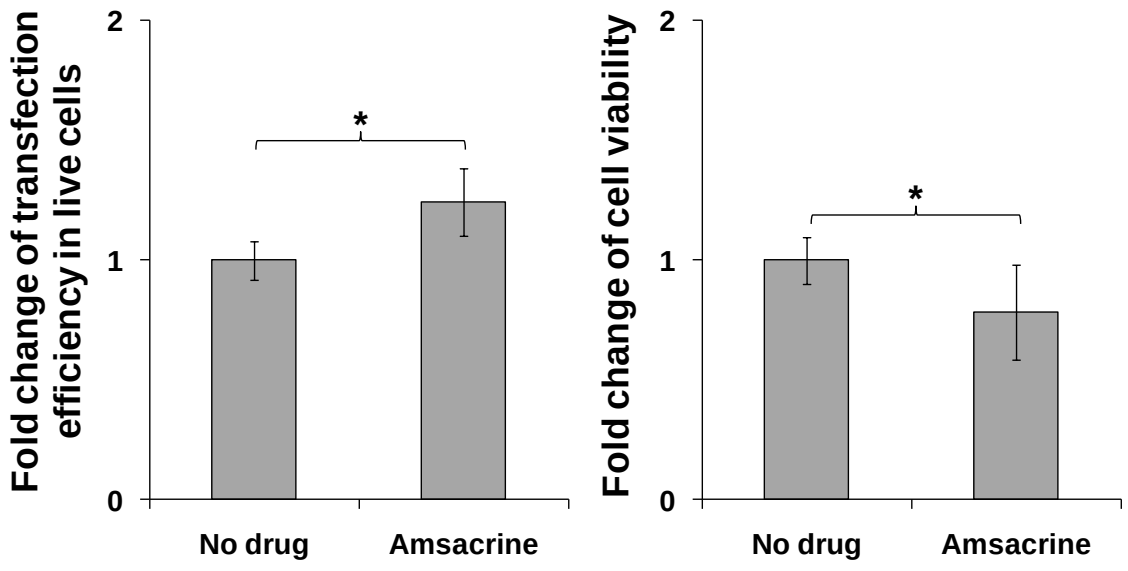

Figure 7.8: Amsacrine treatment (200 nM) increased the transfection efficiency mediated by US and decreased the cell viability. Data represent the averages of n ≥ 3 replicates with standard deviation (*paired Student's t-test, p < 0.05). US conditions: pressure amplitude of 0.78 MPa, total treatment time of 1 min with a pulse length of 0.25 ms at a duty cycle of 25%, Definity® concentration of 1 vol%.

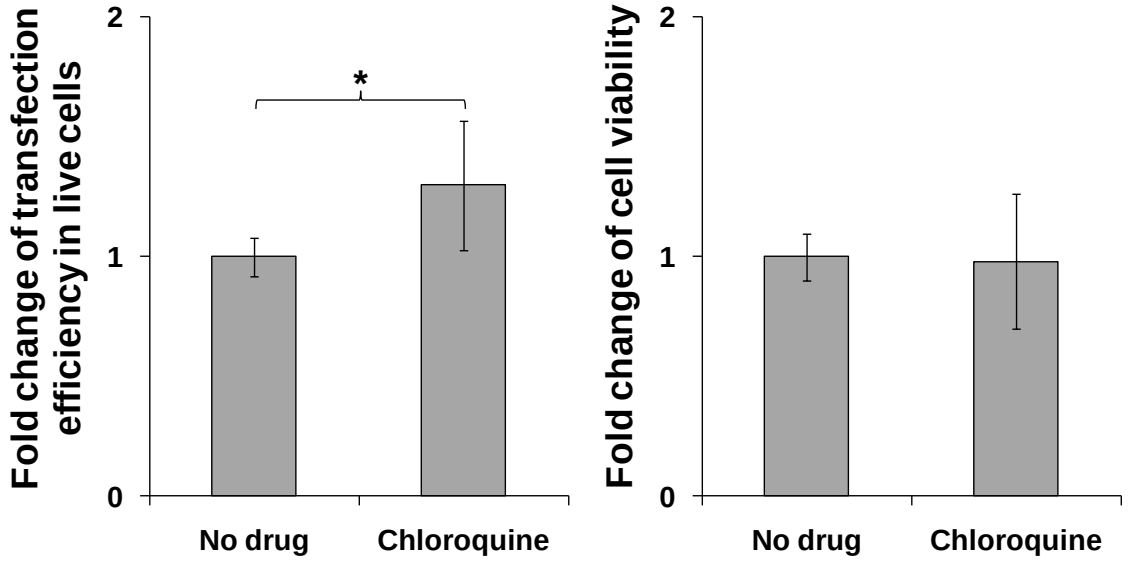

Figure 7.9: Chloroquine treatment (100 µM) increased the transfection efficiency mediated by US without affecting the cell viability. Data represent the averages of n

≥ 3 replicates with standard deviation (*paired Student's t-test, $p < 0.05$). US conditions: pressure amplitude of 0.78 MPa, total treatment time of 1 min with a pulse length of 0.25 ms at a duty cycle of 25%, Definity® concentration of 1 vol%.

Chloroquine is not only a TOP2α inhibitor but also a DNA interchalater (Luthman and Magnusson 1983; Sehested and Jensen 1996; Snyder 2000). As a weak organic base, chloroquine can neutralize the pH of endosomes/lysosomes and autophagosomes/ autophagolysosomes, and therefore possibly prevent DNA degradation (Maxfield 1982; Dijkstra et al. 1984; Erbacher et al. 1996). We previously observed the colocalization of pDNA with LysoTracker®-labeled autophagosomes/autophagolysosomes (Figure 6.7). To test whether chloroquine affected endosomes/lysosomes and autophagosomes/ autophagolysosomes, we measured the geometric mean of the green fluorescence indicating LysoTracker®-labeled endosomes/lysosomes and autophagosomes/ autophagolysosomes after US exposure with or without chloroquine treatment. As shown in Figure 7.10, the peak of the green fluorescence with chloroquine treatment shifted to the left compared to that without chloroquine treatment, indicating a less strong fluorescence of LysoTracker®-labeled endosomes/lysosomes and autophagosomes/ autophagolysosomes with chloroquine treatment. Therefore, it appears that chloroquine may increase transfection efficiency by a combination of down-regulating TOP2α and inhibiting autophagosomes/autophagolysosomes.

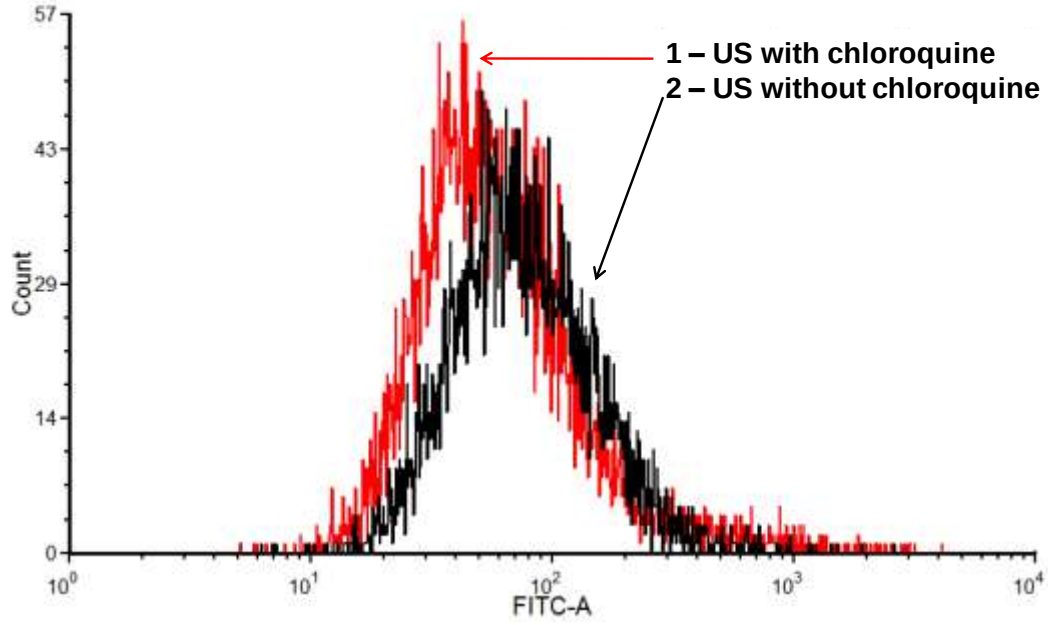

Figure 7.10: A representative FCM histogram showing the geometric mean of green fluorescence among sonicated cells after LysoTracker® staining decreased by an average of 24% (n = 6, paired Student's t-test p = 0.01) with chloroquine treatment. US conditions: pressure amplitude of 0.78 MPa, total treatment time of 1 min with a pulse length of 0.25 ms at a duty cycle of 25%, Definity® concentration of 1 vol%.

Etoposide

Similar like amsacrine, etoposide is also a TOP2α poison that can stabilize the structure of the DNA/TOP2 complex and cause DNA double-strand break (Liu 1989). Treating cells with etoposide for US exposure did not further increase gene transfection efficiency but decreased the cell viability (Figure 7.11).

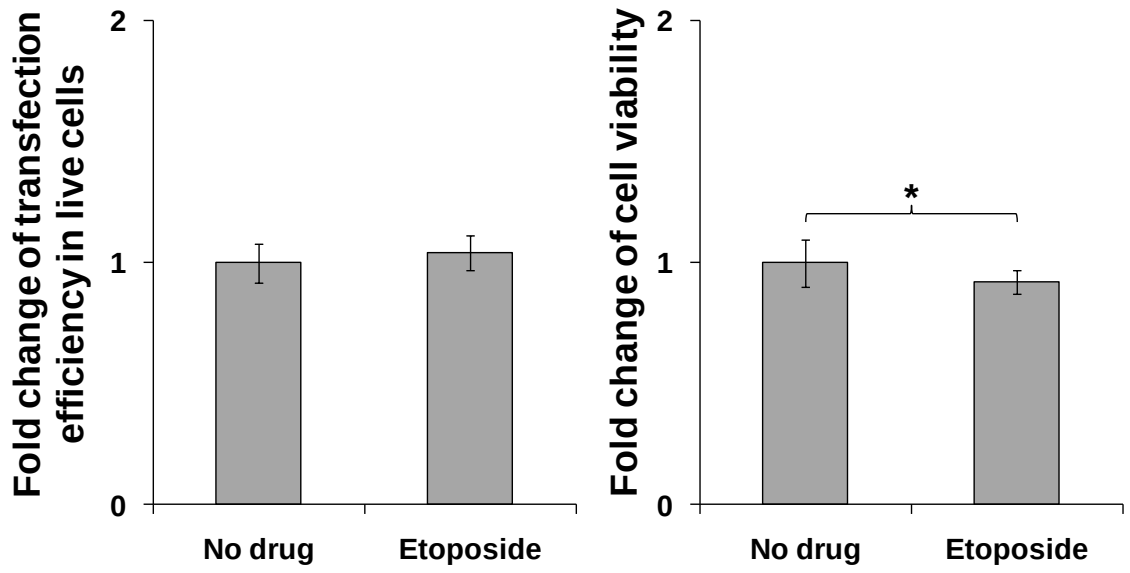

Figure 7.11: Etoposide treatment (200 nM) did not affect the transfection efficiency mediated by US but decreased the cell viability. Data represent the averages of n ≥ 3 replicates with standard deviation (*paired Student's t-test, p < 0.05). US conditions: pressure amplitude of 0.78 MPa, total treatment time of 1 min with a pulse length of 0.25 ms at a duty cycle of 25%, Definity® concentration of 1 vol%.

Mitoxantrone dihydrochloride

Mitoxantrone is another TOP2α poison. DU145 human prostate cancer cells were found to be relatively insensitive to certain TOP2 poisons including etoposide and mitoxantrone (Salido et al. 1999; van Brussel et al. 1999), which could explain the fact that at the concentrations we tested, no further enhancement of gene transfection was observed (Figure 7.12).

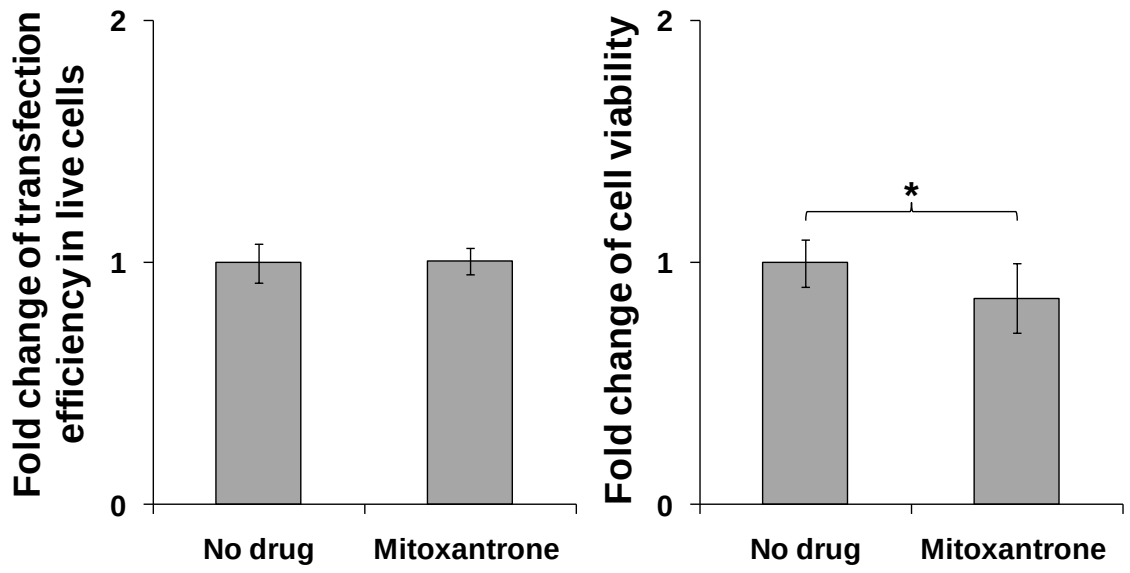

Figure 7.12: Mitoxantrone treatment (200 nM) did not affect the transfection efficiency mediated by US but decreased the cell viability. Data represent the averages of n ≥ 3 replicates with standard deviation (*paired Student's t-test, p < 0.05). US conditions: pressure amplitude of 0.78 MPa, total treatment time of 1 min with a pulse length of 0.25 ms at a duty cycle of 25%, Definity® concentration of 1 vol%.

Aclarubicin

Aclarubicin is another catalytic inhibitor of TOP2α by inhibiting the enzyme in binding to its substrate DNA (Andoh and Ishida 1998). Treating DU145 cells with aclarubicin for US exposure did not increase gene transfection efficiency while cell viability was further decreased by ~ 20% compared to US exposure alone (Figure 7.13).

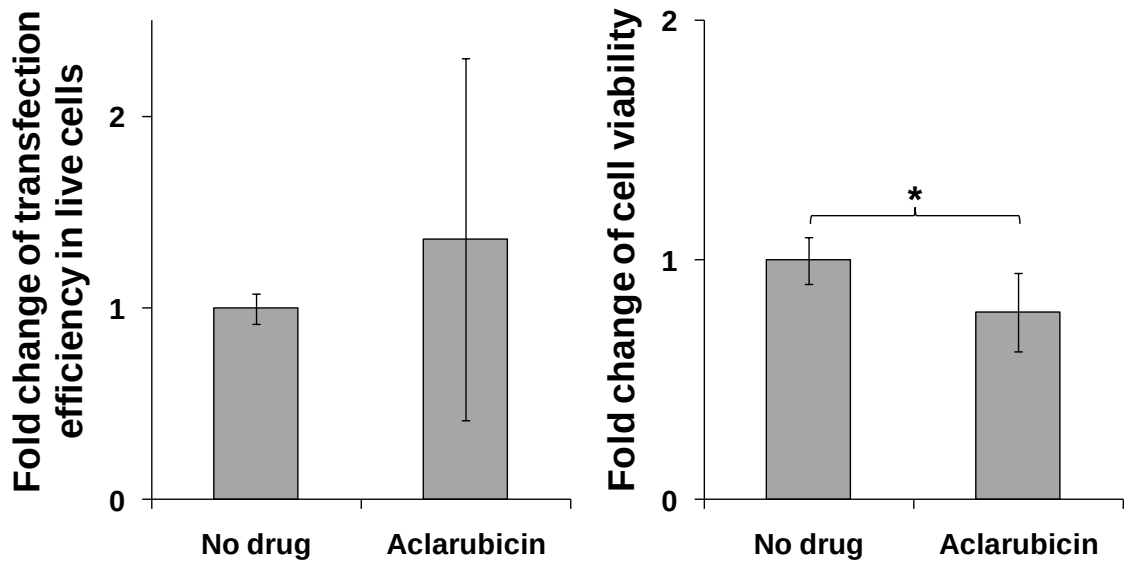

Figure 7.13: Aclarubicin treatment (50 nM) did not affect the transfection efficiency mediated by US but decreased the cell viability. Data represent the averages of n ≥ 3 replicates with standard deviation (*paired Student's t-test, p < 0.05). US conditions: pressure amplitude of 0.78 MPa, total treatment time of 1 min with a pulse length of 0.25 ms at a duty cycle of 25%, Definity® concentration of 1 vol%.

Expressional Regulation of TOP2α and GADD45α

To test whether the above four drugs that increased gene transfection efficiency regulated the expression level of TOP2α or GADD45α in DU145 cells, cells were sonicated with 100 μM chloroquine, 200 nM amsacrine, 0.6 mg/mL EMS, or 2 mM NMDA, separately, and incubated at growth conditions for 8 h. The results of qRT-PCR showed that in cells treated with EMS or NMDA, the expression level of GADD45α was found to be increased by 3 and 1.2 fold, respectively. The treatment with chloroquine decreased the expression level of TOP2α by 43%, and amsacrine decreased the expression level of TOP2α in DU145 cells by 21% (Figure 7.14). These results indicated

that EMS and NMDA enhanced the overexpression of GADD45α, and chloroquine and amsacrine inhibited the expression of TOP2α in DU145 cells.

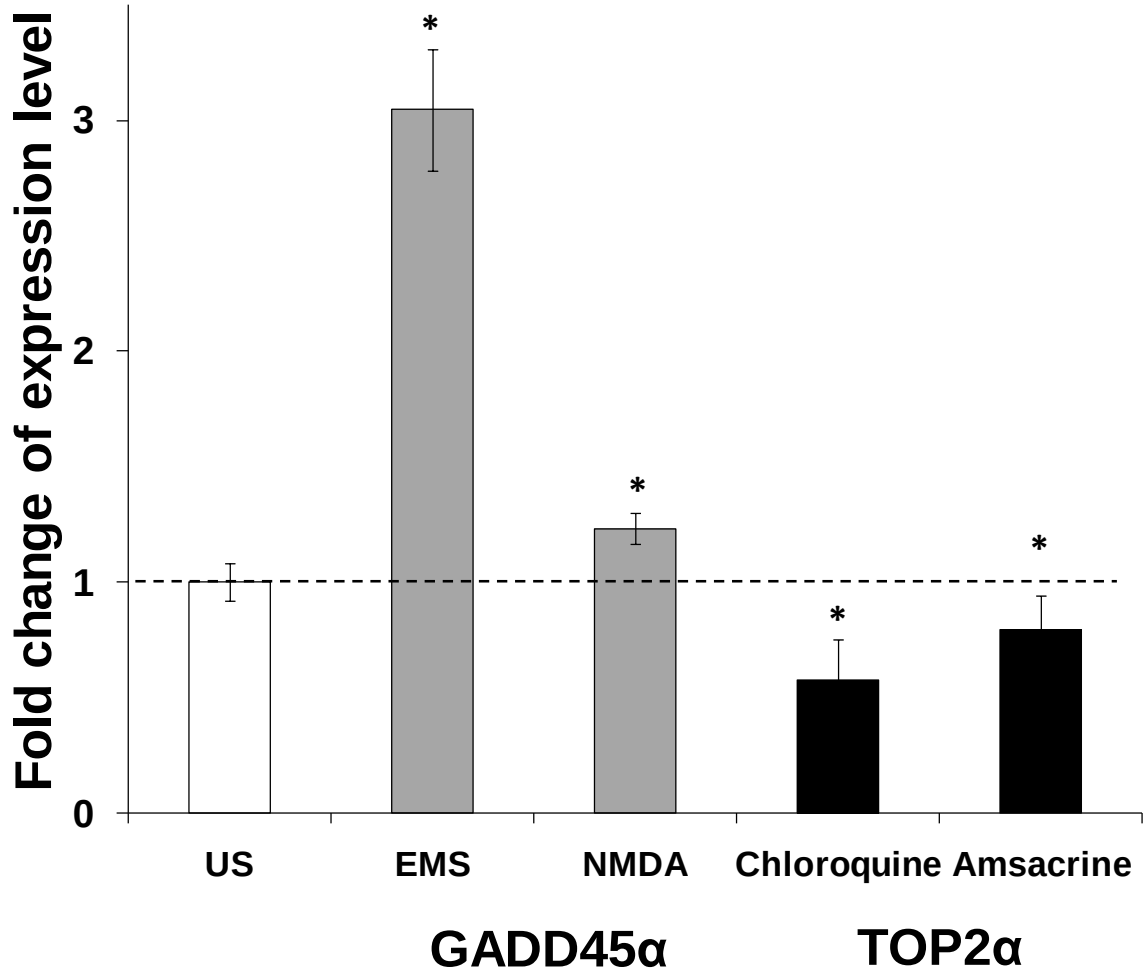

Figure 7.14: Results from qRT-PCR confirmed that the treatment with EMS or NMDA increased the expression level of GADD45α (grey bars), and the treatment with chloroquine or amsacrine decreased the expression level of TOP2α (black bars). Data represent the averages of n = 3 replicates with standard deviation ($p < 0.05$). US conditions: pressure amplitude of 0.78 MPa, total treatment time of 1 min with a pulse length of 0.25 ms at a duty cycle of 25%, Definity® concentration of 1 vol%.

Drugs that Regulate Active Transport and Trafficking

The regulation of DNA trafficking by enhancing active transport or inhibiting lysosomes-associated degradation to increase transfection efficiency was previously studied using gene delivery systems like electroporation and chemical vectors (Luthman and Magnusson 1983; Vaughan et al. 2008). Whether these regulations also facilitate US-mediated gene transfection is of interest. Therefore, in addition to the regulation of the expression levels of TOP2α and GADD45α, we also selected drugs that were found to enhance or suppress the active transport and trafficking in the cytoplasm and tested their bioeffects on US-mediated gene transfection.

Paclitaxel

Paclitaxel (Taxol®) is an anti-tumor drug that is known to stabilize microtubules and thereby prevent cancer cells from division (Horwitz 1994). Some gene delivery vectors including viral and chemical vectors were previously verified to utilize microtubules to reach the nucleus (Bukrinskaya et al. 1998; Suomalainen et al. 1999; Vihinen-Ranta et al. 2000; Ogawa-Goto et al. 2003; Bausinger et al. 2006). It is suggested that plasmid DNA may also utilize microtubules to transport from the cell membrane to the nucleus in other physical gene delivery systems. Stabilizing microtubules was found to increase gene transfection efficiency using electroporation and microinjection (Vaughan and Dean 2006). In our study, when cells were sonicated with paclitaxel, transfection efficiency in live cells was increased by ~ 27%. However, cell viability was decreased by 24% compared to US exposure alone. Because of the further

decrease in cell viability caused by paclitaxel, the overall transfection efficiency among all the cells was not affected compared to US exposure alone (Figure 7.15).

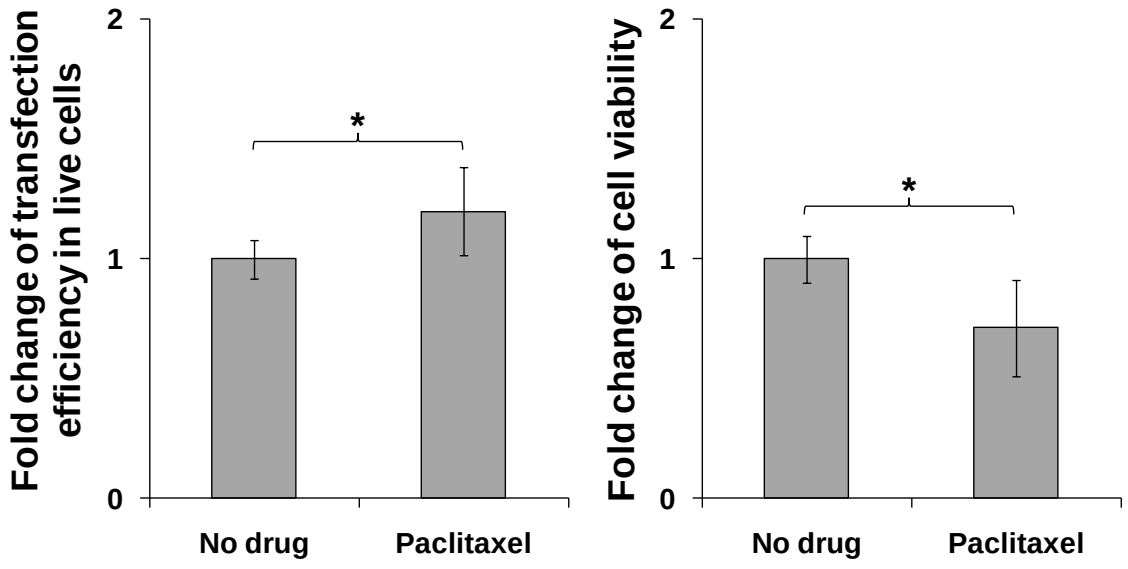

Figure 7.15: Paclitaxel treatment (16 μM) increased the transfection efficiency in live cells but decreased the cell viability. Data represent the averages of n ≥ 3 replicates with standard deviation (*paired Student's t-test, p < 0.05). US conditions: pressure amplitude of 0.78 MPa, total treatment time of 1 min with a pulse length of 0.25 ms at a duty cycle of 25%, Definity® concentration of 1 vol%.

Docetaxel

Docetaxel (Taxotere®) is an analog of paclitaxel. It was demonstrated to have higher affinity for microtubules and thereby stronger cytotoxicity to cancer cells (Pazdur et al. 1993). With docetaxel treatment, the transfection efficiency was increased by 30% in live cells, but the cell viability was decreased by 36% compared to US exposure alone. The overall transfection efficiency among all the cells was decreased because of the decrease in cell viability (Figure 7.16).

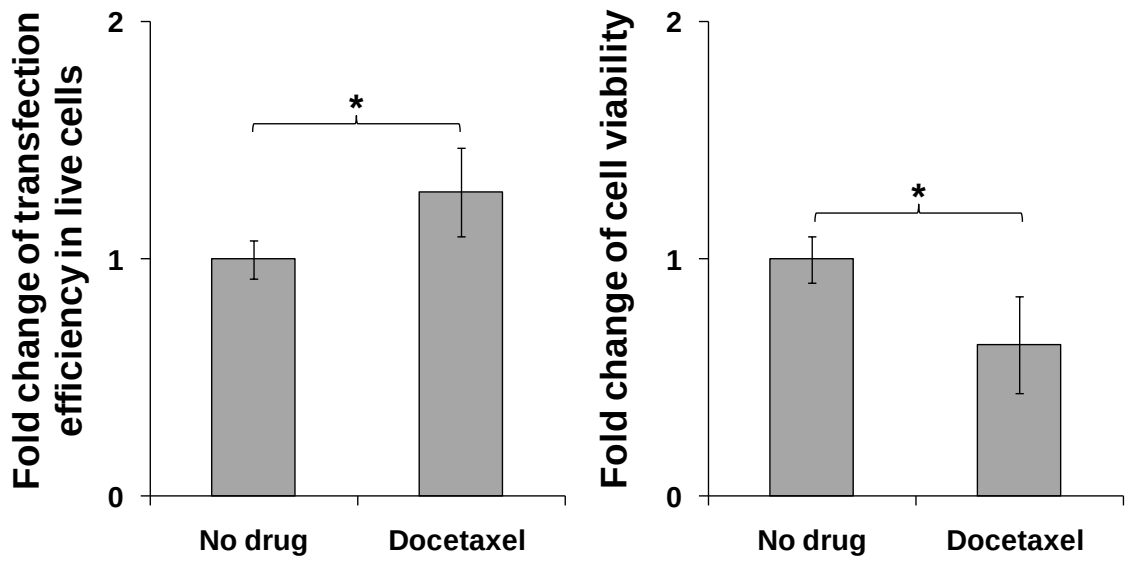

Figure 7.16: Docetaxel treatment (16 μM) increased the transfection efficiency in live cells but decreased the cell viability. Data represent the averages of n ≥ 3 replicates with standard deviation (*paired Student's t-test, p < 0.05). US conditions: pressure amplitude of 0.78 MPa, total treatment time of 1 min with a pulse length of 0.25 ms at a duty cycle of 25%, Definity® concentration of 1 vol%.

Tetracaine Hydrochloride

We found that enhancing active transport using microtubule stabilizing drugs (paclitaxel and docetaxel) could increase transfection efficiency in live cells post US exposure, but cause further damage to cell viability. We were also interested to test if inhibiting transport in the cytoplasm could cause any decrease in gene transfection efficiency. Tetracaine is a local anesthetic that is able to suppress the movement of motor proteins and thereby inhibit the active transport along the cytoskeleton (Ayad and White 1977; Miyamoto et al. 2000). When tetracaine was added to the cell samples for US exposure, gene transfection efficiency was decreased by ~ 25% and the viability of

DU145 cells was not affected (Figure 7.17). This result indicated that inhibiting active transport in cells could decrease gene transfection efficiency after US exposure.

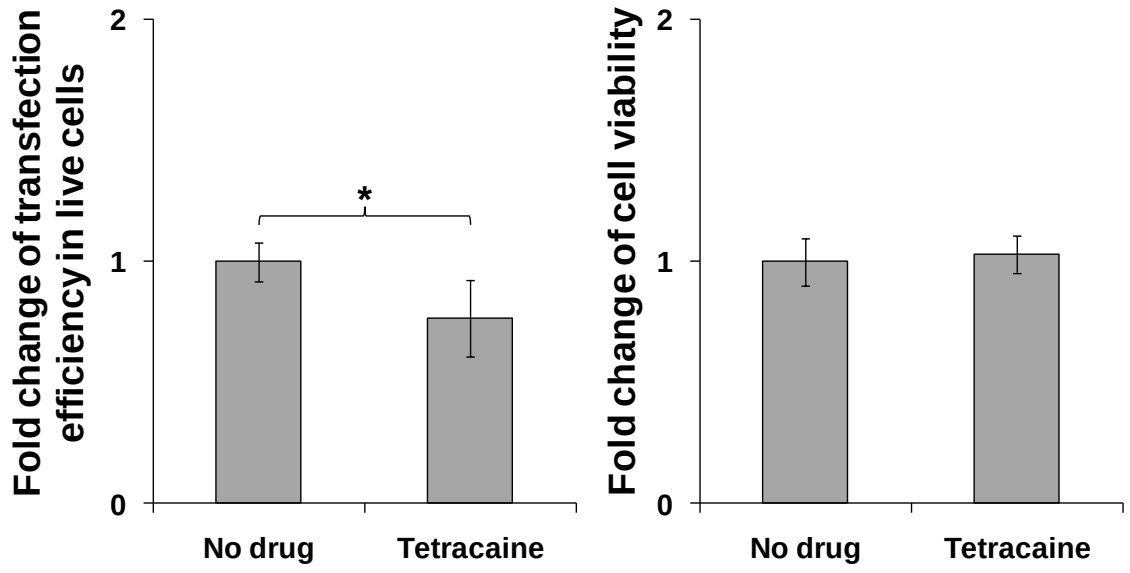

Figure 7.17: Tetracaine treatment (20 μM) decreased the transfection efficiency mediated by US without affecting the cell viability. Data represent the averages of n ≥ 3 replicates with standard deviation (*paired Student's t-test, $p < 0.05$). US conditions: pressure amplitude of 0.78 MPa, total treatment time of 1 min with a pulse length of 0.25 ms at a duty cycle of 25%, Definity® concentration of 2 vol%.

Bafilomycin A1

Bafilomycin A1 was previously found to be able to prevent maturation of autophagic vacuoles (Yamamoto et al. 1998), and therefore might be able to prevent pDNA from degradation. However, when adding 250 nM bafilomycin A1 to the sonication sample, we did not observe any increase in gene transfection efficiency but further decrease in cell viability by ~ 30% (Figure 7.18).

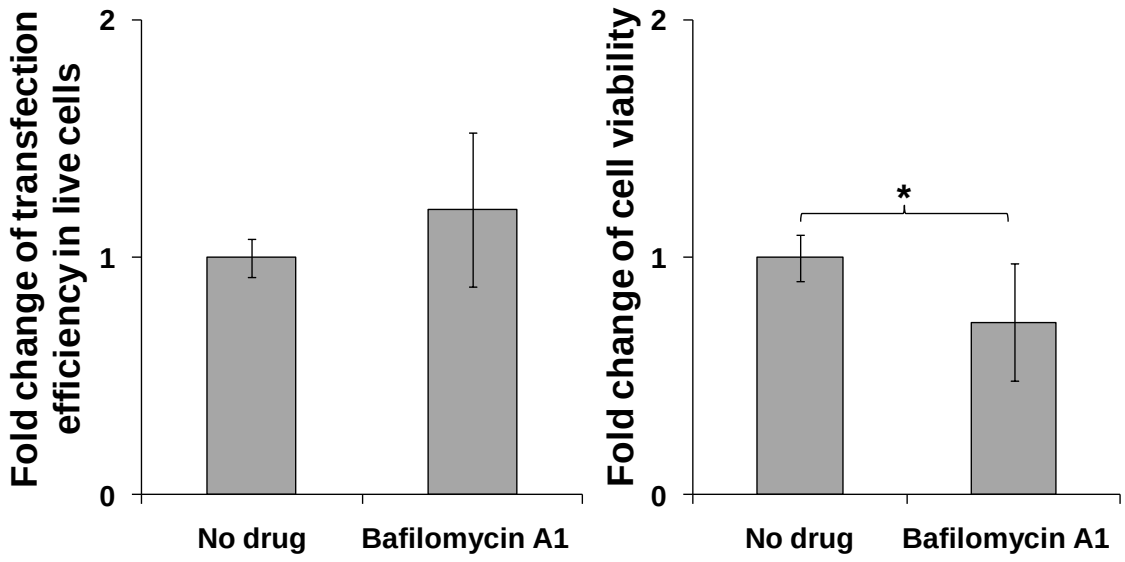

Figure 7.18: Bafilomycin A1 (250 nM) did not affect the transfection efficiency mediated by US but decreased the cell viability. Data represent the averages of n ≥ 3 replicates with standard deviation (*paired Student's t-test, p < 0.05). US conditions: pressure amplitude of 0.78 MPa, total treatment time of 1 min with a pulse length of 0.25 ms at a duty cycle of 25%, Definity® concentration of 1 vol%.

Uptake Efficiency with Drug Treatment

So far we have found the several drugs could enhance gene transfection mediated by US and hypothesized that they acted by influencing DNA trafficking within the cell, as opposed to affecting DNA uptake into the cell. We therefore also tested whether adding these drugs could affect the uptake efficiency of pDNA in DU145 cells. As shown in Figure 7.19, the DNA uptake efficiency mediated by US exposure was not affected by the treatment with drugs.

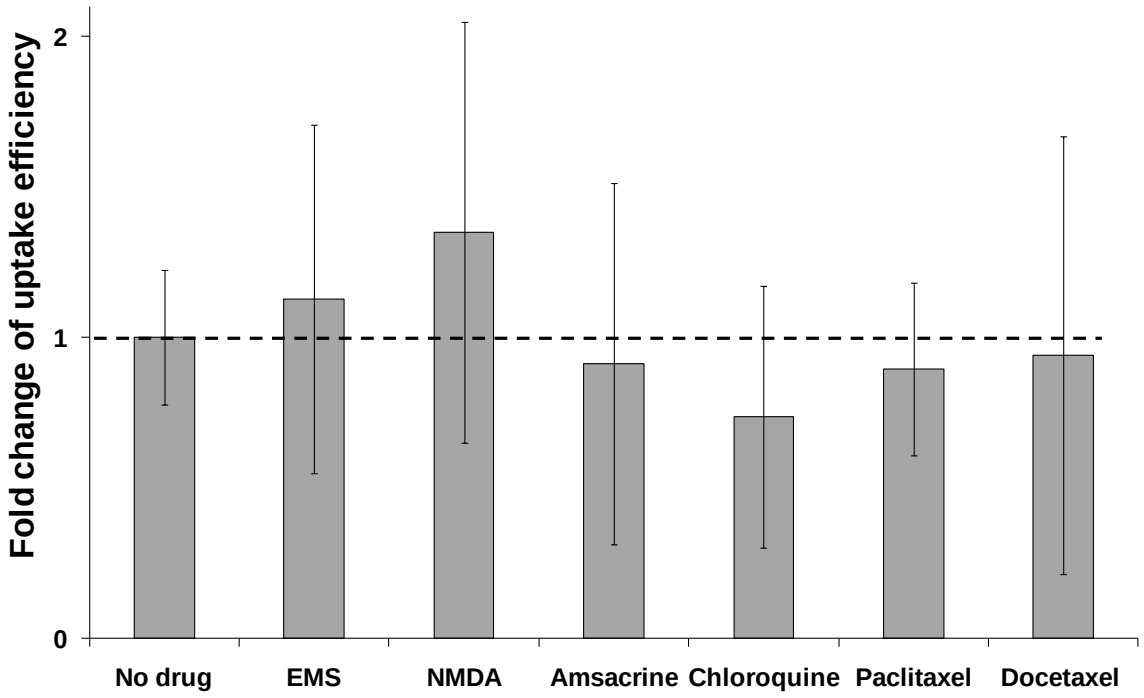

Figure 7.19: Fold change of US-mediated DNA uptake with and without drug treatment of 0.6 mg/mL EMS, 2 mM NMDA, 200 nM amsacrine, 100 µM chloroquine, 16 µM paclitaxel, or 16 µM docetaxel. Data represent the averages of n = 3 replicates and the error bars represent 95% confidence interval (Student's t-test, p > 0.05). US conditions: pressure amplitude of 0.78 MPa, total treatment time of 1 min with a pulse length of 0.25 ms at a duty cycle of 25%, Definity® concentration of 1 vol%.

Treatment with the Regulation of both TOP2α and GADD45α

Previously we found EMS and NMDA increased transfection efficiency post US exposure by inducing the overexpression of GADD45α, and amsacrine and chloroquine enhanced gene transfection mediated by US by inhibiting the expression of TOP2α in DU145 cells. We then regulated the expression levels of GADD45α and TOP2α at the same time and tested the bioeffects on gene transfection.

EMS and Amsacrine

Combine EMS and amsacrine treatment with US exposure, and we increased gene transfection efficiency by ~ 30% without affecting the cell viability (Figure 7.20).

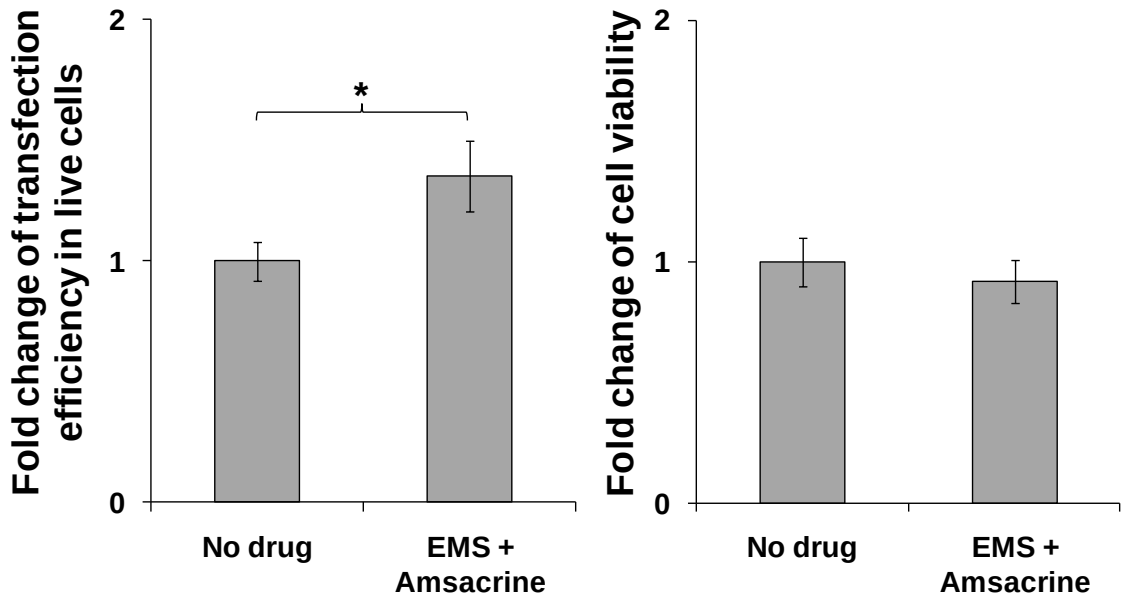

Figure 7.20: Drug treatment with 0.6 mg/mL EMS and 200 nM amsacrine increased the transfection efficiency mediated by US without affecting the cell viability. Data represent the averages of n ≥ 3 replicates with standard deviation (*paired Student's t-test, p < 0.05). US conditions: pressure amplitude of 0.78 MPa, total treatment time of 1 min with a pulse length of 0.25 ms at a duty cycle of 25%, Definity® concentration of 1 vol%.

EMS and Chloroquine

When cells were treated with both EMS and chloroquine for US exposure, gene transfection efficiency was increased by 2 fold and the cell viability was not affected (Figure 7.21).

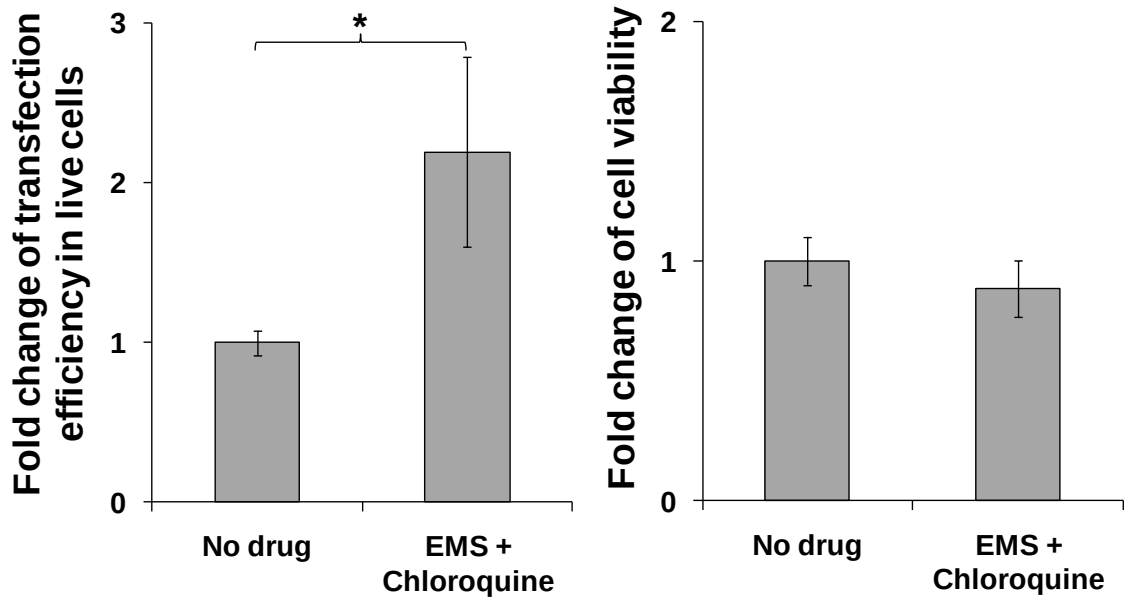

Figure 7.21: Drug treatment with 0.6 mg/mL EMS and 100 μM chloroquine increased the transfection efficiency mediated by US without affecting the cell viability. Data represent the averages of n ≥ 3 replicates with standard deviation (*paired Student's t-test, p < 0.05). US conditions: pressure amplitude of 0.78 MPa, total treatment time of 1 min with a pulse length of 0.25 ms at a duty cycle of 25%, Definity® concentration of 1 vol%.

NMDA and Amsacrine

Combine NMDA and amsacrine treatment with US exposure, and we increased gene transfection efficiency in DU145 cells by ~ 50%. The cell viability was decreased by ~ 10%, but the overall transfection efficiency among all the cells was increased compared to US exposure alone (Figure 7.22).

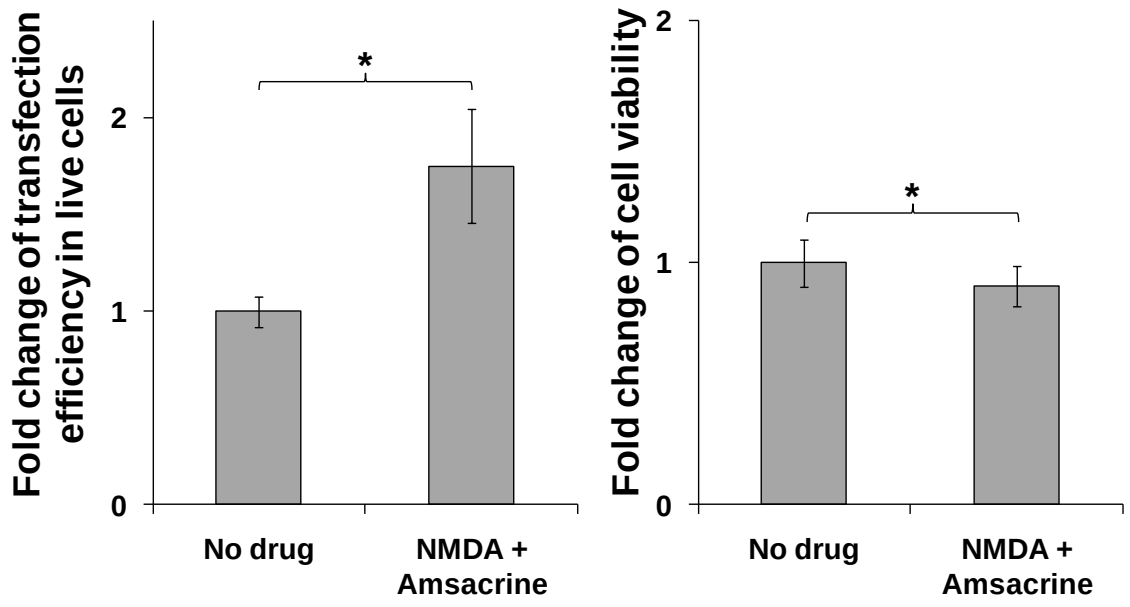

Figure 7.22: Drug treatment with 2 mM NMDA and 200 nM amsacrine increased the transfection efficiency mediated by US but decreased the cell viability. Data represent the averages of n ≥ 3 replicates with standard deviation (*paired Student's t-test, p < 0.05). US conditions: pressure amplitude of 0.78 MPa, total treatment time of 1 min with a pulse length of 0.25 ms at a duty cycle of 25%, Definity® concentration of 1 vol%.

NMDA and Chloroquine

When cells were treated with both NMDA and chloroquine for US exposure, gene transfection efficiency in live cells was increased by ~ 20% and the cell viability was decreased by ~ 10%. The overall transfection efficiency among all the cells was not found to be different from US exposure alone (Figure 7.23).

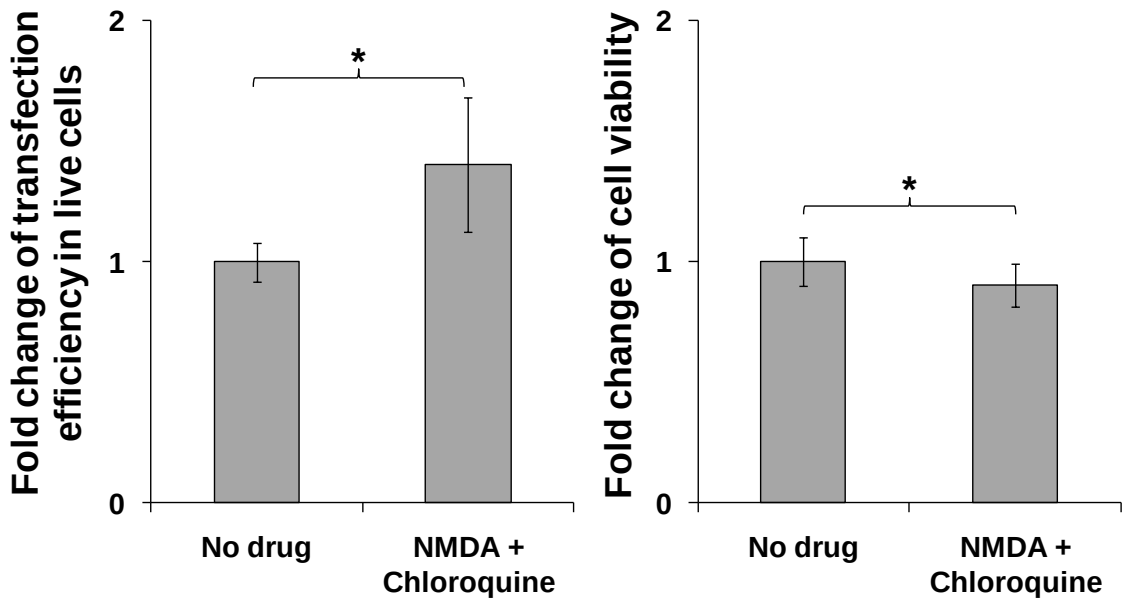

Figure 7.23: Drug treatment with 2 mM NMDA and 100 μM chloroquine increased the transfection efficiency mediated by US but decreased the cell viability. Data represent the averages of n ≥ 3 replicates with standard deviation (*paired Student's t-test, p < 0.05). US conditions: pressure amplitude of 0.78 MPa, total treatment time of 1 min with a pulse length of 0.25 ms at a duty cycle of 25%, Definity® concentration of 1 vol%.

Summarized Results of Drug Treatment

A summary of our findings from the drug treatment combined with US exposure is shown in Figure 7.24 and Appendix D. We found treating cells with EMS, NMDA, Amsacrine, chloroquine, paclitaxel and docetaxel increased transfection efficiency in live cells mediated by US exposure (Figure 7.24a). The overall transfection efficiency among all the cells was dependent on cell viability. EMS and chloroquine did not affect the cell viability, while NMDA, amsacrine, paclitaxel and docetaxel caused damage to the cell viability (Appendix D). Therefore, the transfection efficiency among all the cells was not affected by NMDA and paclitaxel, and decreased by docetaxel (Figure 7.24b).

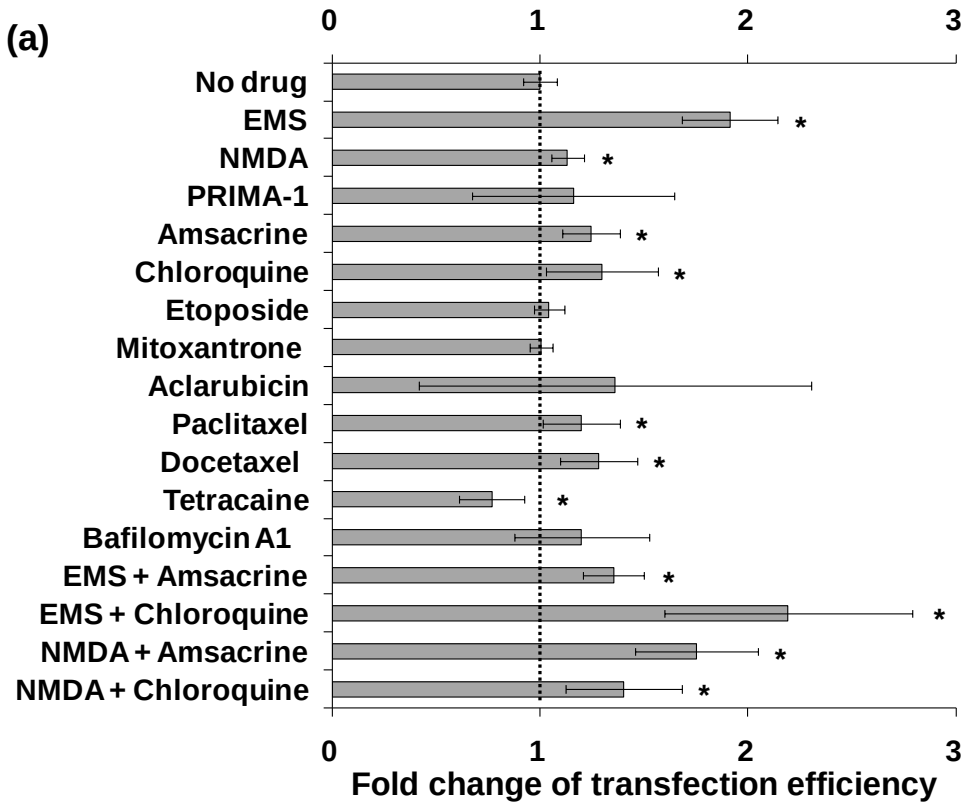
(a)
0
1
2
3
No drug
EMS
NMDA
PRIMA-1
Amsacrine
Chloroquine
Etoposide
Mitoxantrone
Aclarubicin
Paclitaxel
Docetaxel
Tetracaine
Bafilomycin A1
EMS + Amsacrine
EMS + Chloroquine
NMDA + Amsacrine
NMDA + Chloroquine
*
Fold change of transfection efficiency

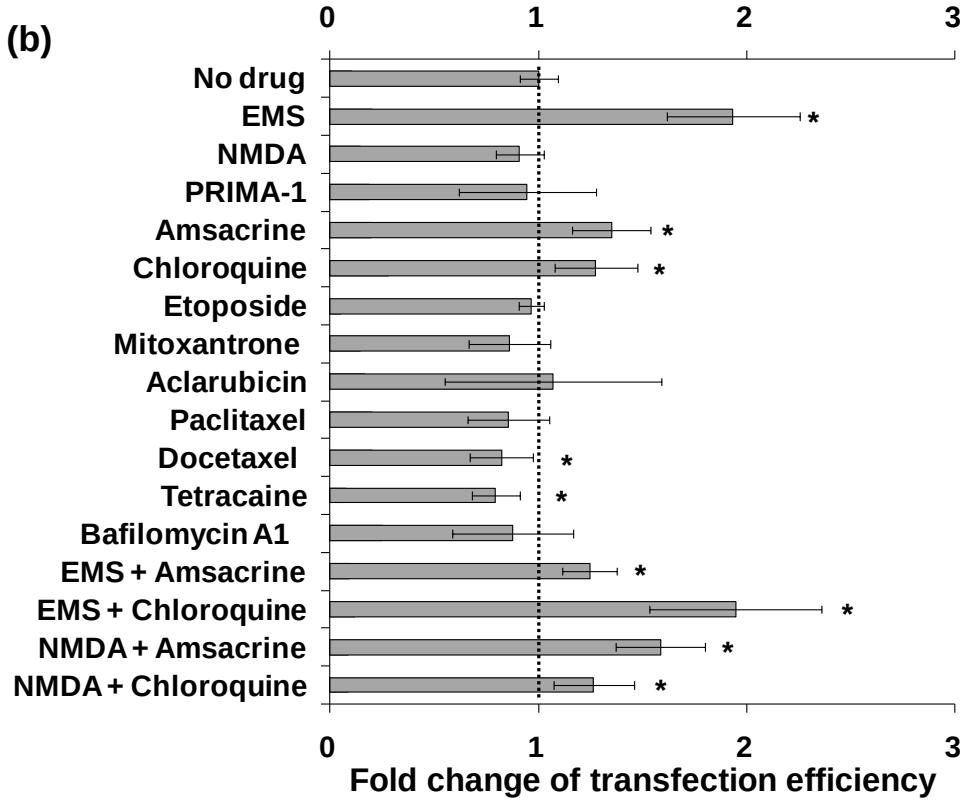
(b)
0
1
2
3
No drug
EMS
NMDA
PRIMA-1
Amsacrine
Chloroquine
Etoposide
Mitoxantrone
Aclarubicin
Paclitaxel
Docetaxel
Tetracaine
Bafilomycin A1
EMS + Amsacrine
EMS + Chloroquine
NMDA + Amsacrine
NMDA + Chloroquine
*
Fold change of transfection efficiency

Figure 7.24: The fold change of gene transfection efficiency in (a) live cells and (b) all cells with drug treatment compared to that without drug treatment. Data represent the averages of n ≥ 3 replicates. The error bars represent 95% confidence interval (*Student's t-test p < 0.05, compared to no drug treatment). The concentration used for each drug: 0.6 mg/mL EMS, 2 mM NMDA, 1 mM PRIMA-1, 200 nM amsacrine, 100 μM chloroquine, 200 nM etoposide, 200 nM mitoxantrone, 50 nM aclarubicin, 16 μM paclitaxel, 16 μM docetaxel, 20 μM tetracaine and 250 nM bafilomycin A1. US conditions: pressure amplitude of 0.78 MPa, total treatment time of 1 min with a pulse length of 0.25 ms at a duty cycle of 25%, Definity® concentration of 1 vol%.

Under the conditions we have tested, PRIMA-1, etoposide, mitoxantrone, aclarubicin and bafilomycin A1 did not affect gene transfection mediated by US (Figure 7.24), but decreased the cell viability (Appendix D). Suppressing active transport by tetracaine decreased transfection efficiency (Figure 7.24) without affecting the cell viability (Appendix D). Combine the treatment to regulate the expression levels of TOP2α and GADD45α at the same time, and we found US-mediated gene transfection was enhanced compared to US exposure alone. The enhancement in transfection with two drugs was not significantly different from that with one drug (Figure 7.24).

Discussion

The heterogeneous bioeffects caused by US may be one of the major reasons responsible for the low gene transfection efficiency. US exposure generates various populations of dead cells, live cells with pDNA uptake, live cells with successful gene transfection, and live cells with neither of the two bioeffects. In this study, we transfected DU145 cells with GFP encoded pDNA using 1 MHz US, and analyzed gene expression in cells with GFP expression and cells with pDNA uptake but no GFP expression using microarray. Genes related to cell cycle were found to play an important role in US-

mediated gene transfection. Cells with successful GFP expression were found to be associated with cell cycle regulation, which is consistent with the independent cell cycle analysis. These findings suggested that slowing down cell cycle was good for gene transfection mediated by US. This would possibly favor the *in vivo* application of US for gene therapy, because cells packed in tissues generally have slow cell cycle.

Among all the genes of interest, GADD45α and TOP2α were chosen for further study because they were two of the most up/down-regulated genes and they were both related to cell cycle regulation. We proposed three strategies to enhance US-mediated gene transfection by up-regulating GADD45α, down-regulating TOP2α, and enhacing or surpressing active transport and trafficking in the cytoplasm. Several drugs were selected according to these strategies to test the bioeffects combined with US exposure.

In the previous chapter we reported that under the optimal US conditions, the maximum pDNA uptake was ~ 30% right after US exposure, while the maximum transfection efficiency was ~ 12% observed at 8 h post US exposure (Figure 6.3). In this study, combine US exposure and the treatment with 0.6 mg/mL EMS and 100 μM chloroquine, or EMS alone, and we further increased transfection efficiency by ~ 2 fold. These results indicated that combining drug treatment with US exposure, we could possibly increase gene transfection efficiency as high as close to the DNA uptake efficiency. Using microtubule stablilizers for US exposure also enhanced gene transfection, and inhibiting active tranport by tetracaine decreased gene transfection efficiency. These results indicated that possible active transport of DNA was happening in cells post US exposure. Facilitating active tranport could potentially enhance gene transfection mediated by US.

It is already known that different cell lines respond differently to either US exposure (Larina et al. 2005) or drug treatment (Fry et al. 1991; Schatten et al. 2000; Lanzi et al. 2001). One cell line also responds differently to similar drugs that are expected to have the same effects. In this study, we used DU145, an androgen-insensitive prostate cancer cell line that generally expresses high level of TOP2α (Pourpak et al. 2007). Since the cellular TOP2α level is related to chemosensitivity to certain TOP2α inhibitors (Fry et al. 1991; Asano et al. 1996; Burden and Osheroff 1998; Bronner et al. 2002), DU145 cells are relatively insensitive to certain TOP2 poisons like etoposide and mitoxantrone (Salido et al. 1999; van Brussel et al. 1999). These factors may contribute to our results that chloroquine and amsacrine enhanced US-mediated gene transfection, while mitoxantrone or etoposide did not show similar effects. Both chloroquine and aclarubicin are catalytic inhibitors of TOP2α. However, in our study, cells reacted differenctly to these two drugs. The treatment with 100 μM chloroquine enhanced gene transfection mediated by US exposure without casuing further damage to the cell viability, while 50 nM aclarubicin decreased the viability of DU145 cells by ~ 20% compared to US exposure alone, but did not affect gene transfection.

Most of these drugs we have tested are anti-tumor durgs, which are able to regulate cell cycle, induce apoptosis or necrosis and kill cancer cells. Therefore, the viability of DU145 cells was likely affected, and that may or may not be a wanted effect depending on the purpose of gene therapy. Some of these drugs have multiple functions and may affect gene transfection through multiple mechanisms. For example, chloroquine is a catalytic inhibitor of TOP2 and also a DNA interchalator that could prevent pDNA from degradation (Luthman and Magnusson 1983). Etoposide as a TOP2 poison was also

tested on its function to enhance GADD45α as a DNA-damaging agent, however, those studies indicated that etoposide treatment had some but limited capability of inducing GADD45α expression (West et al. 2002; Li et al. 2009).

Since the drugs we have tested are mostly toxic to DU145 cells, we chose to add them to the concentrated cell suspension, perform US and incubate cells at the growth conditions for 8 h with a much lower concentration of drugs (a dilution of 50 times). In this way, we expected to have efficient delivery of these drugs in cells and reduce harm to cells. To optimize the effects of drug treatment, more detailed studies may be designed to investigate the time of adding these drugs (before or after US exposure) and the overall treatment time. It is also possible that changing drug concentration could result in different effects on cell viability and gene transfection, although higher concentration of EMS in our study did not show any difference from the lower concentration treatment. Other methods to regulate gene expression, such as siRNA, could also be tested. While the specific drugs examined in this study may be useful directly for possible US-based gene transfection, the greater value of this study may be identification of bottlenecks to DNA delivery, which suggest additional strategies that do no involve toxic chemotherapeutics, such as employing siRNA to modulcate TOP2α, GADD45α and other protein expression, nuclear localization sequences to direct DNA trafficking to the nucleus, cell cycle modulation by various other means and strategies.

Gene transfection efficiency was found to be dependent on cell cycle in some chemical non-viral delivery systems (Mortimer et al. 1999; Brunner et al. 2000). This is the first time when the cell cycle dependency of transfection efficiecy was studied with US as a gene delivery strategy. The fact that GADD45α was overexpressed and TOP2α

was down-regulated in the cells with successful gene transfection, which accumulated at the G1 phase of cell cycle, may offer new clues for the better understanding of the mechanism of US-mediated gene transfection. We verified in this study that by regulating the expression level of GADD45α and TOP2α and other intracellular processes, higher efficiency of US-mediated gene transfection could be achieved.

CHAPTER 8: THE INTEGRITY OF GENE DELIVERY CARRIERS

Introduction

Although US has been widely used in clinics, safety is a concern when designing US systems for drug delivery and gene transfection. In this part of the study, a broad range of US conditions were tested to evaluate the possibility that US exposure can adversely affect the integrity and, therefore, the bioactivity of various therapeutic agents. We carried out studies to examine the effects of US on the integrity of plasmid DNA, siRNA and a viral vector. We selected these models because they are of interest to gene-based therapies and might be more sensitive to damage by US. Possible damage to neuronal cells by US exposure was also examined. The results indicated that US itself did not affect the integrity of gene delivery carriers and cell viability over the range of US conditions tested. US may offer a safe treatment strategy for gene transfection.

Results

To assess whether US damages DNA, we exposed plasmid DNA encoding GFP to US over energy densities ranging from 0 to 12,000 J/cm^2. We selected this range of US conditions because it included and well exceeded those found to be useful for enhanced delivery *in vitro* and *in vivo* in the previous sections. After sonication, the DNA was transfected into cultured cells using a lipid transfection agent as an assessment of DNA integrity. There was no significant difference in transfection efficiency between DNA sonicated at any of the conditions tested compared to non-sonicated controls ($p > 0.05$) as shown in Figure 8.1a. Note that sonication was not used in this study to aid DNA entry

into cells, as has been shown in the previous chapters. The goal of this safety study was to determine if sonication damaged DNA in some way that affected subsequent transfection of cells.

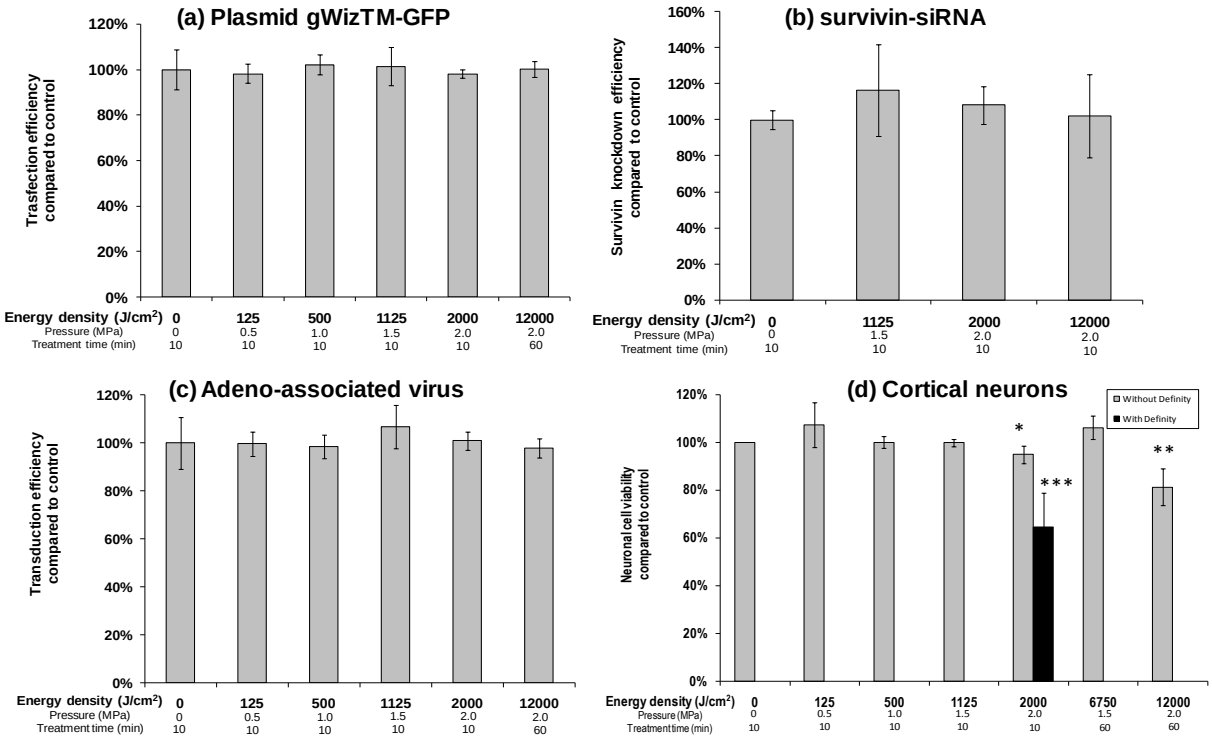

Figure 8.1: Effect of US exposure on plasmid DNA, siRNA, and virus integrity and cortical neuron viability. (a) Plasmid gWizTM-GFP and (b) survivin-siRNA were sonicated and subsequently transfected to DU145 cells by Lipofectamine 2000. Each bar displays the average and standard deviation of (a) the transfection efficiency normalized by the non-sonicated control DNA and (b) the survivin knockdown efficiency normalized by the non-sonicated siRNA (n ≥ 4 replicates). Percent survivin knockdown was determined based on survivin expression levels from cells without siRNA transfection set equal to 0% protein knockdown. Student's t-test showed no significant changes in (a) transfection efficiency and (b) knockdown efficiency at any of the conditions tested relative to the non-sonicated control (p > 0.05). (c) Adeno-associated virus was sonicated and subsequently transduced to HT-1080 cells. Each bar displays the average and standard deviation of the transduction efficiency normalized by non-sonicated control virus (n ≥ 4 replicates). Student's t-test showed no significant changes in transduction efficiency at any of the conditions tested relative to the non-sonicated control (p > 0.05). (d) Cortical neurons were sonicated at different US conditions and, in one case, in the presence of Definity® US contrast agent. Each bar displays the average and standard deviation of the cell

viability normalized by non-sonicated control neurons (n ≥ 4 replicates). Student's t-test showed no significant changes in cell viability at any of the conditions tested relative to the non-sonicated control (p > 0.05), except at the conditions indicated: (*) p = 0.016, (**) p = 0.0013, (***) p = 0.0006.

A similar experiment was carried out to assess the effects of US on the ability of siRNA to knock down expression of a model protein, survivin. As shown in Figure 8.1b, there were no significant differences in the level of protein knockdown between siRNA sonicated at any of the conditions tested compared to non-sonicated controls ($p > 0.05$).

The effects of US on function of an adeno-associated virus are shown in Figure 8.1c. Over the range of conditions examined, there were no significant differences in the level of transduction efficiency between sonicated adeno-associated virus and non-sonicated controls ($p > 0.05$), indicating the integrity of virus was not affected by US.

Finally, the effect of US on the viability of cortical neurons freshly harvested from fetal rats was examined. As shown in Figure 8.1d, sonication at pressures up to 1.5 MPa for up to 60 min (energy density 6,750 J/cm^2) had no significant effect on neuronal cell viability ($p > 0.05$), which is consistent with the previous histology study. However, cell viability was decreased when the acoustic pressure was increased to the highest energy density of 12,000 J/cm^2, which caused cell viability to decrease by 19% ($p = 0.0013$). As a positive control, sonication was carried out at 2,000 J/cm^2 in the presence of Definity® US contrast agent, which served to nucleate cavitation activity. Under these conditions, cell viability was reduced by 35% ($p = 0.0006$). However, the conditions that caused losses of cell viability are much stronger than the ones found to be useful for gene transfection in the previous sections.

Discussion

This study provided an initial assessment of the safety of US exposure for gene delivery. Because of its non-invasive nature, US has the potential to avoid tissue damage. This expected safety, under other US conditions, is well established for clinical use of US for diagnostic imaging and therapeutic heating (Fowlkes and Holland 2000). In this study, exposure of US was found to be well tolerated by cultured cortical neurons *in vitro.* Specifically, viability of cortical neurons was unaffected over most US conditions. Sonication at the highest energy density of 12,000 J/cm^2 significantly reduced cell viability; however, this energy level was well beyond the minimum conditions found to be effective for enhanced delivery.

As a secondary objective, we evaluated the potency of US not only to facilitate gene transfection but also to preserve the biological activity of the gene carriers delivered by it. The sonochemical effects of US such as production of free radicals during cavitation events have been demonstrated to change the activity of drugs (Rosenthal et al. 2004). We carried out experiments designed to assess the functionality of several therapeutic biomolecules of interest after US treatment. This study showed that exposure to US at any of the conditions tested did not significantly affect transfection efficiency of the plasmid DNA, protein knockdown efficiency of the siRNA, or transduction efficiency of the adeno-associated virus. These studies suggest that there is a broad range of US conditions that may be suitable for enhanced gene transfection without damaging the integrity of plasmid DNA, siRNA, adeno-associated virus or cortical neurons. Additional *in vivo* studies will be needed, which eliminate the artifacts of *in vitro* cells in suspension,

such as increased shear stress due to acoustic streaming and cavitational activity, and the inability of cell culture models to fully mimic tissues *in vivo*.

CHAPTER 9: DISCUSSION AND CONCLUSIONS

US-mediated gene transfection is of interest among the current gene delivery systems due to its unique expected advantages, including: low toxicity, low immunogenicity, the potential for repeated application, organ specificity and broad applicability to acoustically accessible organs (Gao et al. 2007). However, the major problem in US-mediated gene transfection is the low transfection efficiency. *In vitro* US exposure generates various populations of dead cells, live cells with pDNA uptake, live cells with successful gene transfection, and live cells with neither of the two bioeffects. In this study, we transfected DU145 cells with GFP encoded pDNA using 1 MHz US. We studied the compromise of cell viability and uptake efficiency; optimized the US conditions for gene transfection; evaluated the capability of US to deliver DNA to the cell nuclei, which is critical to achieve successful transfection; investigated the differences between DNA uptake cells and gene transfection cells; and verified the possibility to further increase transfection efficiency by combining US exposure with drug treatment that regulates intracellular processes.

Various US apparatus systems have been designed and a variety of US exposure conditions (e.g., frequency, energy intensity, pulse length, acoustic pressure) have been tested previously on different types of cells and tissues both *in vitro* and *in vivo* to facilitate drug/gene delivery (Mitragotri 2005). Although the bioeffects caused by US exposure was found to differ due to the US conditions and cell/tissue types, nearly all the studies reported the compromise of cell viability and uptake/transfection efficiency, that

is, high uptake/transfection efficiency was often associated with low cell viability. We found, in this study, changing the US contrast agents or increasing the sonication temperature could possibly increase the uptake efficiency without affecting the cell viability (Figure 4.4), due to the cavitation mechanism of US-facilitated drug/gene delivery. Definity® showed higher uptake efficiency than Optison® under the same US conditions (e.g., 83% – 136% greater), which is consistent with some previous studies (Moran et al. 2000; Li et al. 2004; Miller and Dou 2004b; King et al. 2010). Sonication at 37 ℃ showed higher uptake efficiency than room temperature (e.g., ~ 50% greater in our study), as shown in the present and previous studies (Kim et al. 1996; Nozaki et al. 2003; Zarnitsyn and Prausnitz 2004).

We also found it important to account for the debris from lysed cells when determining the bioeffects caused by US. Therefore in our study, the bioeffects were reported as cell viability, uptake and transfection efficiency among live cells as well as total cells as compared to the "sham" controls. Some previous studies showed high uptake with high viability but this was an artifact of the analysis that did not account for cell debris when determining cell viability. We concluded that the literature did not show that it was possible to achieve high uptake with high viability by optimizing physical parameters. This motivated us to investigate the intracellular processes and study the influence of biological parameters to increased transfection efficiency.

US was found to be able to deliver pDNA into cell nuclei within 30 min in our study and other studies (Duvshani-Eshet and Machluf 2005). This could explain the rapid gene transfection observed within 3 ~ 4 h after US exposure (Figure 6.3), because the protein expression took place after about 3 h once the DNA entered the cell nucleus

(Mehier-Humbert et al. 2005b). Under the optimal US conditions, we found that within 30 min after sonication, up to ~ 30% of cells had DNA uptake and most had a portion of the DNA already in the nuclei (Figure 6.3). Overall, ~ 30% of intracellular DNA was in the nuclei, ~ 30% was in the autophagosomes/autophagolysosomes and the rest was free in the cytoplasm (Figure 6.8). After 4 h, the percentage of cells with DNA uptake decreased to ~ 20% and half of those cells (i.e. ~ 10% of all cells) exhibited expression of the reporter protein GFP (Figure 6.3). The percentage of intracellular DNA remains at ~ 30% in the nuclei, but increased to ~ 60% in the autophagosomes/autophagolysosomes, leaving just ~ 10% free in cytoplasm (Figure 6.8). The maximum transfection efficiency was ~ 12% at 8 h post US exposure (Figure 6.3). At later time up to 24 h, the percentage of cells with DNA uptake decreased continuously to ~ 10%, with most of these cells exhibiting GFP expression. DNA continued to be distributed ~ 30% in the nuclei and most or all of the rest in autophagosomes/autophagolysosomes (Figure 6.8). Further microarray and cell cycle analysis indicated possible cell cycle arrest in the cells with successful gene transfection (Figure 7.3 and 7.4) compared to the uptake cells without GFP expression.

These results suggested that the initial bioeffects caused by US exposure were critical to the results of gene transfection, possibly because of the cavitation mechanisms of US. How much of DNA that US could deliver into the cells initially, determined how much of DNA that could be delivered to the cell nuclei and in turn how much of gene transfection could be achieved later. Once the DNA got into the nuclei, it was transcribed and translated, but could also be lost and degraded due to cell division over time (Gasiorowski and Dean 2005), as we observed the decrease in uptake and transfection

efficiency (Figure 6.3). If this is the case, it would favor the *in vivo* application of US-mediated gene transfection, because cells in tissues are generally slow in the cell cycle, so that once US could deliver DNA into cell nuclei, possible higher and longer transfection could be expected. And the US conditions that cause cell death may not induce tissue damage since the cells tightly packed in tissues have better tolerance to US exposure (Danialou et al. 2002; Li et al. 2003).

The microarray analysis suggested the up-regulation of GADD45α and down-regulation of TOP2α among the cells with gene transfection compared to the uptake cells without GFP expression. Using drugs that regulate the expression of these two genes and the transport and trafficking in the cytoplasm, we found US-mediated transfection efficiency could be further increased. Combine US exposure and the treatment with 0.6 mg/mL EMS and 100 μM chloroquine, or EMS alone, and we further increased transfection efficiency by ~ 2 fold. These results indicated that combining drug treatment with US exposure, we could possibly increase gene transfection efficiency as high as close to the DNA uptake efficiency.

Overall, in this study we have shown that US was able to deliver DNA to the cell nuclei to facilitate rapid gene transfection and by regulating intracellular processes, the transfection efficiency could be further increased. US has the potential to be developed as a safe and efficient tool for gene therapy.

CHAPTER 10: FUTURE WORK

Alternative Cell Lines and *In Vivo* Study

Since different cell lines may respond differently to US exposure, it is of interest to see whether similar regulation of intracellular processes can be found in other types of cells after US-mediated gene transfection, and whether the drug treatment suggested in this study may also increase transfection efficiency in other cell lines. Previous studies using other gene delivery methods have found cells undergoing mitosis were more ready for transfection (Wilke et al. 1996; Tseng et al. 1999). Our studies also suggested that cells with successful gene transfection were associated with cell cycle arrest. It is of interest to test whether slowing down cell cycle or preventing cells from division can improve US-mediated gene transfection. Although we found it difficult to synchronize DU145 human prostate cancer cells, it is worth investigating whether cell synchronization can significantly enhance gene transfection mediated by US using other cell lines.

Some of the major advantages using US as a gene delivery method include that US is non-invasive and easy to apply to nearly any part of the body (Rosenthal et al. 2004), which can be reflected in the *in vivo* application. All the experiments in this study were conducted *in vitro*. The future work may consider transferring these *in vitro* results to *in vivo* studies. Some differences are expected between *in vitro* and *in vivo* studies. For instance, the threshold for inertial cavitation may be higher *in vivo* than *in vitro*, and therefore the US conditions caused damage to cell viability *in vitro* may not damage the

tightly packed cells in tissues *in vivo*. Different types of cells in tissues may also respond differently to the drug treatment tested in DU145 cells in this study.

Quantitative Colocalization Analysis

Current studies on DNA trafficking mainly focused on chemical gene delivery systems (Colin et al. 2000; Fisher et al. 2000; Tachibana et al. 2002; Akita et al. 2004). There are fewer reports of DNA trafficking studies using physical delivery systems (Wilson et al. 1999; Golzio et al. 2002). Compared to endocytosis, the formation mechanism and intracellular itinerary of autophagosomes/autophagolysosomes are not fully clear, which may also limit the studies on DNA trafficking in physical gene delivery systems. The current methods for colocalization analysis of 3D images work well for objects of the similar size and shape but are still limited in the situation of a small object embedded in a large object, in which case the colocalization of DNA in the nucleus is. Plus, the current image analysis methods for colocalization generally provide good qualitative information, but not good quantitative information. The recent development of an imaging flow cytometer may provide a more powerful technique for quantitative colocalization analysis. Several papers have been published showing quantitative colocalization results using the ImageStream® imaging flow cytometer system (Amnis, Seattle, WA) (Pawluczkowycz et al. 2009; Petrovas et al. 2009; Bao et al. 2010; Xu et al. 2010).

It is worth noting that the Cy3/Cy5 labeling process could alter pDNA and affect DNA trafficking, localization, uptake and transfection (Gasiorowski and Dean 2005). For instance, the fluorophores were randomly attached on the plasmids with an alkylating aromatic nitrogen mustard (Belikova et al. 1967) and the bulky fluorophores that coat the

plasmid may block transcription factors from binding to the DNA (Slattum et al. 2003). This could explain our results that transfection efficiency of unlabeled pDNA was higher than labeled pDNA (Figure 6.3c). An alternative peptide nucleic acid (PNA) was designed to specifically bind to a certain sequence of DNA and could possibly address this problem (Gasiorowski and Dean 2005), although further studies are required to evaluate whether labeling DNA with PNA is effective for microscopy imaging and quantitative colocalization analysis.

Combination of US and Other Methods to Facilitate Gene Delivery

In this present work, we combined US exposure with drugs that regulate intracellular processes and found that transfection efficiency could be further increased compared to the treatment with US alone. It is recommended to test the bioeffects of combined treatment of US with some other methods, such as chemical gene delivery vectors, nuclear targeting sequence and "intelligent" microbubbles.

Combination of US Exposure and Drug Treatment

Only a limited number of drugs were tested in this study. There may be other drugs serving the same function that can possibly also enhance gene transfection. To better understand the influence of a particular drug on US-mediated gene transfection, a more variety of concentrations need to be investigated. For instance, 50 μM or less chloroquine was found nontoxic to cells but also ineffective, while 100 μM chloroquine was necessary to augment luciferase expression (Cotten et al. 1990). Similarly, the timing of adding these drugs (e.g., before or after US exposure) and the drug treatment time may also affect the results due to the different pharmaceutical kinetics. Therefore, more completed optimization of the concentrations and the timing of drug treatment may be

needed in future study. Other biological methods to regulate gene expression, such as siRNA, may also be tested.

Combination of US Exposure and Other Delivery Systems

While naked pDNA was used in this present study, future work may consider selecting viral or chemical gene delivery vectors for US-mediated gene transfection. Several studies have reported the combination of US and adenovirus (Chen et al. 2003a), poly(ethylenimine) (Deshpande and Prausnitz 2007), cationic lipids (Unger et al. 1997; Lawrie et al. 1999; Anwer et al. 2000; Koch et al. 2000) had a synergistic effect to increase gene transfection. Synthetic chemical gene vectors have been found effective but non-biodegradable or toxic *in vivo*. While some biodegradable and non-toxic vectors were found difficult to trigger endocytosis for efficient uptake and transfection. US can increase the intracellular uptake and nuclear entry of these large gene delivery vectors, possibly alter the vector-DNA complexes and facilitate the release of DNA. On the other hand, these vectors may increase the stability of DNA, protect the exogenous gene from degrading and facilitate DNA trafficking. US exposure combined with some viral component may possibly achieve more stable transfection for a longer period of time. The combination of the advantages in various gene delivery systems may further enhance gene transfection compared to a single method.

Combination of US Exposure and NLS or DTS

To facilitate DNA entry into the nuclei, nuclear localization signal (NLS) and DNA nuclear targeting sequences (DTS) have been discovered and developed. NLS is a variety of peptides which contains basic amino acids that can be recognized by cytosolic factors to mediate active transport through the nuclear pores complex on the nuclear

envelope (Jans and Hubner 1996). It is reported that the nuclear pore complex can be expanded to ~30 nm during active transport (Dworetzky et al. 1988). DTS is a DNA sequence from the virus SV40 genome that was found to enhance nuclear import (Graessmann et al. 1989; Dean et al. 1999).

Synthetic NLS peptides have been developed to bind to DNA and facilitate DNA delivery into the nuclei using various gene delivery methods (Cartier and Reszka 2002). Several DTS were designed as an enhancer to help nuclear import in several cell lines (Graessmann et al. 1989; Dean 1997; Langle-Rouault et al. 1998). However, few studies used US as the gene delivery method. It is of interest to investigate the combination of US exposure with NLS or DTS, although further studies on the bioconjugation and behavior of the NLS-DNA or DTS-DNA complexes are required.

US Exposure with "Intelligent" Microbubbles

US contrast agents can lower the threshold for cavitation and therefore enhance the bioeffects caused by US. The microbubble-DNA spacing, as well as microbubble-cell spacing and cell-DNA spacing, may have influence on transfection efficiency. Our results also indicated that using different contrast agents could increase US-mediated uptake efficiency without affecting the cell viability, and that the initial amount of DNA that US could deliver might be critical for the results of gene transfection, which could be improved by novel US contrast agents. Future studies may consider developing US contrast agents with multiple functions, not only as the cavitation nuclei, but also as drug carriers and tissue targeting for specific gene delivery purpose (Bekeredjian et al. 2006; Lum et al. 2006). For instance, microbubbles can be prepared to encapsulate generic materials and to contain ligands like antibodies or specific peptides, which would bind to

the specific target cells or tissues and therefore cause a close contact between microbubbles and the target of treatment (Feril 2009).

Overall, to make US a success for gene therapy, future research work needs to study the cell/tissue type dependence of the bioeffects caused by US exposure. Questions related to the mechanism need to be addressed, such as cavitation, DNA trafficking and other intracellular processes that help to facilitate gene transfection. Novel US contrast agents may be designed to enforce the initial bioeffects of US exposure and possibly enhance gene transfection by preventing DNA degradation or further improving specific targeting. The regulation of intracellular processes and the advantages of other delivery systems may be combined with US to make it a safe and efficient tool for gene therapy.

APPENDIX A: CALIBRATION OF ULTRASOUND FIELD

To calibrate the input voltage to the output ultrasound pressure, the membrane hydrophone was located at the desired sample location. Figure A.1 shows the calibration curve for 1 MHz US.

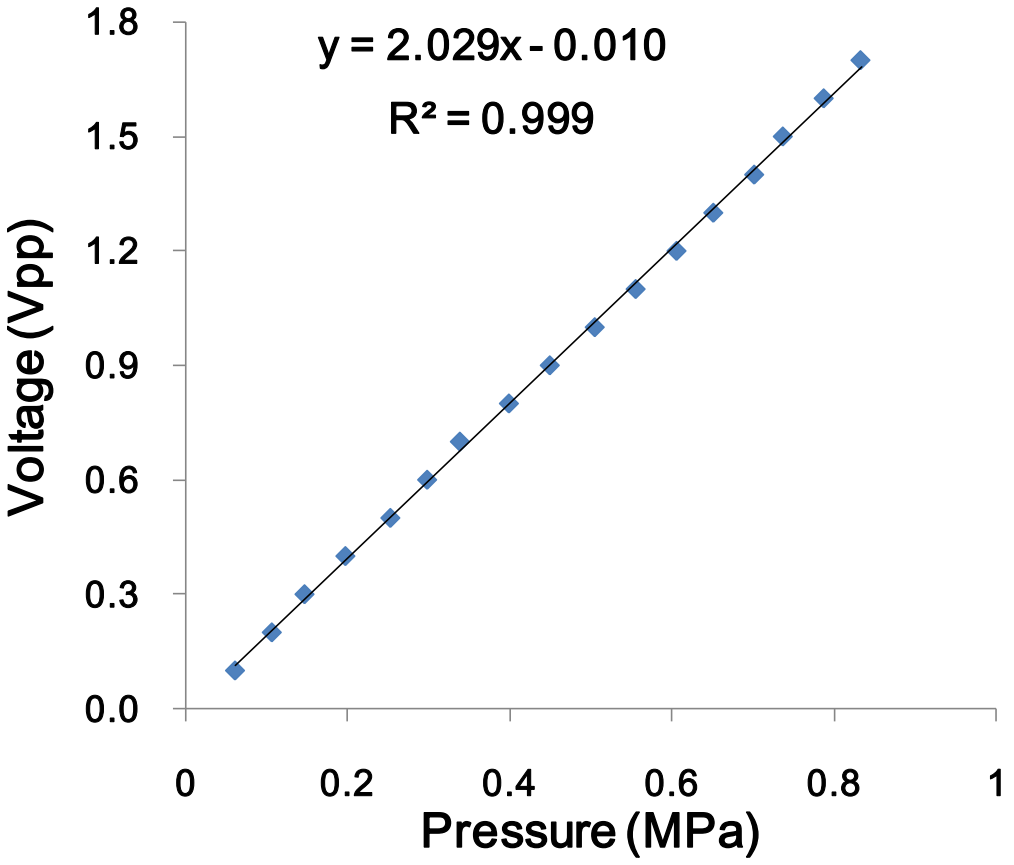

Figure A.1: Calibration of peak-to-peak pressure with the function generator voltage at the location of sample for US exposure.

APPENDIX B: GENES DIFFERENTLY EXPRESSED IN UPTAKE CELLS AND TRANSFECTION CELLS

Totally 78 genes were found differentially expressed between the two groups of cells, 32 of which were up-regulated in transfected cells and 46 were down-regulated relative to cells with pDNA uptake but lacking expression (Table B.1). It is worth noting that there may be multiple Affymetrix probes (Affymetrix_ID) that correspond to one gene.

Table B.1: Differentially expressed genes indentified by microarrays

Affymetrix_ID	Gene Symbol	Gene Title	Fold Change
236898_at	---	Transcribed locus	6.20
1559948_at	---	CDNA FLJ20447 fis, clone KAT05276	2.15
236219_at	---	---	-1.99
212363_x_at	ACTG1	actin, gamma 1	-2.55
212738_at	ARHGAP19	Rho GTPase activating protein 19	-2.81
202672_s_at	ATF3	activating transcription factor 3	2.63
208833_s_at	ATXN10	ataxin 10	-2.05
204092_s_at	AURKA	aurora kinase A	-2.88
208079_s_at	AURKA	aurora kinase A	-2.22
1557257_at	BCL10	B-cell CLL/lymphoma 10	3.29
209642_at	BUB1	BUB1 budding uninhibited by benzimidazoles 1 homolog (yeast)	-2.93
203755_at	BUB1B	BUB1 budding uninhibited by benzimidazoles 1 homolog beta (yeast)	-3.80

225300_at	C15orf23	chromosome 15 open reading frame 23	-2.29
219004_s_at	C21orf45	chromosome 21 open reading frame 45	-2.34
1554314_at	C6orf141	chromosome 6 open reading frame 141	2.06
226386_at	C7orf30	chromosome 7 open reading frame 30	-1.99
213226_at	CCNA2	cyclin A2	-2.39
214710_s_at	CCNB1	cyclin B1	-2.53
201925_s_at	CD55	CD55 molecule, decay accelerating factor for complement (Cromer blood group)	2.66
203213_at	CDC2	cell division cycle 2, G1 to S and G2 to M	-3.17
218542_at	CEP55	centrosomal protein 55kDa	-2.76
211343_s_at	COL13A1	collagen, type XIII, alpha 1	-2.16
218726_at	DKFZp762E1312	hypothetical protein DKFZp762E1312	-2.13
203764_at	DLG7	discs, large homolog 7 (Drosophila)	-2.33
212573_at	ENDOD1	endonuclease domain containing 1	-2.11
1555355_a_at	ETS1	v-ets erythroblastosis virus E26 oncogene homolog 1 (avian)	2.51
218980_at	FHOD3	formin homology 2 domain containing 3	-2.10
207876_s_at	FLNC	filamin C, gamma (actin binding protein 280)	2.22
211458_s_at	GABARAPL1 /// GABARAPL3	GABA(A) receptor-associated protein like 1 /// GABA(A) receptors associated protein like 3	4.09
203725_at	GADD45A	growth arrest and DNA-damage-inducible, alpha	3.09
210002_at	GATA6	GATA binding protein 6	2.94
219539_at	GEMIN6	gem (nuclear organelle) associated protein 6	-2.12
212959_s_at	GNPTAB	N-acetylglucosamine-1-phosphate transferase, alpha and beta subunits	-2.00
212906_at	GRAMD1B	GRAM domain containing 1B	-2.49
230031_at	HSPA5	heat shock 70kDa protein 5 (glucose-regulated	2.51

		protein, 78kDa)	
208687_x_at	HSPA8	heat shock 70kDa protein 8	-3.14
224187_x_at	HSPA8	heat shock 70kDa protein 8	-2.70
210338_s_at	HSPA8	heat shock 70kDa protein 8	-2.27
201609_x_at	ICMT	isoprenylcysteine carboxyl methyltransferase	-2.02
232030_at	KIAA1632	KIAA1632	2.36
218755_at	KIF20A	kinesin family member 20A	-2.86
209408_at	KIF2C	kinesin family member 2C	-2.17
1555832_s_at	KLF6	Kruppel-like factor 6	2.50
203068_at	KLHL21	kelch-like 21 (Drosophila)	2.21
204162_at	KNTC2	kinetochore associated 2	-3.30
211762_s_at	KPNA2 /// LOC728860	karyopherin alpha 2 (RAG cohort 1, importin alpha 1) /// karyopherin alpha 2 (RAG cohort 1, importin alpha 1) /// similar to Importin alpha-2 subunit (Karyopherin alpha-2 subunit) (SRP1-alpha) (RAG cohort protein 1) /// similar to Importin alpha-2 subunit (Karyopherin alpha-2 subunit) (SRP1-alpha) (RAG cohort protein 1)	-2.82
230298_at	LOC153364	similar to metallo-beta-lactamase superfamily protein	-2.17
214719_at	LOC283537	hypothetical protein LOC283537	-2.50
228089_x_at	LOC374395	similar to RIKEN cDNA 1810059G22	-2.08
227099_s_at	LOC387763	hypothetical LOC387763	5.77
242329_at	LOC401317	hypothetical LOC401317	3.28
225436_at	LOC58489	hypothetical protein from EUROIMAGE 588495	-2.44
202209_at	LSM3	LSM3 homolog, U6 small nuclear RNA associated (S. cerevisiae)	-2.42

203362_s_at	MAD2L1	MAD2 mitotic arrest deficient-like 1 (yeast)	-2.57
36711_at	MAFF	v-maf musculoaponeurotic fibrosarcoma oncogene homolog F (avian)	2.33
203640_at	MBNL2	muscleblind-like 2 (Drosophila)	2.14
203625_x_at	MCAM	melanoma cell adhesion molecule	-3.43
211042_x_at	MCAM	melanoma cell adhesion molecule /// melanoma cell adhesion molecule	-2.58
226657_at	MGC33894	transcript expressed during hematopoiesis 2	3.35
209585_s_at	MINPP1	multiple inositol polyphosphate histidine phosphatase, 1	-2.52
217980_s_at	MRPL16	mitochondrial ribosomal protein L16	-2.30
224206_x_at	MYNN	myoneurin	2.48
221805_at	NEFL	neurofilament, light polypeptide 68kDa	-2.59
204641_at	NEK2	NIMA (never in mitosis gene a)-related kinase 2	-1.98
218014_at	NUP85	nucleoporin 85kDa	-2.31
219148_at	PBK	PDZ binding kinase	-2.34
209382_at	POLR3C	polymerase (RNA) III (DNA directed) polypeptide C (62kD)	2.08
224509_s_at	RTN4IP1	reticulon 4 interacting protein 1 /// reticulon 4 interacting protein 1	-2.10
202037_s_at	SFRP1	secreted frizzled-related protein 1	-2.09
230165_at	SGOL2	shugoshin-like 2 (S. pombe)	-2.02
56256_at	SIDT2	SID1 transmembrane family, member 2	2.17
244070_at	SYNE1	spectrin repeat containing, nuclear envelope 1	5.58
219682_s_at	TBX3	T-box 3 (ulnar mammary syndrome)	2.22
202644_s_at	TNFAIP3	tumor necrosis factor, alpha-induced protein 3	3.34
201292_at	TOP2A	topoisomerase (DNA) II alpha 170kDa	-4.57

201291_s_at	TOP2A	topoisomerase (DNA) II alpha 170kDa	-4.26
218145_at	TRIB3	tribbles homolog 3 (Drosophila)	2.32
210705_s_at	TRIM5	tripartite motif-containing 5	2.11
204033_at	TRIP13	thyroid hormone receptor interactor 13	-2.07
212320_at	TUBB	tubulin, beta	-2.12
214023_x_at	TUBB2B	tubulin, beta 2B	2.20
219192_at	UBAP2	ubiquitin associated protein 2	2.09
233952_s_at	ZNF295	zinc finger protein 295	2.49
219228_at	ZNF331	zinc finger protein 331	2.99
1554248_at	ZNF638	zinc finger protein 638	3.63
214138_at	ZNF79	zinc finger protein 79	2.75

APPENDIX C: DNA ELECTROPHORESIS

DNA electrophoresis was carried out after qRT-PCR to confirm the expression of the two genes of interest: TOP2α and GADD45α (Figure C.1).

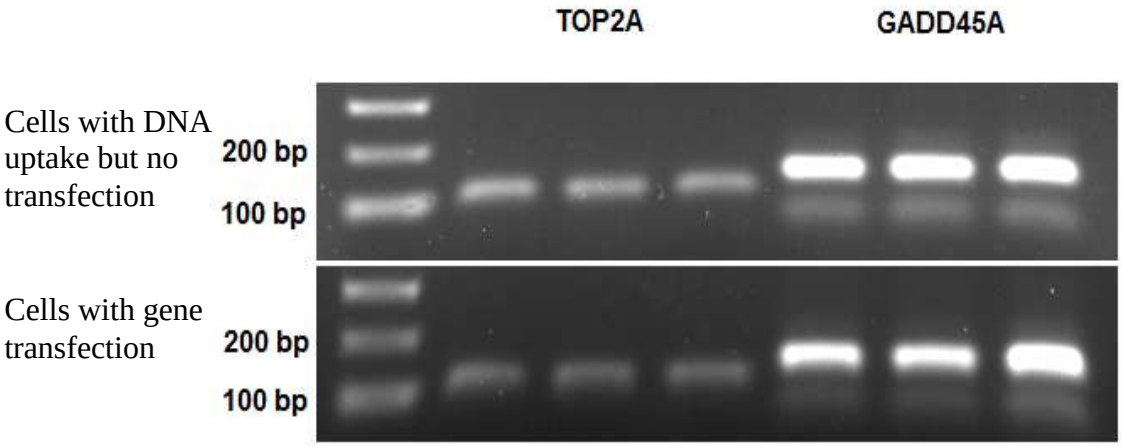

Figure C.1: DNA electrophoresis after qRT-PCR. The upper image shows the expression of TOP2α and GADD45α in the cells with DNA uptake but no transfection. The bottom image shows that in the cells with gene transfection.

APPENDIX D: CELL VIABILITY WITH DRUG TREATMENT

Cell viability after US exposure was not affected by EMS, chloroquine, tetracaine, but decreased with the treatment of NMDA, PRIMA-1, amsacrine, etoposide, mitoxantrone, aclarubicin, paclitaxel, docetaxel and bafilomycin A1 (Figure D.1).

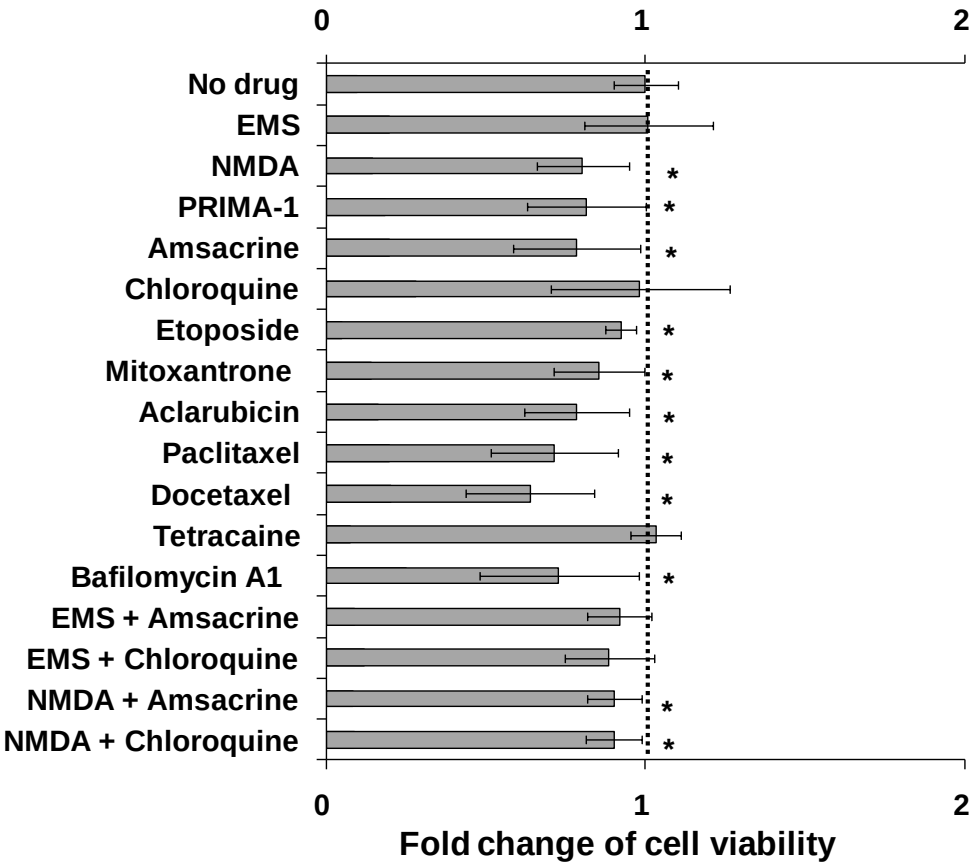

Figure D.1: The fold change of cell viability with drug treatment compared to that without drug treatment. Data represent the averages of n ≥ 3 replicates. The error bars represent 95% confidence interval (*Student's t-test $p < 0.05$, compared to no drug treatment). The concentration used for each drug: 0.6 mg/mL EMS, 2 mM NMDA, 1 mM PRIMA-1, 200 nM amsacrine, 100 µM chloroquine, 200 nM etoposide, 200 nM mitoxantrone, 50 nM aclarubicin, 16 µM paclitaxel, 16 µM docetaxel, 20 µM tetracaine and 250 nM bafilomycin A1. US conditions: pressure amplitude of 0.78 MPa, total treatment time of 1 min with a pulse length of 0.25 ms at a duty cycle of 25%, Definity® concentration of 1 vol%.

REFERENCES

Abdollahi A, Domhan S, Jenne JW, Hallaj M, Dell'Aqua G, Mueckenthaler M, Richter A, Martin H, Debus J, Ansorge W, Hynynen K, Huber PE. Apoptosis signals in lymphoblasts induced by focused ultrasound. FASEB J 2004;18:1413-4.

Akita H, Ito R, Khalil IA, Futaki S, Harashima H. Quantitative three-dimensional analysis of the intracellular trafficking of plasmid DNA transfected by a nonviral gene delivery system using confocal laser scanning microscopy. Mol Ther 2004;9:443-51.

Akowuah EF, Gray C, Lawrie A, Sheridan PJ, Su CH, Bettinger T, Brisken AF, Gunn J, Crossman DC, Francis SE, Baker AH, Newman CM. Ultrasound-mediated delivery of timp-3 plasmid DNA into saphenous vein leads to increased lumen size in a porcine interposition graft model. Gene Ther 2005;12:1154-7.

Alter A, Rozenszajn LA, Miller HI, Rosenschein U. Ultrasound inhibits the adhesion and migration of smooth muscle cells in vitro. Ultrasound in Medicine & Biology 1998;24:711-21.

Andoh T, Ishida R. Catalytic inhibitors of DNA topoisomerase ii. Biochim Biophys Acta 1998;1400:155-71.

Andre F, Mir LM. DNA electrotransfer: Its principles and an updated review of its therapeutic applications. Gene Ther 2004;11 Suppl 1:S33-42.

Anwer K, Kao G, Proctor B, Anscombe I, Florack V, Earls R, Wilson E, McCreery T, Unger E, Rolland A, Sullivan SM. Ultrasound enhancement of cationic lipid-mediated gene transfer to primary tumors following systemic administration. Gene Ther 2000;7:1833-9.

Asano T, An T, Zwelling LA, Takano H, Fojo AT, Kleinerman ES. Transfection of a human topoisomerase ii alpha gene into etoposide-resistant human breast tumor cells sensitizes the cells to etoposide. Oncol Res 1996;8:101-10.

Asher RC. Ultrasonic sensors. Bristol: Institute of Physics Publishing, 1997.

Ashush H, Rozenszajn LA, Blass M, Barda-Saad M, Azimov D, Radnay J, Zipori D, Rosenschein U. Apoptosis induction of human myeloid leukemic cells by ultrasound exposure. Cancer Res 2000;60:1014-20.

Atchley AA, Frizzell LA, Apfel RE, Holland CK, Madanshetty S, Roy RA. Thresholds for cavitation produced in water by pulsed ultrasound. Ultrasonics 1988;26:280-5.

Auerbach AB. Production of functional transgenic mice by DNA pronuclear microinjection. Acta Biochim Pol 2004;51:9-31.

Ayad SR, White A. The effect of the local anaesthetic, tetracaine, on the isoprenaline and prostaglandin e1 stimulation of camp in normal and malignant cell lines. Exp Cell Res 1977;107:201-6.

Azuma H, Tomita N, Kaneda Y, Koike H, Ogihara T, Katsuoka Y, Morishita R. Transfection of nfkappab-decoy oligodeoxynucleotides using efficient ultrasound-

mediated gene transfer into donor kidneys prolonged survival of rat renal allografts. Gene Ther 2003;10:415-25.

Bao J, Lu Z, Joseph JJ, Carabenciov D, Dimond CC, Pang L, Samsel L, McCoy JP, Jr., Leclerc J, Nguyen P, Gius D, Sack MN. Characterization of the murine sirt3 mitochondrial localization sequence and comparison of mitochondrial enrichment and deacetylase activity of long and short sirt3 isoforms. J Cell Biochem 2010;110:238-47.

Bao S, Thrall BD, Miller DL. Transfection of a reporter plasmid into cultured cells by sonoporation in vitro. Ultrasound in Medicine & Biology 1997;23:953-9.

Bausinger R, von Gersdorff K, Braeckmans K, Ogris M, Wagner E, Brauchle C, Zumbusch A. The transport of nanosized gene carriers unraveled by live-cell imaging. Angew Chem Int Ed Engl 2006;45:1568-72.

Bekeredjian R, Chen S, Frenkel PA, Grayburn PA, Shohet RV. Ultrasound-targeted microbubble destruction can repeatedly direct highly specific plasmid expression to the heart. Circulation 2003;108:1022-6.

Bekeredjian R, Katus HA, Kuecherer HF. Therapeutic use of ultrasound targeted microbubble destruction: A review of non-cardiac applications. Ultraschall Med 2006;28:134-40.

Belikova AM, Zarytova VF, Grineva NI. Synthesis of ribonucleosides and diribonucleoside phosphates containing 2-chloroethylamine and nitrogen mustard residues. Tetrahedron Lett 1967;37:3557-62.

Bouakaz A, Frinking PJ, de Jong N, Bom N. Noninvasive measurement of the hydrostatic pressure in a fluid-filled cavity based on the disappearance time of micrometer-sized free gas bubbles. Ultrasound Med Biol 1999;25:1407-15.

Brayman AA, Miller MW. Sonolysis of albunex-supplemented, 40% hematocrit human erythrocytes by pulsed 1-mhz ultrasound: Pulse number, pulse duration and exposure vessel rotation dependence. Ultrasound Med Biol 1999;25:307-14.

Brisson M, Tseng WC, Almonte C, Watkins S, Huang L. Subcellular trafficking of the cytoplasmic expression system. Hum Gene Ther 1999;10:2601-13.

Bronner C, Hopfner R, Mousli M. Transcriptional regulation of the human topoisomerase iialpha gene. Anticancer Res 2002;22:605-12.

Brunner S, Sauer T, Carotta S, Cotten M, Saltik M, Wagner E. Cell cycle dependence of gene transfer by lipoplex, polyplex and recombinant adenovirus. Gene Ther 2000;7:401-7.

Bukrinskaya A, Brichacek B, Mann A, Stevenson M. Establishment of a functional human immunodeficiency virus type 1 (hiv-1) reverse transcription complex involves the cytoskeleton. J Exp Med 1998;188:2113-25.

Burden DA, Osheroff N. Mechanism of action of eukaryotic topoisomerase ii and drugs targeted to the enzyme. Biochim Biophys Acta 1998;1400:139-54.

Butte A. The use and analysis of microarray data. Nature Reviews Drug Discovery 2002;1:951-60.

Callans LS, Gadacz TR. Fragmentation of human gallstones using ultrasound and electrohydraulic lithotripsy: Experimental and clinical experience. Surgery 1990;107:121-7.

Campbell P, Prausnitz MR. Future directions for therapeutic ultrasound. Ultrasound Med Biol 2007;33:657.

Carstensen EL, Law WK, McKay ND, Muir TG. Demonstration of nonlinear acoustical effects at biomedical frequencies and intensities. Ultrasound in Medicine & Biology 1980;6:359-68.

Cartier R, Reszka R. Utilization of synthetic peptides containing nuclear localization signals for nonviral gene transfer systems. Gene Ther 2002;9:157-67.

Champoux JJ. DNA topoisomerases: Structure, function, and mechanism. Annu Rev Biochem 2001;70:369-413.

Check E. A tragic setback. Nature 2002;420:116-8.

Check E. Second cancer case halts gene-therapy trials. Nature 2003;421:305.

Chen S, Kroll MH, Shohet RV, Frenkel P, Mayer SA, Grayburn PA. Bioeffects of myocardial contrast microbubble destruction by echocardiography. Echocardiography 2002;19:495-500.

Chen S, Shohet RV, Bekeredjian R, Frenkel P, Grayburn PA. Optimization of ultrasound parameters for cardiac gene delivery of adenoviral or plasmid deoxyribonucleic acid by ultrasound-targeted microbubble destruction. J Am Coll Cardiol 2003a;42:301-8.

Chen W-S, Brayman AA, Matula TJ, Crum LA. Inertial cavitation dose and hemolysis produced in vitro with or without optison? Ultrasound in Medicine & Biology 2003b;29:725-37.

Chen W-S, Matula TJ, Brayman AA, Crum LA. A comparison of the fragmentation thresholds and inertial cavitation doses of different ultrasound contrast agents. The Journal of the Acoustical Society of America 2003c;113:643-51.

Cheung VG, Morley M, Aguilar F, Massimi A, Kucherlapati R, Childs G. Making and reading microarrays. Nat Genet 1999;21:15-9.

Christiansen JP, French BA, Klibanov AL, Kaul S, Lindner JR. Targeted tissue transfection with ultrasound destruction of plasmid-bearing cationic microbubbles. Ultrasound Med Biol 2003;29:1759-67.

Chu G, Hayakawa H, Berg P. Electroporation for the efficient transfection of mammalian cells with DNA. Nucleic Acids Res 1987;15:1311-26.

Cochran SA, Prausnitz MR. Sonoluminescence as an indicator of cell membrane disruption by acoustic cavitation. Ultrasound Med Biol 2001;27:841-50.

Colin M, Maurice M, Trugnan G, Kornprobst M, Harbottle RP, Knight A, Cooper RG, Miller AD, Capeau J, Coutelle C, Brahimi-Horn MC. Cell delivery, intracellular

trafficking and expression of an integrin-mediated gene transfer vector in tracheal epithelial cells. Gene Ther 2000;7:139-52.

Conti E, Izaurralde E. Nucleocytoplasmic transport enters the atomic age. Curr Opin Cell Biol 2001;13:310-9.

Corish P, Tyler-Smith C. Attenuation of green fluorescent protein half-life in mammalian cells. Protein Eng 1999;12:1035-40.

Cotten M, Langle-Rouault F, Kirlappos H, Wagner E, Mechtler K, Zenke M, Beug H, Birnstiel ML. Transferrin-polycation-mediated introduction of DNA into human leukemic cells: Stimulation by agents that affect the survival of transfected DNA or modulate transferrin receptor levels. P Natl Acad Sci USA 1990;87:4033-7.

Croaker GM, Wass EJ, Iland HJ. Electric field-mediated gene-transfer into k562 cells - optimization of parameters affecting efficiency. Leukemia 1990;4:502-7.

Crystal RG. Transfer of genes to humans: Early lessons and obstacles to success. Science 1995;270:404-10.

Cullen DK, LaPlaca MC. Neuronal response to high rate shear deformation depends on heterogeneity of the local strain field. J Neurotrauma 2006;23:1304-19.

Danialou G, Comtois AS, Dudley RW, Nalbantoglu J, Gilbert R, Karpati G, Jones DH, Petrof BJ. Ultrasound increases plasmid-mediated gene transfer to dystrophic muscles without collateral damage. Mol Ther 2002;6:687-93.

Dass CR. Lipoplex-mediated delivery of nucleic acids: Factors affecting in vivo transfection. J Mol Med 2004;82:579-91.

Datta S, Coussios CC, McAdory LE, Tan J, Porter T, De Courten-Myers G, Holland CK. Correlation of cavitation with ultrasound enhancement of thrombolysis. Ultrasound Med Biol 2006;32:1257-67.

Dean DA. Import of plasmid DNA into the nucleus is sequence specific. Exp Cell Res 1997;230:293-302.

Dean DA, Dean BS, Muller S, Smith LC. Sequence requirements for plasmid nuclear import. Exp Cell Res 1999;253:713-22.

Deretic V. Autophagy in innate and adaptive immunity. Trends Immunol 2005;26:523-8.

Deshpande MC, Prausnitz MR. Synergistic effect of ultrasound and pei on DNA transfection in vitro. J Control Release 2007;118:126-35.

Dijkstra J, Van Galen M, Scherphof GL. Effects of ammonium chloride and chloroquine on endocytic uptake of liposomes by kupffer cells in vitro. Biochim Biophys Acta 1984;804:58-67.

Duvshani-Eshet M, Baruch L, Kesselman E, Shimoni E, Machluf M. Therapeutic ultrasound-mediated DNA to cell and nucleus: Bioeffects revealed by confocal and atomic force microscopy. Gene Ther 2006;13:163-72.

Duvshani-Eshet M, Machluf M. Therapeutic ultrasound optimization for gene delivery: A key factor achieving nuclear DNA localization. J Control Release 2005;108:513-28.

Dworetzky SI, Lanford RE, Feldherr CM. The effects of variations in the number and sequence of targeting signals on nuclear uptake. J Cell Biol 1988;107:1279-87.

Eisenbraun MD, Fuller DH, Haynes JR. Examination of parameters affecting the elicitation of humoral immune responses by particle bombardment-mediated genetic immunization. DNA Cell Biol 1993;12:791-7.

el Khader K, Ibn Attya A, Mamoun M, Koutani A, Hachimi M, Lakrissa A. [role of ultrasound lithotripsy in the treatment of lithiasis of the lower urinary tract. Apropos of 38 cases]. J Urol (Paris) 1995;101:165-8.

Erbacher P, Roche AC, Monsigny M, Midoux P. Putative role of chloroquine in gene transfer into a human hepatoma cell line by DNA lactosylated polylysine complexes. Experimental Cell Research 1996;225:186-94.

Eskelinen EL. Maturation of autophagic vacuoles in mammalian cells. Autophagy 2005;1:1-10.

Everbach EC, Francis CW. Cavitational mechanisms in ultrasound-accelerated thrombolysis at 1 mhz. Ultrasound in Medicine and Biology 2000;26:1153-60.

Fan W, Richter G, Cereseto A, Beadling C, Smith KA. Cytokine response gene 6 induces p21 and regulates both cell growth and arrest. Oncogene 1999;18:6573-82.

Fasbender A, Zabner J, Zeiher BG, Welsh MJ. A low rate of cell proliferation and reduced DNA uptake limit cationic lipid-mediated gene transfer to primary cultures of ciliated human airway epithelia. Gene Ther 1997;4:1173-80.

Fechheimer M, Boylan JF, Parker S, Sisken JE, Patel GL, Zimmer SG. Transfection of mammalian cells with plasmid DNA by scrape loading and sonication loading. P Natl Acad Sci USA 1987;84:8463-7.

Feril LB, Jr. Ultrasound-mediated gene transfection. Methods Mol Biol 2009;542:179-94.

Fischer AJ, Stanke JJ, Omar G, Askwith CC, Burry RW. Ultrasound-mediated gene transfer into neuronal cells. J Biotechnol 2006;122:393-411.

Fisher KD, Ulbrich K, Subr V, Ward CM, Mautner V, Blakey D, Seymour LW. A versatile system for receptor-mediated gene delivery permits increased entry of DNA into target cells, enhanced delivery to the nucleus and elevated rates of transgene expression. Gene Ther 2000;7:1337-43.

Fowlkes JB, Holland CK. Mechanical bioeffects from diagnostic ultrasound: Aium consensus statements. American institute of ultrasound in medicine. J Ultrasound Med 2000;19:69-72.

Fregeau CJ, Bleackley RC. Factors influencing transient expression in cytotoxic t cells following deae dextran-mediated gene transfer. Somat Cell Mol Genet 1991;17:239-57.

Frinking PJ, Bouakaz A, de Jong N, Ten Cate FJ, Keating S. Effect of ultrasound on the release of micro-encapsulated drugs. Ultrasonics 1998;36:709-12.

Frinking PJ, de Jong N. Acoustic modeling of shell-encapsulated gas bubbles. Ultrasound Med Biol 1998;24:523-33.

Fry AM, Chresta CM, Davies SM, Walker MC, Harris AL, Hartley JA, Masters JRW, Hickson ID. Relationship between topoisomerase ii level and chemosensitivity in human tumor cell lines. Cancer Res 1991;51:6592-5.

Fushimi K, Verkman AS. Low viscosity in the aqueous domain of cell cytoplasm measured by picosecond polarization microfluorimetry. J Cell Biol 1991;112:719-25.

Gao X, Kim K-S, Liu D. Nonviral gene delivery: What we know and what is next. The AAPS Journal 2007;9:E92-E104.

Gasiorowski JZ, Dean DA. Postmitotic nuclear retention of episomal plasmids is altered by DNA labeling and detection methods. Molecular Therapy 2005;12:460-7.

Gehl J. Electroporation: Theory and methods, perspectives for drug delivery, gene therapy and research. Acta Physiol Scand 2003;177:437-47.

Golzio M, Teissié J, Rols M-P. Direct visualization at the single-cell level of electrically mediated gene delivery. P Natl Acad Sci USA 2002;99:1292-7.

Goswami PC, Roti Roti JL, Hunt CR. The cell cycle-coupled expression of topoisomerase iialpha during s phase is regulated by mrna stability and is disrupted by heat shock or ionizing radiation. Mol Cell Biol 1996;16:1500-8.

Graessmann M, Menne J, Liebler M, Graeber I, Graessmann A. Helper activity for gene expression, a novel function of the sv40 enhancer. Nucleic Acids Res 1989;17:6603-12.

Gu Z, Qi J, Shen H, Liu J, Chen J. Percutaneous nephroscopic with holmium laser and ultrasound lithotripsy for complicated renal calculi. Lasers Med Sci 2010;25:577-80.

Guo DP, Li XY, Sun P, Wang ZG, Chen XY, Chen Q, Fan LM, Zhang B, Shao LZ, Li XR. Ultrasound/microbubble enhances foreign gene expression in ecv304 cells and murine myocardium. Acta Biochim Biophys Sin (Shanghai) 2004;36:824-31.

Guo FY. Clinical studies on ultrasound lithotripsy in intrahepatic bile-duct via abdomen. J Tongji Med Univ 1995;15:108-11.

Guzman HR, McNamara AJ, Nguyen DX, Prausnitz MR. Bioeffects caused by changes in acoustic cavitation bubble density and cell concentration: A unified explanation based on cell-to-bubble ratio and blast radius. Ultrasound Med Biol 2003;29:1211-22.

Guzman HR, Nguyen DX, Khan S, Prausnitz MR. Ultrasound-mediated disruption of cell membranes. Ii. Heterogeneous effects on cells. J Acoust Soc Am 2001;110:597-606.

Guzman HR, Nguyen DX, McNamara AJ, Prausnitz MR. Equilibrium loading of cells with macromolecules by ultrasound: Effects of molecular size and acoustic energy. J Pharm Sci 2002;91:1693-701.

Haar GT, Coussios C. High intensity focused ultrasound: Physical principles and devices. Int J Hyperthermia 2007;23:89-104.

Hallow DM, Mahajan AD, McCutchen TE, Prausnitz MR. Measurement and correlation of acoustic cavitation with cellular bioeffects. Ultrasound Med Biol 2006;32:1111-22.

Hallow DM, Mahajan AD, Prausnitz MR. Ultrasonically targeted delivery into endothelial and smooth muscle cells in ex vivo arteries. J Control Release 2007;118:285-93.

Harkin DP, Bean JM, Miklos D, Song Y-H, Truong VB, Englert C, Christians FC, Ellisen LW, Maheswaran S, Oliner JD, Haber DA. Induction of gadd45 and jnk/sapk-dependent apoptosis following inducible expression of brca1. Cell 1999;97:575-86.

Heller LC, Ugen K, Heller R. Electroporation for targeted gene transfer. Expert Opin Drug Deliv 2005;2:255-68.

Hoff L, Sontum PC, Hovem JM. Oscillations of polymeric microbubbles: Effect of the encapsulating shell. J Acoust Soc Am 2000;107:2272-80.

Hofmann A, Zakhartchenko V, Weppert M, Sebald H, Wenigerkind H, Brem G, Wolf E, Pfeifer A. Generation of transgenic cattle by lentiviral gene transfer into oocytes. Biol Reprod 2004;71:405-9.

Horwitz SB. Taxol (paclitaxel): Mechanisms of action. Ann Oncol 1994;5 Suppl 6:S3-6.

Huber PE, Jenne J, Debus J, Wannenmacher MF, Pfisterer P. A comparison of shock wave and sinusoidal-focused ultrasound-induced localized transfection of hela cells. Ultrasound Med Biol 1999;25:1451-7.

Hundt W, Yuh EL, Bednarski MD, Guccione S. Gene expression profiles, histologic analysis, and imaging of squamous cell carcinoma model treated with focused ultrasound beams. AJR Am J Roentgenol 2007;189:726-36.

Hutcheson JD, Schlicher RK, Hicks HK, Prausnitz MR. Saving cells from ultrasound-induced apoptosis: Quantification of cell death and uptake following sonication and effects of targeted calcium chelation. Ultrasound Med Biol 2010;36:1008-21.

Hynynen K, McDannold N, Sheikov NA, Jolesz FA, Vykhodtseva N. Local and reversible blood-brain barrier disruption by noninvasive focused ultrasound at frequencies suitable for trans-skull sonications. Neuroimage 2005;24:12-20.

Ingber DE. Mechanical signaling and the cellular response to extracellular matrix in angiogenesis and cardiovascular physiology. Circ Res 2002;91:877-87.

Jahreiss L, Menzies FM, Rubinsztein DC. The itinerary of autophagosomes: From peripheral formation to kiss-and-run fusion with lysosomes. Traffic 2008;9:574-87.

Jans DA, Hubner S. Regulation of protein transport to the nucleus: Central role of phosphorylation. Physiol Rev 1996;76:651-85.

Juhasz G, Neufeld TP. Autophagy: A forty-year search for a missing membrane source. PLoS Biol 2006;4:e36.

Kalejta RF, Brideau AD, Banfield BW, Beavis AJ. An integral membrane green fluorescent protein marker, us9-gfp, is quantitatively retained in cells during propidium iodide-based cell cycle analysis by flow cytometry. Exp Cell Res 1999;248:322-8.

Karshafian R, Samac S, Bevan PD, Burns PN. Microbubble mediated sonoporation of cells in suspension: Clonogenic viability and influence of molecular size on uptake. Ultrasonics 2010;50:691-7.

Kastan MB, Zhan Q, el-Deiry WS, Carrier F, Jacks T, Walsh WV, Plunkett BS, Vogelstein B, Fornace AJ, Jr. A mammalian cell cycle checkpoint pathway utilizing p53 and gadd45 is defective in ataxia-telangiectasia. Cell 1992;71:587-97.

Kearsey JM, Coates PJ, Prescott AR, Warbrick E, Hall PA. Gadd45 is a nuclear cell cycle regulated protein which interacts with p21cip1. Oncogene 1995;11:1675-83.

Kennedy JE. High-intensity focused ultrasound in the treatment of solid tumours. Nat Rev Cancer 2005;5:321-7.

Keyhani K, Guzman HR, Parsons A, Lewis TN, Prausnitz MR. Intracellular drug delivery using low-frequency ultrasound: Quantification of molecular uptake and cell viability. Pharm Res 2001;18:1514-20.

Kim HJ, Greenleaf JF, Kinnick RR, Bronk JT, Bolander ME. Ultrasound-mediated transfection of mammalian cells. Hum Gene Ther 1996;7:1339-46.

Kimmel E. Cavitation bioeffects. Crit Rev Biomed Eng 2006;34:105-61.

King DA, Malloy MJ, Roberts AC, Haak A, Yoder CC, O'Brien WD, Jr. Determination of postexcitation thresholds for single ultrasound contrast agent microbubbles using double passive cavitation detection. J Acoust Soc Am 2010;127:3449-55.

King R. Gene delivery to mammalian cells by microinjection. Methods Mol Biol 2004;245:167-74.

Kinoshita M, Hynynen K. Mechanism of porphyrin-induced sonodynamic effect: Possible role of hyperthermia. Radiat Res 2006;165:299-306.

Klein TM, Wolf ED, Wu R, Sanford JC. High-velocity microprojectiles for delivering nucleic-acids into living cells. Nature 1987;327:70-3.

Kober LO, Ellwart JW, Brettel H. Effect of the pulse length of ultrasound on cell membrane damage in vitro. J Acoust Soc Am 1989;86:6-7.

Koch S, Pohl P, Cobet U, Rainov NG. Ultrasound enhancement of liposome-mediated cell transfection is caused by cavitation effects. Ultrasound Med Biol 2000;26:897-903.

Koike H, Tomita N, Azuma H, Taniyama Y, Yamasaki K, Kunugiza Y, Tachibana K, Ogihara T, Morishita R. An efficient gene transfer method mediated by ultrasound and microbubbles into the kidney. J Gene Med 2005;7:108-16.

Kondo I, Ohmori K, Oshita A, Takeuchi H, Fuke S, Shinomiya K, Noma T, Namba T, Kohno M. Treatment of acute myocardial infarction by hepatocyte growth factor

gene transfer: The first demonstration of myocardial transfer of a "Functional" Gene using ultrasonic microbubble destruction. J Am Coll Cardiol 2004;44:644-53.

Kurata S, Tsukakoshi M, Kasuya T, Ikawa Y. The laser method for efficient introduction of foreign DNA into cultured-cells. Experimental Cell Research 1986;162:372-8.

Laabich A, Li G, Cooper NG. Characterization of apoptosis-genes associated with nmda mediated cell death in the adult rat retina. Brain Res Mol Brain Res 2001;91:34-42.

Lambert JM, Gorzov P, Veprintsev DB, Soderqvist M, Segerback D, Bergman J, Fersht AR, Hainaut P, Wiman KG, Bykov VJ. Prima-1 reactivates mutant p53 by covalent binding to the core domain. Cancer Cell 2009;15:376-88.

Lan HY, Mu W, Tomita N, Huang XR, Li JH, Zhu HJ, Morishita R, Johnson RJ. Inhibition of renal fibrosis by gene transfer of inducible smad7 using ultrasound-microbubble system in rat uuo model. J Am Soc Nephrol 2003;14:1535-48.

Langle-Rouault F, Patzel V, Benavente A, Taillez M, Silvestre N, Bompard A, Sczakiel G, Jacobs E, Rittner K. Up to 100-fold increase of apparent gene expression in the presence of epstein-barr virus orip sequences and ebna1: Implications of the nuclear import of plasmids. J Virol 1998;72:6181-5.

Lanzi C, Cassinelli G, Cuccuru G, Supino R, Zuco V, Ferlini C, Scambia G, Zunino F. Cell cycle checkpoint efficiency and cellular response to paclitaxel in prostate cancer cells. Prostate 2001;48:254-64.

Larina IV, Evers BM, Esenaliev RO. Optimal drug and gene delivery in cancer cells by ultrasound-induced cavitation. Anticancer Res 2005;25:149-56.

Lawrie A, Brisken AF, Francis SE, Tayler DI, Chamberlain J, Crossman DC, Cumberland DC, Newman CM. Ultrasound enhances reporter gene expression after transfection of vascular cells in vitro. Circulation 1999;99:2617-20.

Lechardeur D, Sohn KJ, Haardt M, Joshi PB, Monck M, Graham RW, Beatty B, Squire J, O'Brodovich H, Lukacs GL. Metabolic instability of plasmid DNA in the cytosol: A potential barrier to gene transfer. Gene Therapy 1999;6:482-97.

Leighton TG. The acoustic bubble. Academic Press, London, UK, 1994.

Li P, Armstrong WF, Miller DL. Impact of myocardial contrast echocardiography on vascular permeability: Comparison of three different contrast agents. Ultrasound Med Biol 2004;30:83-91.

Li T, Tachibana K, Kuroki M. Gene transfer with echo-enhanced contrast agents: Comparison between albunex, optison, and levovist in mice--initial results. Radiology 2003;229:423-8.

Li Y, Qian H, Li X, Wang H, Yu J, Liu Y, Zhang X, Liang X, Fu M, Zhan Q, Lin C. Adenoviral-mediated gene transfer of gadd45a results in suppression by inducing apoptosis and cell cycle arrest in pancreatic cancer cell. J Gene Med 2009;11:3-13.

Liang HD, Lu QL, Xue SA, Halliwell M, Kodama T, Cosgrove DO, Stauss HJ, Partridge TA, Blomley MJ. Optimisation of ultrasound-mediated gene transfer (sonoporation) in skeletal muscle cells. Ultrasound Med Biol 2004;30:1523-9.

Liebermann DA, Hoffman B. Gadd45 in stress signaling. J Mol Signal 2008;3:15.

Liu DX, Zhang GS, Gao X, Song YK, Vollmer R, Stolz DB, Gasiorowski JZ, Dean DA. Hydroporation as the mechanism accounting for efficient gene transfer by hydrodynamic delivery. Molecular Therapy 2004;9:S307-S8.

Liu LF. DNA topoisomerase poisons as antitumor drugs. Annu Rev Biochem 1989;58:351-75.

Liu Y, Paliwal S, Bankiewicz KS, Bringas JR, Heart G, Mitragotri S, Prausnitz MR. Ultrasound-enhanced drug transport and distribution in the brain. AAPS PharmSciTech 2010;11:1005-17.

Livak KJ, Schmittgen TD. Analysis of relative gene expression data using real-time quantitative pcr and the 2-[delta][delta]ct method. Methods 2001;25:402-8.

Luby-Phelps K, Mujumdar S, Mujumdar RB, Ernst LA, Galbraith W, Waggoner AS. A novel fluorescence ratiometric method confirms the low solvent viscosity of the cytoplasm. Biophys J 1993;65:236-42.

Ludtke JJ, Sebestyen MG, Wolff JA. The effect of cell division on the cellular dynamics of microinjected DNA and dextran. Mol Ther 2002;5:579-88.

Lukacs GL, Haggie P, Seksek O, Lechardeur D, Freedman N, Verkman AS. Size-dependent DNA mobility in cytoplasm and nucleus. J Biol Chem 2000;275:1625-9.

Lum AF, Borden MA, Dayton PA, Kruse DE, Simon SI, Ferrara KW. Ultrasound radiation force enables targeted deposition of model drug carriers loaded on microbubbles. J Control Release 2006;111:128-34.

Luthman H, Magnusson G. High efficiency polyoma DNA transfection of chloroquine treated cells. Nucl Acids Res 1983;11:1295-308.

Lynn JG, Zwemer RL, Chick AJ, Miller AE. A new method for the generation and use of focused ultrasound in experimental biology. J Gen Physiol 1942;26:179-93.

Manome Y, Nakayama N, Nakayama K, Furuhata H. Insonation facilitates plasmid DNA transfection into the central nervous system and microbubbles enhance the effect. Ultrasound Med Biol 2005;31:693-702.

Marshall E. Gene therapy death prompts review of adenovirus vector. Science 1999;286:2244-5.

Maxfield FR. Weak bases and ionophores rapidly and reversibly raise the ph of endocytic vesicles in cultured mouse fibroblasts. Journal of Cell Biology 1982;95:676-81.

McDannold N, Vykhodtseva N, Hynynen K. Use of ultrasound pulses combined with definity for targeted blood-brain barrier disruption: A feasibility study. Ultrasound Med Biol 2007;33:584-90.

McDonald D, Vodicka MA, Lucero G, Svitkina TM, Borisy GG, Emerman M, Hope TJ. Visualization of the intracellular behavior of hiv in living cells. J Cell Biol 2002;159:441-52.

Mehier-Humbert S, Bettinger T, Yan F, Guy RH. Plasma membrane poration induced by ultrasound exposure: Implication for drug delivery. J Control Release 2005a;104:213-22.

Mehier-Humbert S, Bettinger T, Yan F, Guy RH. Ultrasound-mediated gene delivery: Kinetics of plasmid internalization and gene expression. J Control Release 2005b;104:203-11.

Melchior F, Gerace L. Mechanisms of nuclear protein import. Curr Opin Cell Biol 1995;7:310-8.

Mesiwala AH, Farrell L, Wenzel HJ, Silbergeld DL, Crum LA, Winn HR, Mourad PD. High-intensity focused ultrasound selectively disrupts the blood-brain barrier in vivo. Ultrasound in Medicine and Biology 2002;28:389-400.

Miao CH, Brayman AA, Loeb KR, Ye P, Zhou L, Mourad P, Crum LA. Ultrasound enhances gene delivery of human factor ix plasmid. Hum Gene Ther 2005;16:893-905.

Michel MS, Erben P, Trojan L, Schaaf A, Kiknavelidze K, Knoll T, Alken P. Acoustic energy: A new transfection method for cancer of the prostate, cancer of the bladder and benign kidney cells. Anticancer Res 2004;24:2303-8.

Miller AD. Human gene therapy comes of age. Nature 1992;357:455-60.

Miller DL. A review of the ultrasonic bioeffects of microsonation, gas-body activation, and related cavitation-like phenomena. Ultrasound Med Biol 1987;13:443-70.

Miller DL, Averkiou MA, Brayman AA, Everbach EC, Holland CK, Wible JH, Jr., Wu J. Bioeffects considerations for diagnostic ultrasound contrast agents. J Ultrasound Med 2008;27:611-32; quiz 33-6.

Miller DL, Bao S, Morris JE. Sonoporation of cultured cells in the rotating tube exposure system. Ultrasound Med Biol 1999;25:143-9.

Miller DL, Dou C. Membrane damage thresholds for 1- to 10-mhz pulsed ultrasound exposure of phagocytic cells loaded with contrast agent gas bodies in vitro. Ultrasound Med Biol 2004a;30:973-7.

Miller DL, Dou C. Membrane damage thresholds for pulsed or continuous ultrasound in phagocytic cells loaded with contrast agent gas bodies. Ultrasound Med Biol 2004b;30:405-11.

Miller MW, Miller DL, Brayman AA. A review of in vitro bioeffects of inertial ultrasonic cavitation from a mechanistic perspective. Ultrasound Med Biol 1996;22:1131-54.

Mink A, Gati I, Szekely J. [nasolith removal with ultrasound lithotripsy]. HNO 1991;39:116-7.

Mitragotri S. Healing sound: The use of ultrasound in drug delivery and other therapeutic applications. Nat Rev Drug Discov 2005;4:255-60.

Miyamoto Y, Muto E, Mashimo T, Iwane AH, Yoshiya I, Yanagida T. Direct inhibition of microtubule-based kinesin motility by local anesthetics. Biophys J 2000;78:940-9.

Moran CM, Anderson T, Pye SD, Sboros V, McDicken WN. Quantification of microbubble destruction of three fluorocarbon-filled ultrasonic contrast agents. Ultrasound Med Biol 2000;26:629-39.

Moran CM, Watson RJ, Fox KA, McDicken WN. In vitro acoustic characterisation of four intravenous ultrasonic contrast agents at 30 mhz. Ultrasound Med Biol 2002;28:785-91.

Mortimer I, Tam P, MacLachlan I, Graham RW, Saravolac EG, Joshi PB. Cationic lipid-mediated transfection of cells in culture requires mitotic activity. Gene Ther 1999;6:403-11.

Muir TG, Carstensen EL. Prediction of nonlinear acoustic effects at biomedical frequencies and intensities. Ultrasound in Medicine & Biology 1980;6:345-57.

Mulligan RC. The basic science of gene therapy. Science 1993;260:926-32.

Nelson EM, Tewey KM, Liu LF. Mechanism of antitumor drug action: Poisoning of mammalian DNA topoisomerase ii on DNA by 4'-(9-acridinylamino)-methanesulfon-m-anisidide. Proc Natl Acad Sci U S A 1984;81:1361-5.

Neu M, Fischer D, Kissel T. Recent advances in rational gene transfer vector design based on poly(ethylene imine) and its derivatives. J Gene Med 2005;7:992-1009.

Newman CM, Bettinger T. Gene therapy progress and prospects: Ultrasound for gene transfer. Gene Ther 2007;14:465-75.

Ng KY, Liu Y. Therapeutic ultrasound: Its application in drug delivery. Med Res Rev 2002;22:204-23.

Ng YY, Hou CC, Wang W, Huang XR, Lan HY. Blockade of nfkappab activation and renal inflammation by ultrasound-mediated gene transfer of smad7 in rat remnant kidney. Kidney Int Suppl 2005;S83-91.

Nicolazzi C, Garinot M, Mignet N, Scherman D, Bessodes M. Cationic lipids for transfection. Curr Med Chem 2003;10:1263-77.

Nozaki T, Ogawa R, Feril LB, Jr., Kagiya G, Fuse H, Kondo T. Enhancement of ultrasound-mediated gene transfection by membrane modification. J Gene Med 2003;5:1046-55.

Nozaki T, Ogawa R, Watanabe A, Nishio R, Fuse H, Kondo T. Ultrasound-mediated gene transfection: Problems to be solved and future possibilities. Journal of Medical Ultrasonics 2006;33:135-42.

Ogawa-Goto K, Tanaka K, Gibson W, Moriishi E, Miura Y, Kurata T, Irie S, Sata T. Microtubule network facilitates nuclear targeting of human cytomegalovirus capsid. J Virol 2003;77:8541-7.

Ohl CD, Arora M, Ikink R, de Jong N, Versluis M, Delius M, Lohse D. Sonoporation from jetting cavitation bubbles. Biophys J 2006;91:4285-95.

Paliwal S, Mitragotri S. Ultrasound-induced cavitation: Applications in drug and gene delivery. Expert Opin Drug Deliv 2006;3:713-26.

Pan H, Zhou Y, Izadnegahdar O, Cui J, Deng CX. Study of sonoporation dynamics affected by ultrasound duty cycle. Ultrasound Med Biol 2005;31:849-56.

Papathanasiou MA, Kerr NC, Robbins JH, McBride OW, Alamo I, Jr., Barrett SF, Hickson ID, Fornace AJ, Jr. Induction by ionizing radiation of the gadd45 gene in cultured human cells: Lack of mediation by protein kinase c. Mol Cell Biol 1991;11:1009-16.

Pawluczkowycz AW, Beurskens FJ, Beum PV, Lindorfer MA, van de Winkel JG, Parren PW, Taylor RP. Binding of submaximal c1q promotes complement-dependent cytotoxicity (cdc) of b cells opsonized with anti-cd20 mabs ofatumumab (ofa) or rituximab (rtx): Considerably higher levels of cdc are induced by ofa than by rtx. J Immunol 2009;183:749-58.

Pazdur R, Kudelka AP, Kavanagh JJ, Cohen PR, Raber MN. The taxoids: Paclitaxel (taxol) and docetaxel (taxotere). Cancer Treat Rev 1993;19:351-86.

Petrovas C, Chaon B, Ambrozak DR, Price DA, Melenhorst JJ, Hill BJ, Geldmacher C, Casazza JP, Chattopadhyay PK, Roederer M, Douek DC, Mueller YM, Jacobson JM, Kulkarni V, Felber BK, Pavlakis GN, Katsikis PD, Koup RA. Differential association of programmed death-1 and cd57 with ex vivo survival of cd8+ t cells in hiv infection. J Immunol 2009;183:1120-32.

Pierce AD. Acoustics: An introduction to its physical principles and applications. New York: McGraw-Hill, 1981.

Pislaru SV, Pislaru C, Kinnick RR, Singh R, Gulati R, Greenleaf JF, Simari RD. Optimization of ultrasound-mediated gene transfer: Comparison of contrast agents and ultrasound modalities. Eur Heart J 2003;24:1690-8.

Plank C, Schillinger U, Scherer F, Bergemann C, Remy JS, Krotz F, Anton M, Lausier J, Rosenecker J. The magnetofection method: Using magnetic force to enhance gene delivery. Biol Chem 2003;384:737-47.

Poling BE, Prausnitz JM, O'Connell JP. The properties of gases and liquids, 5th ed. New York: McGraw-Hill, 2001.

Pollard H, Toumaniantz G, Amos JL, Avet-Loiseau H, Guihard G, Behr JP, Escande D. Ca2+-sensitive cytosolic nucleases prevent efficient delivery to the nucleus of injected plasmids. Journal of Gene Medicine 2001;3:153-64.

Pourpak A, Landowski TH, Dorr RT. Ethonafide-induced cytotoxicity is mediated by topoisomerase ii inhibition in prostate cancer cells. J Pharmacol Exp Ther 2007;321:1109-17.

Rahim A, Taylor SL, Bush NL, ter Haar GR, Bamber JC, Porter CD. Physical parameters affecting ultrasound/microbubble-mediated gene delivery efficiency in vitro. Ultrasound Med Biol 2006;32:1269-79.

Raz D, Zaretsky U, Einav S, Elad D. Cellular alterations in cultured endothelial cells exposed to therapeutic ultrasound irradiation. Endothelium 2005;12:201-13.

Roberts WW, Hall TL, Ives K, Wolf JS, Jr., Fowlkes JB, Cain CA. Pulsed cavitational ultrasound: A noninvasive technology for controlled tissue ablation (histotripsy) in the rabbit kidney. J Urol 2006;175:734-8.

Rols MP, Delteil C, Serin G, Teissie J. Temperature effects on electrotransfection of mammalian cells. Nucleic Acids Res 1994;22:540.

Rosenthal I, Sostaric JZ, Riesz P. Sonodynamic therapy--a review of the synergistic effects of drugs and ultrasound. Ultrason Sonochem 2004;11:349-63.

Sakakima Y, Hayashi S, Yagi Y, Hayakawa A, Tachibana K, Nakao A. Gene therapy for hepatocellular carcinoma using sonoporation enhanced by contrast agents. Cancer Gene Ther 2005;12:884-9.

Salido M, Larran J, Lopez A, Vilches J, Aparicio J. Etoposide sensitivity of human prostatic cancer cell lines pc-3, du 145 and lncap. Histol Histopathol 1999;14:125-34.

Schatten H, Ripple M, Balczon R, Weindruch R, Chakrabarti A, Taylor M, Hueser CN. Androgen and taxol cause cell type-specific alterations of centrosome and DNA organization in androgen-responsive lncap and androgen-independent du145 prostate cancer cells. J Cell Biochem 2000;76:463-77.

Schena M, Shalon D, Davis RW, Brown PO. Quantitative monitoring of gene expression patterns with a complementary DNA microarray. Science 1995;270:467-70.

Scherer F, Anton M, Schillinger U, Henke J, Bergemann C, Kruger A, Gansbacher B, Plank C. Magnetofection: Enhancing and targeting gene delivery by magnetic force in vitro and in vivo. Gene Ther 2002;9:102-9.

Schlicher RK, Hutcheson JD, Radhakrishna H, Apkarian RP, Prausnitz MR. Changes in cell morphology due to plasma membrane wounding by acoustic cavitation. Ultrasound Med Biol 2010;36:677-92.

Schlicher RK, Radhakrishna H, Tolentino TP, Apkarian RP, Zarnitsyn V, Prausnitz MR. Mechanism of intracellular delivery by acoustic cavitation. Ultrasound Med Biol 2006;32:915-24.

Schneider M, Bussat P, Barrau MB, Bodino F, Gotti C, Hybl E, Pelaprat ML, Yan F. A new ultrasound contrast agent based on biodegradable polymeric microballoons. Invest Radiol 1991;26 Suppl 1:S190-1; discussion S8-200.

Sehested M, Jensen PB. Mapping of DNA topoisomerase ii poisons (etoposide, clerocidin) and catalytic inhibitors (aclarubicin, icrf-187) to four distinct steps in the topoisomerase ii catalytic cycle. Biochem Pharmacol 1996;51:879-86.

Sheikov N, McDannold N, Vykhodtseva N, Jolesz F, Hynynen K. Cellular mechanisms of the blood-brain barrier opening induced by ultrasound in presence of microbubbles. Ultrasound Med Biol 2004;30:979-89.

Shimamura M, Sato N, Taniyama Y, Yamamoto S, Endoh M, Kurinami H, Aoki M, Ogihara T, Kaneda Y, Morishita R. Development of efficient plasmid DNA transfer into adult rat central nervous system using microbubble-enhanced ultrasound. Gene Ther 2004;11:1532-9.

Shirahata Y, Ohkohchi N, Itagak H, Satomi S. New technique for gene transfection using laser irradiation. J Invest Med 2001;49:184-90.

Skorpikova J, Dolnikova M, Hrazdira I, Janisch R. Changes in microtubules and microfilaments due to a combined effect of ultrasound and cytostatics in hela cells. Folia Biol (Praha) 2001;47:143-7.

Slattum PS, Loomis AG, Machnik KJ, Watt MA, Duzeski JL, Budker VG, Wolff JA, Hagstrom JE. Efficient in vitro and in vivo expression of covalently modified plasmid DNA. Mol Ther 2003;8:255-63.

Snyder RD. Use of catalytic topoisomerase ii inhibitors to probe mechanisms of chemical-induced clastogenicity in chinese hamster v79 cells. Environ Mol Mutagen 2000;35:13-21.

Sonne C, Xie F, Lof J, Oberdorfer J, Phillips P, Carr Everbach E, Porter TR. Differences in definity and optison microbubble destruction rates at a similar mechanical index with different real-time perfusion systems. J Am Soc Echocardiogr 2003;16:1178-85.

Subramanian A, Ranganathan P, Diamond SL. Nuclear targeting peptide scaffolds for lipofection of nondividing mammalian cells. Nat Biotechnol 1999;17:873-7.

Suomalainen M, Nakano MY, Keller S, Boucke K, Stidwill RP, Greber UF. Microtubule-dependent plus- and minus end-directed motilities are competing processes for nuclear targeting of adenovirus. J Cell Biol 1999;144:657-72.

Tabuchi Y, Ando H, Takasaki I, Feril LB, Jr., Zhao QL, Ogawa R, Kudo N, Tachibana K, Kondo T. Identification of genes responsive to low intensity pulsed ultrasound in a human leukemia cell line molt-4. Cancer Lett 2007;246:149-56.

Tabuchi Y, Kondo T, Ogawa R, Mori H. DNA microarray analyses of genes elicited by ultrasound in human u937 cells. Biochem Biophys Res Commun 2002;290:498-503.

Tachibana R, Harashima H, Ide N, Ukitsu S, Ohta Y, Suzuki N, Kikuchi H, Shinohara Y, Kiwada H. Quantitative analysis of correlation between number of nuclear plasmids and gene expression activity after transfection with cationic liposomes. Pharm Res 2002;19:377-81.

Tang S-C, Sambanis A. Development of genetically engineered human intestinal cells for regulated insulin secretion using raav-mediated gene transfer. Biochem Biophys Res Commun 2003;303:645-52.

Taniyama Y, Tachibana K, Hiraoka K, Aoki M, Yamamoto S, Matsumoto K, Nakamura T, Ogihara T, Kaneda Y, Morishita R. Development of safe and efficient novel nonviral gene transfer using ultrasound: Enhancement of transfection efficiency of naked plasmid DNA in skeletal muscle. Gene Ther 2002;9:372-80.

Tata DB, Dunn F, Tindall DJ. Selective clinical ultrasound signals mediate differential gene transfer and expression in two human prostate cancer cell lines: Lncap and pc-3. Biochem Biophys Res Commun 1997;234:64-7.

Terhorst B, Lutzeyer W, Cichos M, Pohlman R. [destruction of urinary calculi by ultrasound. Ii. Ultrasound lithotripsy of bladder calculi]. Urol Int 1972;27:458-69.

Toth C, Hodi I, Holman E. [percutaneous ultrasound lithotripsy of staghorn calculi]. Z Urol Nephrol 1988;81:293-7.

Tseng WC, Haselton FR, Giorgio TD. Mitosis enhances transgene expression of plasmid delivered by cationic liposomes. Biochim Biophys Acta 1999;1445:53-64.

Tsunoda S, Mazda O, Oda Y, Iida Y, Akabame S, Kishida T, Shin-Ya M, Asada H, Gojo S, Imanishi J, Matsubara H, Yoshikawa T. Sonoporation using microbubble br14 promotes pdna/sirna transduction to murine heart. Biochem Biophys Res Commun 2005;336:118-27.

Tu J, Matula TJ, Brayman AA, Crum LA. Inertial cavitation dose produced in ex vivo rabbit ear arteries with optison?By 1-mhz pulsed ultrasound. Ultrasound in Medicine & Biology 2006;32:281-8.

Uberti D, Meli E, Memo M. Expression of cell-cycle-related proteins and excitoxicity. Amino Acids 2002;23:27-30.

Uchida M, Shimatsu Y, Onoe K, Matsuyama N, Niki R, Ikeda JE, Imai H. Production of transgenic miniature pigs by pronuclear microinjection. Transgenic Res 2001;10:577-82.

Unger EC, McCreery TP, Sweitzer RH. Ultrasound enhances gene expression of liposomal transfection. Invest Radiol 1997;32:723-7.

Urick RJ. Priciples of underwater sound. New York: McGraw-Hill, 1983.

Vaezy S, Zderic V. Hemorrhage control using high intensity focused ultrasound. International Journal of Hyperthermia 2007;23:203-11.

van Brussel JP, van Steenbrugge GJ, Romijn JC, Schroder FH, Mickisch GH. Chemosensitivity of prostate cancer cell lines and expression of multidrug resistance-related proteins. Eur J Cancer 1999;35:664-71.

van Loo ND, Fortunati E, Ehlert E, Rabelink M, Grosveld F, Scholte BJ. Baculovirus infection of nondividing mammalian cells: Mechanisms of entry and nuclear transport of capsids. J Virol 2001;75:961-70.

van Wamel A, Bouakaz A, Versluis M, de Jong N. Micromanipulation of endothelial cells: Ultrasound-microbubble-cell interaction. Ultrasound Med Biol 2004;30:1255-8.

Vaughan EE, Dean DA. Intracellular trafficking of plasmids during transfection is mediated by microtubules. Mol Ther 2006;13:422-8.

Vaughan EE, DeGiulio JV, Dean DA. Intracellular trafficking of plasmids for gene therapy: Mechanisms of cytoplasmic movement and nuclear import. Curr Gene Ther 2006;6:671-81.

Vaughan EE, Geiger RC, Miller AM, Loh-Marley PL, Suzuki T, Miyata N, Dean DA. Microtubule acetylation through hdac6 inhibition results in increased transfection efficiency. Molecular Therapy 2008;16:1841-7.

Vihinen-Ranta M, Yuan W, Parrish CR. Cytoplasmic trafficking of the canine parvovirus capsid and its role in infection and nuclear transport. J Virol 2000;74:4853-9.

Wang S, Joshi S, Lu S. Delivery of DNA to skin by particle bombardment. Methods Mol Biol 2004;245:185-96.

Wang X, Liang HD, Dong B, Lu QL, Blomley MJ. Gene transfer with microbubble ultrasound and plasmid DNA into skeletal muscle of mice: Comparison between commercially available microbubble contrast agents. Radiology 2005;237:224-9.

Wang XW, Zhan Q, Coursen JD, Khan MA, Kontny HU, Yu L, Hollander MC, O'Connor PM, Fornace AJ, Harris CC. Gadd45 induction of a g2/m cell cycle checkpoint. P Natl Acad Sci USA 1999;96:3706-11.

Wells DJ. Electroporation and ultrasound enhanced non-viral gene delivery in vitro and in vivo. Cell Biol Toxicol 2010;26:21-8.

West A, Priante G, Lahdetie J. Stage-specific expression of gadd45 induced by x-irradiation in rat spermatogenesis. Int J Radiat Biol 2002;78:29-39.

Whitworth M, Bricker L, Neilson JP, Dowswell T. Ultrasound for fetal assessment in early pregnancy. Cochrane Database Syst Rev 2010;CD007058.

Wilke M, Fortunati E, van den Broek M, Hoogeveen AT, Scholte BJ. Efficacy of a peptide-based gene delivery system depends on mitotic activity. Gene Ther 1996;3:1133-42.

Wilson GL, Dean BS, Wang G, Dean DA. Nuclear import of plasmid DNA in digitonin-permeabilized cells requires both cytoplasmic factors and specific DNA sequences. J Biol Chem 1999;274:22025-32.

Xu C, Lo A, Yammanuru A, Tallarico AS, Brady K, Murakami A, Barteneva N, Zhu Q, Marasco WA. Unique biological properties of catalytic domain directed human anti-caix antibodies discovered through phage-display technology. PLoS One 2010;5:e9625.

Yamamoto A, Tagawa Y, Yoshimori T, Moriyama Y, Masaki R, Tashiro Y. Bafilomycin a1 prevents maturation of autophagic vacuoles by inhibiting fusion between autophagosomes and lysosomes in rat hepatoma cell line, h-4-ii-e cells. Cell Struct Funct 1998;23:33-42.

Yamamoto M, Okumura S, Schwencke C, Sadoshima J, Ishikawa Y. High efficiency gene transfer by multiple transfection protocol. Histochem J 1999;31:241-3.

Yang NS, Burkholder J, Roberts B, Martinell B, McCabe D. In vivo and in vitro gene transfer to mammalian somatic cells by particle bombardment. Proc Natl Acad Sci U S A 1990;87:9568-72.

Yoshizawa S, Ikeda T, Ito A, Ota R, Takagi S, Matsumoto Y. High intensity focused ultrasound lithotripsy with cavitating microbubbles. Med Biol Eng Comput 2009;47:851-60.

Young LS, Searle PF, Onion D, Mautner V. Viral gene therapy strategies: From basic science to clinical application. J Pathol 2006;208:299-318.

Zarnitsyn VG, Prausnitz MR. Physical parameters influencing optimization of ultrasound-mediated DNA transfection. Ultrasound Med Biol 2004;30:527-38.

Zhang G, Budker V, Wolff JA. High levels of foreign gene expression in hepatocytes after tail vein injections of naked plasmid DNA. Hum Gene Ther 1999;10:1735-7.

Zhang G, Gao X, Song YK, Vollmer R, Stolz DB, Gasiorowski JZ, Dean DA, Liu D. Hydroporation as the mechanism of hydrodynamic delivery. Gene Therapy 2004;11:675-82.

Zhao J, Tenev T, Martins LM, Downward J, Lemoine NR. The ubiquitin-proteasome pathway regulates survivin degradation in a cell cycle-dependent manner. J Cell Sci 2000;113 Pt 23:4363-71.

Zhou S, Schmelz A, Seufferlein T, Li Y, Zhao J, Bachem MG. Molecular mechanisms of low intensity pulsed ultrasound in human skin fibroblasts. J Biol Chem 2004;279:54463-9.

VITA

YING LIU

Ying Liu was born in Zibo, P.R.China on June 19, 1980. She attended Zhejiang University in Hangzhou, China in 1998 and received a B.A. in Bioengineering in July 2002 and a M.S in Biochemical Engineering in March 2005. In August 2005, she attended the Georgia Institute of Technology in Atlanta, Georgia where she was accepted as a Ph.D. candidate in the School of Chemical and Biomolecular Engineering. Her dissertation title was "THE IMPACT OF PHYSICAL AND BIOLOGICAL FACTORS ON INTRACELLULAR UPTAKE, TRAFFICKING AND GENE TRANSFECTION AFTER ULTRASOUND EXPOSURE". She defended her doctoral thesis on March 7, 2011 and obtained her Ph.D. in Chemical Engineering with a minor in Bioengineering in May 2011.